LB/DON/150/2016
DMT 03/10

REINFORCEMENT OF CARBOXYLATED NITRILE RUBBER LATEX FILMS BY SURFACE MODIFIED NANOSILICA

LIBRARY
UNIVERSITY OF MORATUWA, SRI LANKA
MORATUWA

Ramasinghege Lumbini Paramitha Ramasinghe

(168026E)

TH 3701
+ CD ROM

Thesis submitted in partial fulfillment of the requirements for the degree
Master of Science by Research

Department of Materials Science and Engineering

University of Moratuwa

Sri Lanka

620"18"
620.1(043)

October 2018

TH3701

TH3701

DECLARATION

I declare that this is my own work and this thesis does not incorporate without acknowledgement any material previously submitted for a Degree or Diploma in any other University or Institute of higher learning and to the best of my knowledge and belief it does not contain any material previously published or written by another person except where the acknowledgement is made in the text.

Also, I hereby grant to the University of Moratuwa the non-exclusive right to reproduce and distribute my thesis in whole or in part in print, electronic or other medium. I retain the right to use this content in whole or in part in the future work (such as articles or books).

Signature: Date:

The above candidate has carried out research for the Master's thesis under my supervision.

Signature of the supervisor: Date:

Name of the Supervisor: Dr. (Mrs.) N.M.V.K. Liyanage

Abstract

Carboxylated acrylonitrile butadiene rubber (XNBR) is synthetic elastomer which inherent number of physical and chemical properties such as comparable barrier protection, good puncture and chemical resistance and high durability under storage.

Although that there is a problem associated with synthetic elastomers that they are typically not self-reinforcing elastomers. Therefore, reinforcing fillers are incorporated to improve the properties of the compounds.

Silica is extensively used for latex products. Nanofillers can impart more advanced properties to the final nanocomposite than micro fillers. Surface modification has been introduced to avoid the incompatibility between inorganic filler silica and organic XNBR matrix.

Role of surface modifiers in this study play dual role, as a capping agent: to control the size of nanoparticles & as a coupling agent: to develop compatibility between rubber and filler. Synthetic surface modifiers i.e. Polymethacrylic acid & Polymethacrylic acid ethyl hexyl acrylate and natural surface modifiers i.e. cellulose, collagen, chitosan & gelatin were used in this study.

The FTIR analysis confirm that the surface of nanosilica particles has been successfully modified with acrylic polymers, forming ester bonds between carboxylic groups of acrylic polymers and surface silanol groups of nanosilica. TGA confirms the successful surface modification resulting lower weight loss; indicating small number of free surface silanols groups are present on the silica surface. XRD analysis revealed the amorphous nature of unmodified and all modified nanosilica particles. SEM results help to monitor the particle shape, size and agglomerations of synthesized particles.

Evaluation of XNBR vulcanizate properties of micro silica, unmodified nanosilica, acrylic polymer modified nanosilica and natural polymer modified nanosilica filled vulcanizates was carried out. The results show that addition of small quantities of nanosilica causes an increase of mechanical properties of XNBR vulcanizates, while high filler loading of nanosilica appear to decrease the mechanical properties due to the aggregation of nanosilica particles. 2% PMAA and 2% cellulose modified nanosilica filled vulcanizates show balance strength with stretch & comfort properties for the glove manufacturing.

TABLE OF CONTENT

LIST OF FIGURES

LIST OF TABLES

LIST OF ABBREVIATIONS

XNBR	Carboxylated acrylonitrile butadiene rubber
PMAA	Polymethacrylic acid homopolymer
P(MAA-EHA)	Polymethacrylic acid ethylhexyl acrylate copolymer
PEG	Poly ethylene glycol
ZDEC	Zinc diethyldithiocarbamate
KOH	Potassium hydroxide
MAA	Methacrylic acid
FTIR	Fourier transform infrared
TGA	Thermogravimetric analysis
SEM	Scanning electron microscopy
ZnO	Zinc oxide
SP	Styrenated phenol
UMNS	Unmodified nanosilica
VN_3	Ball milled micro silica
MNS_{M1}	1% Polymethacrylic acid modified nanosilica
$MNS_{M1.5}$	1.5% Polymethacrylic acid modified nanosilica
MNS_{M2}	2% Polymethacrylic acid modified nanosilica
$MNS_{M2.5}$	2.5% Polymethacrylic acid modified nanosilica
$MNS_{M/E1}$	1% Polymethacrylic acid ethylhexyl acrylate modified nanosilica
$MNS_{M/E1.5}$	1.5%Polymethacrylic acid ethylhexyl acrylate modified nanosilica
$MNS_{M/E2}$	2% Polymethacrylic acid ethylhexyl acrylate modified nanosilica
*MNS_{M2}	2% Polymethacrylic acid modified commercial nanosilica
*$MNS_{M/E1.5}$	1.5%Polymethacrylic acid ethylhexyl acrylate modified commercial nanosilica
CE	Cellulose

CO	Collagen
CHO	Chitosan
GE	Gelatin
*MNS_{CE2}	2% cellulose modified nanosilica
*MNS_{CO2}	2% collagen modified nanosilica
*MNS_{CHO2}	2% chitosan modified nanosilica
*MNS_{GE2}	2% gelatin modified nanosilica
MMS_{CE2}	2% cellulose modified microsilica
MMS_{CO2}	2% collagen modified microsilica
MMS_{CHO2}	2% chitosan modified microsilica
MMS_{GE2}	2% gelatin modified microsilica
TS	Tensile strength
EB (%)	Elongation at break (%)
M300	Modulus at 300% elongation
TRS	Tear strength

ACKNOWLEDGEMENT

I wish to express my gratitude to my supervisor Dr. Kalyani Liyanage for the useful comments, remarks and guidance through the learning process of this master thesis. Furthermore, I would like to thank the research committee, Drs. Shantha Amarasinghe and Shantha M. Egodage for reviewing the research as well for the support on the way. Also, I greatly appreciate the assistance that I received from the staff of Department of Materials Science and Engineering. This includes Mr. M.A.P.C. Gunawardhana, Mr. R.R.P. Perera, and Mr. M.T.M.R. Jayaweera. Further, I would like to thank Departments of Civil Engineering and Chemical and Process Engineering at University of Moratuwa. Financial support by SRC/LT/2016/05 university research fund is greatly acknowledged.

I would like to thank my family and my loved ones, who have supported me throughout the entire process, both by keeping me harmonious and helping me putting pieces together. My warm hearted thanks to my friends Bhagya Gannoruwa and Nuwan Pannilawithana for their endless support and encouragement to achieve this goal.

Ramasinghe R.L.P.

CHAPTER 01

1 INTRODUCTION

Elastomeric materials have been the one of key topics in contemporary immense research and development area. Consequently, their application areas also have been intensifying. Elastomers are a specific class of polymers comprise with long chain and high molecular weight molecules with no or minor crystallinity at rest. These long chain molecules are easily entangled with each other. In the state of unstrained these long chains are coiled. When stress is applied; uncoiling of polymer chains could be observed acquiring high extensions of elastomeric materials. Then stress is removed; polymer chains return back to its coiled state with rapid recovery. Crosslinking is introduced to elastomers to overcome unnecessary elasticity behavior and induce an additional strength according to the requirement of the application.

The polymer coils elucidate the basic characteristics of elastomers; remarkably high extensibility and recovery. Some elastomers are naturally reinforced, attaining high strength, i.e. natural rubber form tiny crystallites during extension. Natural rubber is a product form principally from the rubber tree, *Hevea brasiliensis*. Over the years, there is a growing concern on the potential allergy caused by natural rubber proteins. These proteins affect number of dermal allergies, ordinarily in the form of skin rashes and eczema. Some people are susceptible to allergic reactions after frequent contact with latex, especially latex gloves. Allergy to latex has been a growing health issue over the years. As a consequence, novel synthetic elastomeric materials have been introduced to the polymer industry such as a styrene– butadiene rubber or a carboxyl-group-containing ionomer-based elastomers such as carboxylated acrylonitrile butadiene rubber latex (XNBR) which is also known as nitrile rubber latex (Ain & Azura, 2011).

XNBR is a terpolymer of acrylonitrile, butadiene and a carboxyl group containing monomers such as acrylic or methacrylic acid. Incorporation of carboxyl groups enhance intra and inter molecular interactions, acquiring enhanced physical and chemical properties of the elastomers. In consequence of the high polarity of existing

carboxylic groups, they are considered as polar rubbers and polarity depends on the percentage of carboxyl groups.

Most synthetic elastomers are unable to obtain self-reinforcing ability and are consequently they inherent low strength when unfilled. Unlike natural rubbers, synthetic elastomers are not capable to crystallize when they are stretched. Therefore, synthetic elastomers demand reinforcing fillers to improve their tensile and tear strength. Fillers are widely incorporated in elastomers as small hard particles. Their effects are highly depend on the type of elastomer. In the crystallizing types, they are not able to enhance post crystallization strength to a high degree (determined in conventional tensile testing); due to cease the strength reduction occurs with the crystallization. In most of the elastomeric applications, crystallization may not be able to occur, and then fillers are able to show their full potential.

Fillers utilize in a range of schemes such as polymeric, organic, biomimetic and biological materials. In polymeric systems, fillers not only utilize as a cost reduction material but also as a reinforcing substance of the compounds. Carbon black and silica are the most extensively used fillers in rubber industry. Carbon black is the foremost reinforcing filler for tire industry and many other rubber and plastic industries (Yimin Zhang et al., 2001). Carbon black obtrudes color restriction of the vulcanized products. In contrast, non-black fillers provide the high possibility that add any color and be discoverd in the products. Non-black fillers can be employed to provide a number of appropriate properties to elastomeric compounds, containing:

- increased tensile strength
- increased tear strength
- lower hysteresis
- increased abrasion resistance
- chemical compatibility or chemical resistance
- lower cost (Mujkanović, Vasiljević, Ostojić, & Zvornik)

The non-black fillers used in elastomers are precipitated silica, amorphous silica, calcium carbonate, talc, kaolin clay, barite, diatomite, etc. Precipitated silica , kaolin

clay and calcium carbonate are the most widely used non-black fillers in polymer industry as by volume and by functionality (Mujkanović et al.).

These fine fillers can act as tiny crystallites, when the surface interaction between filler and elastomer is high and noticeably increase the tensile strength of non-crystallizing elastomers. Elastomer nanocomposites reinforced with low volume of nanofillers ominously improve the mechanical, thermal, barrier and flame-retardant properties.

The performance of the particulate fillers on elastomeric applications intensely relies on number of parameters such as filler morphology, volume fraction, and filler-filler and filler-rubber interactions. The most significant parameter is the filler-rubber interaction. Due to the filler-rubber interactions, polymer chains of matrix adsorb onto the filler particle surface. And this interactions can be regulated by changing the nature of filler-rubber interactions. Thus, surface modifiers are introduced to enhance the filler-rubber interactions and create homogenous distribution throughout the rubber matrix. Surface modifiers are mostly bi-functional molecules which are able to create molecular bridges at the interface between the rubber matrix and the filler surface. In this way, the rubber-filler interaction is amplified and thus the reinforcing capability of silica is enhanced (Bokobza, 2004).

For nanofillers it is difficult to disperse well in rubber matrix due to its high surface energy which leads to the huge agglomerations. Hence, the overall objective of this study was to investigate the effects of surface modified nanosilica in reinforcement of XNBR latex vulcanizates. Both synthetic and natural polymers (NPs) were used as the surface modifiers. The selected surface modifiers were expected play dual role; as a capping agent to prevent agglomeration of synthesized of nanosilica particles and as a coupling agent to confer rubber-filler interactions. The specific objectives of this investigation are:

- To synthesis stable aqueous dispersions of nanosilica
- To prepare stable nitrile latex/nanosilica blends, and
- To enhance physical properties of nitrile rubber/nanosilica composites

CHAPTER 02

2 LITERATURE REVIEW

2.1 XNBR

Chemical structures of the monomers present in XNBR latex, are given below;

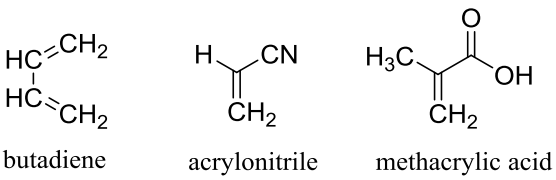

Figure 2.1: Monomers of XNBR

The contribution of each monomer on the inclusive properties of the final product turn out from one latex can be outlined as follows: acrylonitrile monomer units offer tensile strength and solvent resistance due to presence of –CN (cyanide) groups, butadiene monomer units provide the elasticity to the polymer due to its simple liner structure and methacrylic acid monomer units provide tensile strength and stability of latex due to presence of carboxylic acid groups (Tennakoon, 2015).

2.2 Fillers

Three classes of fillers are generally recognized for elastomer; reinforcing, semi-reinforcing, and non-reinforcing. These definitions are a little vague as the effects of a given filler can vary from polymer to polymer. One way of distinguishing them is by their effect on pure natural rubber (Skelhorn, 2003).

2.2.1 Filler characteristics

The filler characteristics are significant in selecting fillers for elastomeric applications.

2.2.1.1 Cost

Depending on factors such as morphology, color, purity and surface treatment of fillers, large price variations can be anticipated even within one type of filler. Though the filler cost is low, transport costs can also be very noteworthy and may well govern when selecting the filler type. Factors other than the raw material cost also must be taken into account in evaluating whether cost savings will be acquired. Some of the significant deliberations are: effects of processing and effects on other ingredients of filler on the elastomer compounding. In spite of the above, fillers are primarily used due to their capability on cost savings while retaining the other physical and chemical properties (Rothon, 2002).

2.2.1.2 Chemical composition

Though the bulk chemical composition of fillers decides most of their physical properties such as thermal conductivity, density, refractive index, etc. However, the ultimate composite properties, are highly influenced by particle morphology. The main deliberations are the ability of fillers being insoluble and inert during utilization, and not be a root for degradation of the polymer matrix (Rothon, 2002).

2.2.1.3 Specific gravity

Most polymers have specific gravities in the range 0.9-1.4. Most fillers have significantly higher specific gravities in the range 2.3-2.8 and their loading at distinctive levels can enhance the specific gravity of the final composite reasonably. This is often a disadvantage especially for light weight requirements, but there are some instances where fillers are used to control density. Therefore, when selecting a type of a filler specific gravity also become very important parameter depending on the requirement of final product (Rothon, 2002).

2.2.1.4 Hardness

The hardness of fillers is significant for polymer applications. Hard fillers, like crystalline silica, are frequently employed when high abrasion resistance is compulsory while soft fillers are preferred where the abrasion and wearing resistance properties are not much important for the final application (Rothon, 2002).

2.2.1.5 Thermal properties

The key principal thermal properties are thermal conductivity, coefficient of expansion specific heat, and stability for the polymer applications. The importance of thermal properties when selecting a type of filler also depends on the requirements of the final application (Rothon, 2002).

2.2.1.6 Optical properties

The most significant optical properties for fillers are color and refractive index. Most applications are willing to implement fillers with colorless, or white. Although, the presence of traces of impurities can provide remarkable deleterious effects on the requirement of the application. Color issues may not be picked up in the filler powder, and may only become visible in the final composite (Rothon, 2002).

2.2.1.7 Morphology

Particle size and shape are key factors when determining the performance of particulate fillers in all polymers types.

Active fillers can identified by three main characteristic sizes: primary particles, aggregates and agglomerates. Figure 2.2 shows the particle size diverge from primary particles to large agglomerates. The term, primary particle, is generally used to the smallest unit that the filler can sensibly thought to be composed of. Assemblies of these primary particles are stated to as aggregates or agglomerates, depending on the strength of interaction. In filler technology, very strong assemblies are called aggregates, and weaker ones, are called agglomerates (Rothon, 2002).

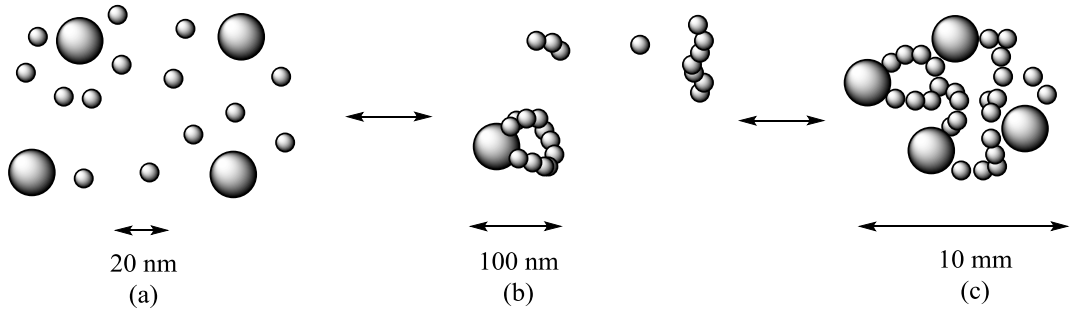

Figure 2.2: Characteristic sizes of fillers (a) Primary particles (b) Aggregates (c) Agglomerates

2.2.1.8 Particle size

Particle size is the most commonly used parameter for filler morphology. This is the main parameter for characterization of fillers as reinforcing fillers, semi-reinforcing fillers and non-reinforcing fillers as illustrated in Figure 2.3. Fillers with particle size greater than 10,000 nm (10 μm) can reduce the performance of rubber instead of reinforcing, because if the size of the filler particle exceeds the polymer inter chain distance, it introduces an area of localized stress and act as an impurity. Therefore, fillers with particle size greater than 10 μm, are not generally used. Fillers with particle size between 1,000 and 10,000 nm (1 to 10 μm) have no significant effect on physical properties of rubber and are used primarily as diluents. Semi-reinforcing fillers range from 100 to 1000 nm (0.1 to 1μm). Reinforcing fillers have particle size range from 10 nm to 100 nm (0.01 to 0.1 μm) and they can significantly increase physical properties of elastomers (C. Brinker, 1988).

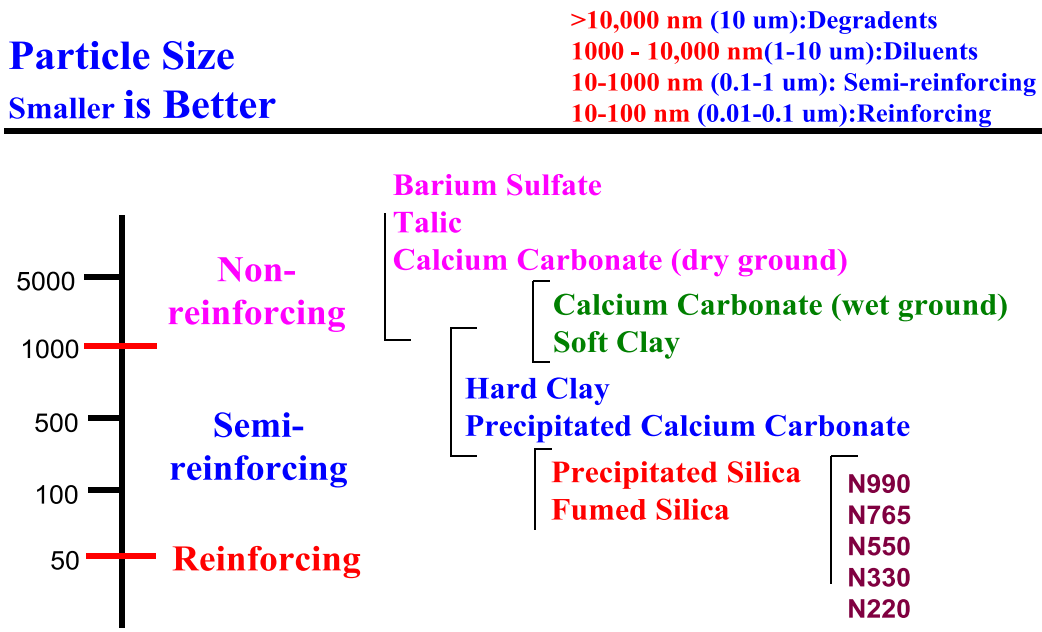

Figure 2.3: Particle sizes of different types of fillers (C. Brinker, 1988)

2.2.1.9 Particle shape

Particle shape is another crucial factor for fillers used in polymers which can have ability to affect processing parameters and composite properties. Distinctive particulate filler shapes are illustrated in Figure 2.4. Anisotropy, or aspect ratio, is also predominantly significant, in surpassing parameters such as heat distortion temperature and stiffness (Rothon, 2002).

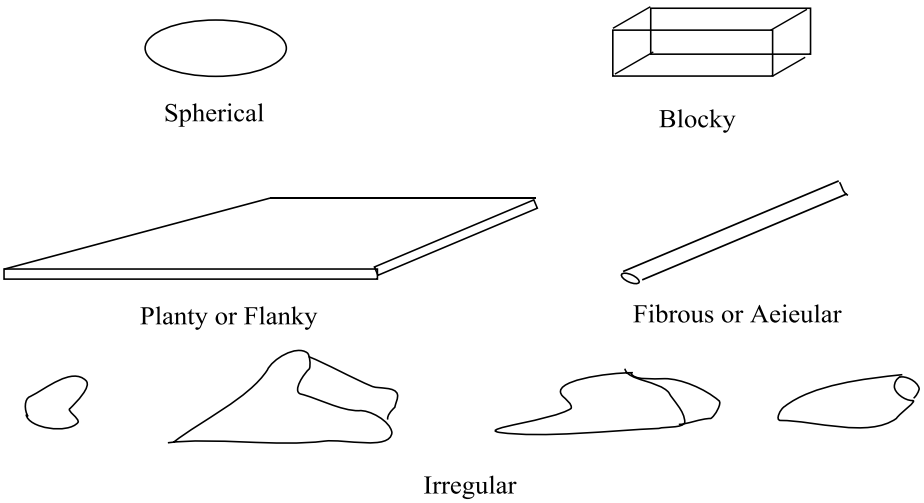

Figure 2.4: Idealized shapes of typical fillers (Rothon, 2002)

2.2.2 Types of fillers

There are number of reinforcing fillers are available: carbon blacks, nano clay, precipitated and fumed silica and some special minerals like *Halloysite*. Semi-reinforcing fillers are some clays (frequently mentioned to as hard clays), thermal blacks and precipitated calcium carbonates. Non-reinforcing fillers comprise natural calcium carbonates and other clays (often termed soft clays).

Particulate fillers are specifically small in sized, and can considerably influence on number of the vital elastomeric properties as described earlier. Carbon black, clays, precipitated silica, and natural carbonates are the foremost fillers used in general purpose elastomeric applications. The principal role of most fillers in elastomeric systems is show enhancements in some, or all, of the following: tensile strength, modulus, tear strength, and abrasion resistance.

Properties if reinforcing fillers filled elastomers are affected by diverse combinations of the following filler properties: filler shape and size, filler structure, filler dispersion and rubber-filler interaction (Skelhorn, 2003).

2.2.2.1 Filler classification

Fillers used in elastomers can be classified based on various parameters such as particle shape, size, origin etc. (Skelhorn, 2003).

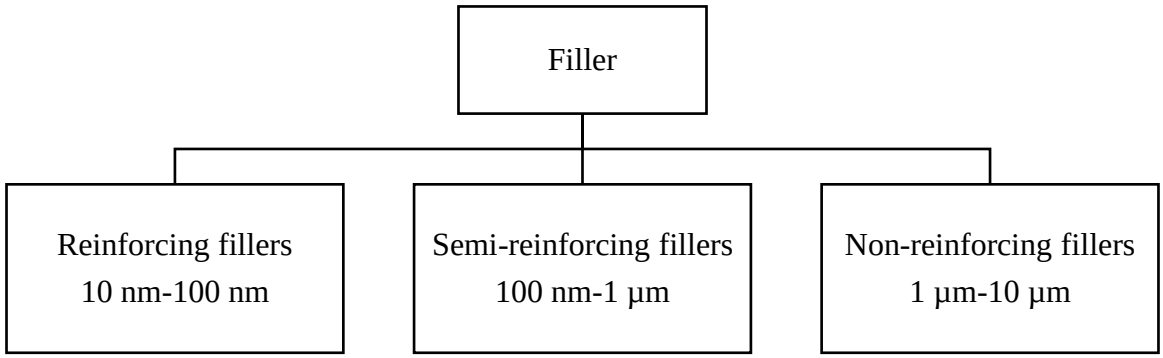

Figure 2.5: Classification of fillers based on particle size (Skelhorn, 2003)

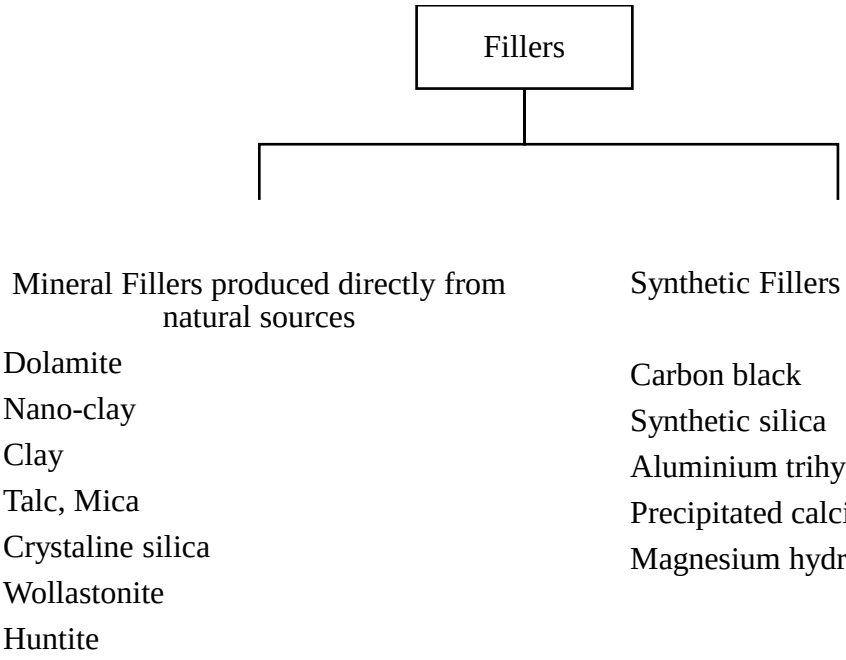

Figure 2.6: Classification of fillers based on origin (Skelhorn, 2003)

2.2.2.2 Silica

Silica can be synthesized comprising several morphological features of carbon blacks and two of such forms are widely used in elastomer technology; i.e. precipitated silica and pyrolytic or fumed silica.

2.2.2.3 Surface chemistry of silica

The final particles which make up the silica can be considered as polymers of silicic acid, consisting of interlinked SiO_4 tetrahedra. At the surface, the structure aborts with either a siloxane group (Si-O-Si) with the oxygen on the surface due to the aggregation of silica atoms, or one of several forms of silanol groups (-Si-OH). The surface silanols can be separated into three groups which have been discovered by using Si-Nuclear Magnetic Resonance (NMR)- or infrared spectroscopy (Vansant, Van Der Voort, & Vrancken, 1995).The three types of silanol groups are named as follows;

- Isolated single hydroxyl group on a silicon atom
- Vicinal two hydroxyl groups on adjacent silicon atoms

- Geminal two hydroxyl groups on adjacent silicon atoms

In first type of silanol groups (isolated groups or free silanols), the surface silica atom has a single OH group and three bonds into the bulk structure (See Figure 2.7). In vicinal silanols (or bridged silanols), where two single silanol groups, attached to different silicon atoms, are close enough to hydrogen bond. Germinal silanols comprise of two hydroxyl groups that are attached to one silicon atom. The germinal silanols are too close to hydrogen bond each other, whereas the free hydroxyl groups are too far separated (C. J. Brinker & Scherer, 2013; Vansant et al., 1995).

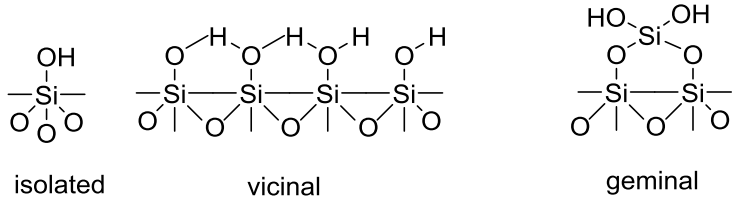

Figure 2.7: Types of hydroxyl species on silica surface (C. J. Brinker & Scherer, 2013)

The surface structure of amorphous silica is highly disordered, thus a regular arrangement of hydroxyl groups cannot expect. Hence the surface of amorphous silica gel may be enclosed by isolated as well as vicinal hydroxyl groups. Irrespective of whether a surface contains either types or only isolated hydroxyl groups (as in crystalline silica), complete surface coverage can be achieved when the surface is fully hydroxylated. On exposing silica to water, it is further able to adsorb water physically by means of hydrogen bonding (Vansant et al., 1995).

2.2.3 Nano fillers

As stated by the National Nanotechnology Initiative Strategic Plan in 2004, nanotechnology is "the understanding and control of matter at dimensions of roughly 1-100 nanometers" and it has become one of the most popular field of development and research in many technical disciplines in the last 20 years. This is due to the nanometer-scale structures are capable to take advantage of physical and chemical properties of matter that are discovered only at this scale. Principally, the use of nanoparticles has led to the development of advanced polymeric matrix

nanocomposites for the realization of high-performance products (Paul & Robeson, 2008). The nanoparticles are characterized by a high interfacial area for volume, furnishing improved molecular interactions with the polymeric matrix leading to the increased properties with respect to traditional composites (Koo, 2006).

The most used nano-oxides in elastomers are silica (SiO_2), alumina (Al_2O_3), and titania (TiO_2) in the form of nano scale particles. These particles are characterized by small dimensions (in the range from 7 to 40 nm in diameter), high specific surface areas (between 50 and 380 m^2/g), and, generally, spherical nonporous structures (Koo, 2006).

Fumed nanosilica particles are produced by the hydrolysis of silicon tetrachloride at elevated temperatures. Moreover, sol-gel or precipitation techniques are practiced to produce NS particles.

2.2.4 Sol-gel process

A sol is a colloidal suspension of solid particles in a liquid. An aerosol is a colloidal suspension of particles in a gas and emulsion is a suspension of liquid droplets in another liquid. Precursors (starting compounds) used in sol-gel process comprise of a metal or metalloid element surrounded by various ligands for formation of a colloid. Metal alkoxides are members of the family of metal organic compounds, which have an organic ligand attached to a metal or metalloid atom (C. J. Brinker & Scherer, 2013).

2.2.4.1 Theory for sol-gel process of silicates

Silicon is the most copious metal in the earth's crust. Hydrolysis and condensation of silicates to formpolysilicate gels and particles have been seen in many natural systems. The synthesis of polysilicate gels from alkoxide precursors closely followed the pioneer research in 1824 by Ebelmen *et al* (Andrianov, 1955). Moreover, Ebelmen *et al* have discovered that the hydrolysis of tetraethylorthosilicate (TEOS) yield silicate solutions (C. J. Brinker & Scherer, 2013). In 1850 Mendeleyev conceived the novel idea of hydrolysis of $SiCl_4$ to produce ($Si(OH)_4$) which

undergoes repeated condensation reactions to form high-molecular weight polysiloxanes.

The +4 oxidation state is the only important one in the chemistry of silicon in naturally occurring systems (Baes & Mesmer, 1976), and the coordination number of silicon is most often four. Therefore, silicon is less electropositive and comparatively less prone to nucleophilic attack compared to transition metals. These factors make the kinetics of hydrolysis and condensation of silicon significantly slower than transition metal systems or group III systems (C. J. Brinker, 1994).

Freundlich *et al* have prepared silicic acid by acidifying a soluble silicate as follows (Freundlich & Hatfield, 1926):

$$Na_2SiO_3 + H_2O + 2HCl \longrightarrow Si(OH)_4 + 2NaCl \qquad (1)$$

As in organic polymer systems, $Si(OH)_4$ might polymerize into siloxane chains that can then subject to branching and cross-linking. However, Iler defines, that there is no relation or similarity between polymerization of silicic acid in an aqueous system and condensation-type organic polymers (Iler, 1979). Iler recognizes three stages of polymerization as follows:

(1) Polymerization of monomers to form particles

(2) Growth of particles

(3) Linking of particles into branched chains, networks, and finally gels.

NMR results obviously confirm Iler's interpretation that condensation occurs to aggregate the silica particles to exploit the number of silica particle to maximize the number of Si-O-Si bonds while minimalizing the number terminal silanol groups (Iler, 1979). Consequently, three-dimensional particles are rapidly created as rings to which monomers add. Particles are formed in most compact state leaving silanol groups on the outer part surface of silica particles. According to Iler, the three-dimensional particles function as nuclei. Then according to the Ostwald ripening mechanism particle growth occurs whereby particles grow in size and decline in number as highly soluble small particles dissolve and reprecipitate on larger particles, less soluble nuclei. Then growth terminates when the difference in

solubility between the smallest and largest particles becomes only a few ppm. Due to greater solubility, growth continues to larger sizes at higher temperatures (C. J. Brinker & Scherer, 2013). Thus, particle size can be controlled by monitoring the reaction parameters which are responsible for the difference of solubility to achieve particles in nano meter range.

Iler splits the polymerization process into three domains depending pH as pH < 2, 2 < pH < 7, and pH >7. pH 2 and 7 act as boundaries. A pH of 2 seems as a boundary, due to the point of zero charge (PZC), where the surface charge is zero, and the isoelectric point (IEP), where the electrical mobility of the silica particles is zero, both are in the range of pH 1-3. pH 7 seems as a boundary due to both solubility and dissolution rates are maximized and silica particles are significantly ionized at or above pH 7. So that particle growth occurs without aggregation or gelation. For all pH ranges, the addition of salt promotes aggregation and gel formation (C. J. Brinker, 1994).

During the polymerization between pH 2 and 6, the gel time decrease gradually. Generally, it is believed that, above the IEP the condensation rate is proportional to the presence of amount of (OH^-) groups as mentioned in the equation (2).

$$\equiv Si\text{-}OH + OH^- \longrightarrow \equiv Si\text{-}O^- + H_2O \quad (2)$$

$$\equiv Si\text{-}O^- + HO\text{-}Si \longrightarrow \equiv Si\text{-}O\text{-}Si\equiv + OH^- \quad (3)$$

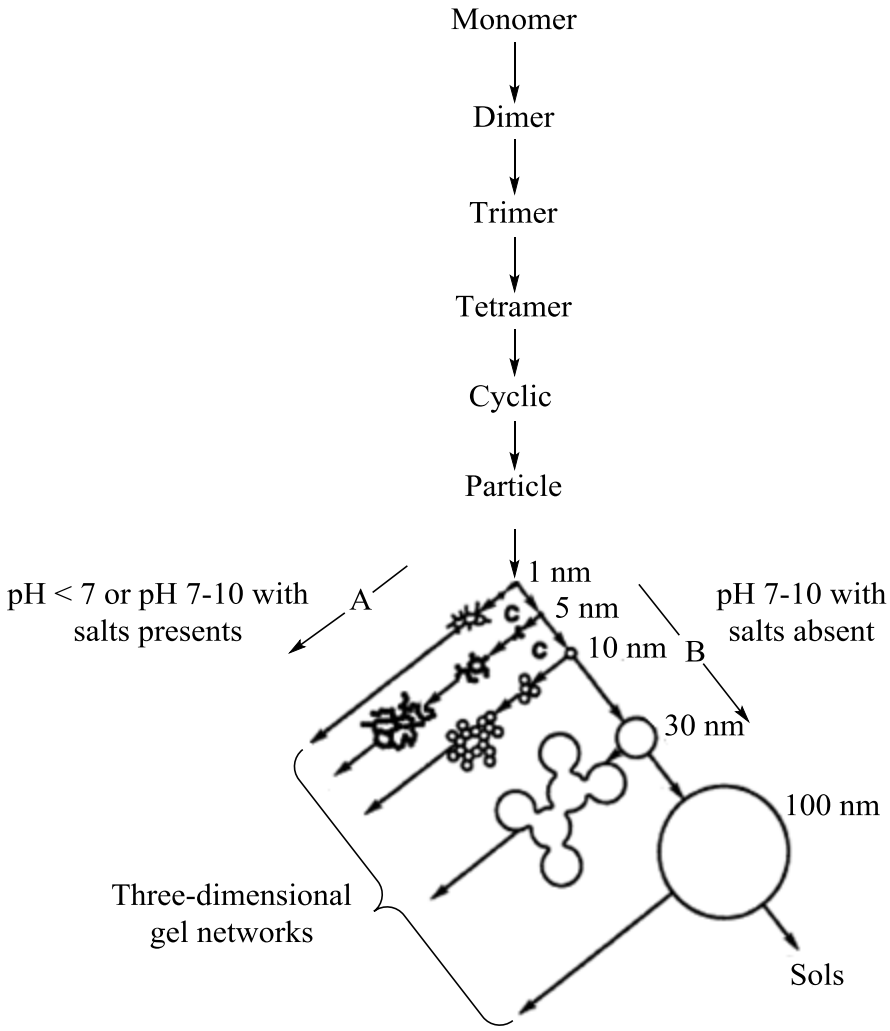

Figure 2.8: Polymerization behavior of aqueous silica (C. J. Brinker, 1994)

Therefore, according to equation (2) condensation happens practically between less condensed, neutral species and more condensed species. As stated by Figure 2.8, condensation pathway of the synthesized particles can be characterized as monomer, dimer, trimer, and tetramer respectively. Tetramers tend to form into cyclize due to the extensive reduction of the monomer population and vicinity of chain ends. Further growth can be occur through addition of other low-molecular-weight species and monomer to cyclic species to generate particles and by aggregation of particles to create chains and networks (C. J. Brinker, 1994; Iler, 1979).

The particle growth above about pH 7 is discriminated from that below pH 7 by at least due to following proposed two factors:

1) Above pH 7, particle aggregation is unlikely due to the significant surface charge of the particles. In contrast, near the IEP (pH 1-3) particles growth and aggregation processes can be occur simultaneously due to the zero electrostatic particle repulsion.

2) Growth of primary particles occurred due to the greater solubility and the greater size dependence of silica above pH 7, as explained by the Ostwald ripening mechanism. Ostwald ripening mechanism explain the growth process as smaller and more soluble particles dissolve and reprecipitate on larger. Growth ends when the solubility difference between the smallest and largest particles becomes insignificant.

Above pH 7, according to the Ostwald ripening mechanism particle growth until the particles are diameter range of 5-10 nm, occurs at room temperature and at higher temperatures growth continues to larger sizes due to the enhanced silica solubility. However, at lower pH values, growth until the particles are 2-4 nm in diameter. (C. J. Brinker & Scherer, 2013).

It has been observed that Polymerization below pH 2, gel time is increased if polymerization is less than pH 2. The polymerization rate is proportional to (H^+). According to the proposed mechanism for acid-catalyzed polymerization involves a siliconium ion intermediate ($\equiv Si^+$) (C. J. Brinker & Scherer, 2013).

$$\equiv Si\text{-}OH + H_3O^+ \longrightarrow \equiv Si^+ + 2H_2O \quad (4)$$

$$\equiv Si^+ + HO\text{-}Si \longrightarrow \equiv Si\text{-}O\text{-}Si\equiv + H^+ \quad (5)$$

The solubility of silica particles below pH 2 is quite low in the absence of fluoride ion (C. J. Brinker & Scherer, 2013). At moderate acidities (pH 0-2) the silicate species are not highly ionized. Therefore, formation and aggregation of primary particles occur simultaneously, and contribution of Ostwald ripening is low to the growth after the particle size exceed 2 nm. Hence gel networks are made out of exceedingly small primary particles as illustrated in Figure 2.8. In this study, pH value of aqueous colloidal system was maintained below pH 2 to inhibit the effect of Ostwald ripening and keep the particles in nano meter range.

The most frequently used metal alkoxide precursors are tetraethoxysilane, $Si(OCH_2CH_3)_4$, abbreviated TEOS and Tetramethoxysilane, $Si(OCH_3)_4$ abbreviated TMOS, in sol-gel processing of silicate. Silica gels are most frequently created by hydrolyzing the alkoxides in the solution of alcohols with a mineral acid or base catalyst. The following three bimolecular nucleophilic reactions are proposed to explain the sol-gel process (C. J. Brinker, 1990).

$$\equiv Si\text{-}OH + RO\text{-}Si\equiv \longrightarrow \equiv Si\text{-}O\text{-}Si\equiv + ROH \quad (6)$$

$$\equiv Si\text{-}OR + H_2O \longrightarrow \equiv Si\text{-}OH + ROH \quad (7)$$

$$\equiv Si\text{-}OH + HO\text{-}Si\equiv \longrightarrow \equiv Si\text{-}O\text{-}Si\equiv + H_2O \quad (8)$$

The hydrolysis reaction replaces alkoxide groups with hydroxyl groups. Consequent condensation reactions involving the silanol groups produce siloxane bonds plus the by-products alcohol, (equation 6) or water, (equation 7).The reverse of hydrolysis is esterification, in which hydroxyl groups are replaced with alkoxides. The reverse of condensation is siloxane bond alcoholysis, (equation 6) or hydrolysis, (equation 7).

The hydrolysis reaction appears to be specific acid or base catalyzed (C. Brinker, 1988; McNeil, DiCaprio, Walsh, & Pratt, 1980). Acid catalysts protonate the alkoxide group, creating a better leaving group (ROH) and escaping the necessity for proton transfer in the transition state. Base catalysts dissociate water, producing a stronger nucleophile (OH^-) (Voronkov, IUzhelevsk'ii, & Mileshkevich, 1978). The condensation reaction depends on the acidity of the silica reactants. Acidic silanols are deprotonated; strong nucleophiles, =SiO~, are created at above pH 2, while weakly acidic silanols or ethoxides are protonated, thus good leaving groups (H_2O or ROH) are formed at below pH 2, and the necessity of charge transfer in the transition state is avoided. The hydrolysis rate of siloxane bonds upsurges at above pH 4 and at very low pH values (Iler, 1979). Similar behavior could be expected for alcoholysis reactions of siloxane bonds. The esterification of silanols is reported to proceed much faster under acid-catalyzed conditions.

According to the Iler's recommendation that siloxane networks might be achieved under conditions where depolymerization is least likely to occur. Siloxane bonds cannot be hydrolyzed once they are formed due to the irreversible reaction of

condensation. The solubility of silica is greatly reduced when water is replaced by high amount of methanol and low amount of water mixture (Iler, 1979). Consequently Iler's hypothesis might be recognized under conditions in which silicon alkoxides are hydrolyzed with small amounts of water especially below pH 7, at which the solubility and the dissolution rate are minimized.

2.2.4.2 Theory for synthesis of nanosilica

The formation of nanosilica particles can be separated into two stages: nucleation and growth. Two models have been suggested to describe the growth stage such as monomer addition (Matsoukas & Gulari, 1988, 1989) and controlled aggregation (Bogush, Tracy, & Zukoski, 1988; Bogush & Zukoski, 1991). This growth stage is the main phenomena to control the particles size in nano scale. The monomer addition model defines that, initial burst of nucleation occurs followed by particle growth through the addition of hydrolyzed monomers and nucleation is not continuously occurred. By contrast, the aggregation model explains that the nucleation occurs continuously throughout the reaction and the resulting nuclei (primary particles) will aggregate together to form dimmer, trimmer, and larger particles (secondary particles) as mentioned in Figure 2.8. Both models clue to the formation of either spherical or gel network depending on the reaction conditions.

2.3 Nanocomposite

Polymeric nanocomposites signify a novel class of composite materials that usually display superior properties than traditional micro composites in terms of mechanical properties, thermal and dimensional stability, gas permeability, fire and chemical resistance, optical and electrical properties, etc., at lower loading levels (Alexandre & Dubois, 2000; Gojny, Wichmann, Köpke, Fiedler, & Schulte, 2004).

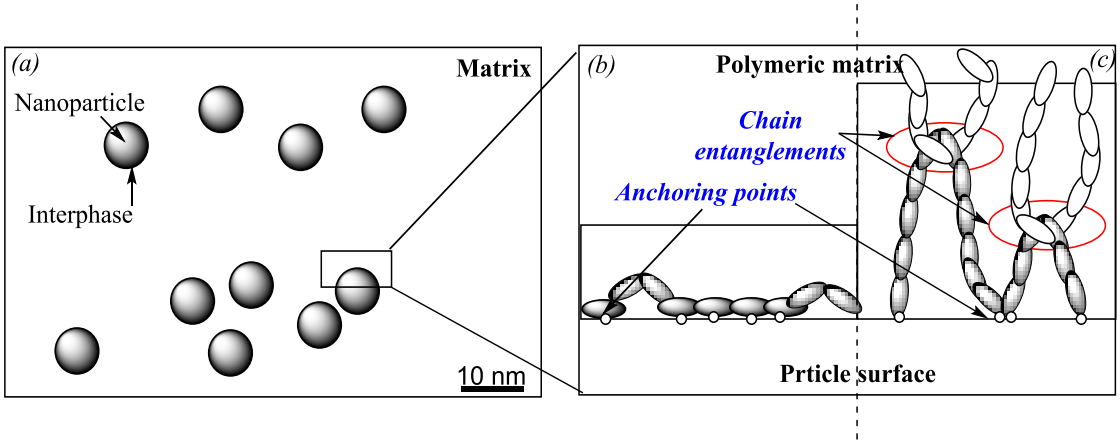

Figure 2.9: Schematic representation of the interphase in a polymer nanocomposite (Rallini & Kenny, 2017)

2.4 Filler surface modification

Most inorganic particulate fillers have poor compatibility with hydrocarbon polymers due to their polar in nature. The poor compatibility nature between inorganic fillers and organic polymers can arise number of processing problems such as poor dispersion, long wetting times and high viscosities, and poor mechanical properties. To overcome the above mentioned problem surface modification has been introduced as a very important weapon in compounding.

Two main classes of filler surface modifiers can be recognized: coupling and non-coupling, are illustrated in Figure 2.10.

The non-coupling surface modifiers has a strong interaction with the filler surface. Therefore, these modifiers are not compatible with the polymer matrix. Fatty acid treatments are typical of this class of modifier (Rothon, 2002).

The coupling surface modifiers has a strong interaction with both the filler phase and the polymer phase. The examples of this category are functionalised polymers and organosilanes (Rothon, 2002).

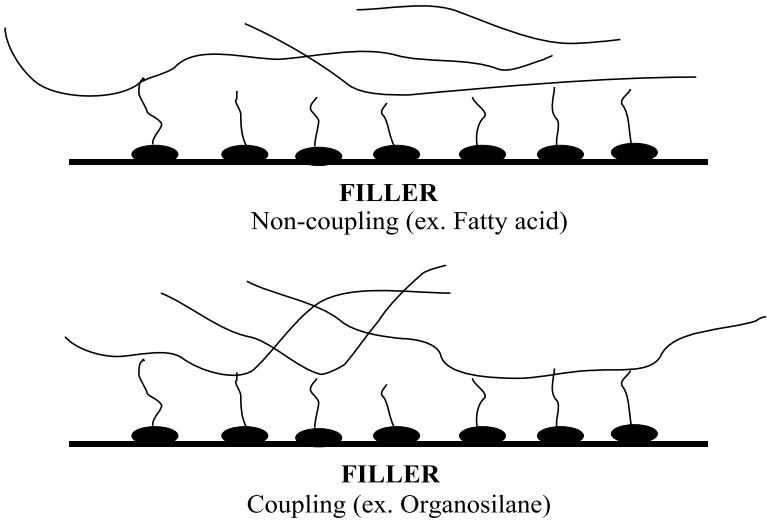

Figure 2.10: The two main types of filler surface modifiers (Rothon, 2002)

2.4.1 Role of surface modifiers in present investigation

In this study, the selected surface modifiers play a dual role. One as a capping agent which helps to prevent particle aggregation, due to surfactant adsorption layer on the particles surface and the other as a coupling agent, to confer compatibility between organic polymer matrix and inorganic filler matrix in lattices.

The aqueous colloidal synthetic approach becomes an attractive pathway due to its simplicity and affordability for aqueous synthesis. In these processes, a surface modifier is critically needed as a capping agent (Nguyen, 2013). The metal oxides would form a continuous phase in the absence of capping agent, instead of discrete nanoparticles. In colloid science, it is well-accepted that the capping agent has ability to prevent particle aggregation, via adsorption of capping layer on to the particle surfaces. The selective adsorption of capping agent has been employed to control the growth direction, thus particles shape to non-spherical forms, such as disk or rod (Yin & Alivisatos, 2005). These evidence confirm that the capping layer formed during particle growth is capable of intensifying the reaction kinetics. Yet, the role of capping agent on particle growth remains unquantified.

In general, particle formation in solution-based synthesis process involves two stages: nucleation and growth. Surface modifiers, which can be termed as “capping

agent" would have ability to influence both stages. Capping agent micelles can form a template for nucleation. The influence of capping agent length on the micelles size has been quantitatively verified (Oliver et al., 2013). Hence, length of capping agent can influence critical nuclei size, which can be predicted by the classical nucleation theory (Erdemir, Lee, & Myerson, 2009).

As mentioned earlier, inorganic particles in nano scale have been successively incorporated to polymers to develop their tribological performance and toughness. Nano size inorganic particles tend to agglomerate easily due to their high surface energy. Therefore, it is very difficult to obtain well disperse nanoparticles in polymer phase. The dispersion in water or other liquid environments of nanosilica depends on its functional groups presence on the surface. Unmodified silica typically contains silanol groups formed via the reaction between molecular water and siloxanes during manufacturing. The presence of -OH groups on silica surface makes the silica hydrophilic. The main disadvantage of using hydrophilic particles is that the -OH groups form hydrogen bonds between two neighboring particles leading to the formation of strong aggregates. As a consequence, if added in a polymeric matrix, in which the interaction polymer/filler become weaker than the interparticle forces, the dispersion could be very difficult (Jasso-Gastinel & Kenny, 2016).

In addition, hydrophilic filler and hydrophobic polymers are not compatible in nature, due to the poor interfacial interaction. Incorporation of nano-size fillers into polymer is still the most convenient way for preparation of polymeric nano-composites. In case of polymer composites, significance of surface modification of the nanosilica has already verified to minimize filler/filler interaction and to enhance filler/ polymer interaction. With the recent developments in nanoscience and nanotechnology, the correlation of polymer nanocomposites properties with surface modification of nanoparticles is also becoming a point of great interests. Therefore, surface modifier could be introduced as a coupling agent for both filler and polymer. The hydrophilic behavior can be also used to modify the particles by the surface adsorption of surfactants or short chain polymers using the electrostatic interaction and the hydrogen bonds (Jasso-Gastinel & Kenny, 2016).

In simply, surface modification of inorganic fillers means introduction of organic coatings onto the filler surface, which can be carried out by developing physical and chemical interactions between the fillers and the modifiers.

2.4.2 Types of surface modifiers

Surface modifiers can be classified as synthetic and natural surface modifiers. In present study both synthetic and natural surface modifiers have been used.

2.4.2.1 Synthetic polymers

Silane is a bifunctional compound which is well studied and developed to the commercial stage to implement as a coupling agent to enhance the reinforcing efficiency of silica. It is consist of two functionally active end groups, i.e., the readily hydrolysable alkoxy group and the organo-functional group. The alkoxy group can chemically react with the silanol groups on silica surface to obtain stable siloxane linkages whereas the organo-functional group, which is relatively non-polar, is more compatible with rubbers and also can participate in the sulfur vulcanization to form chemical linkages with rubbers. As a consequence, silane act as a coupling agent creating a bridge between silica filler and rubber matrix to improve the filler-rubber interaction and, thus, give a remarkable development in properties of silica filler filled compounds.

Silane coupling agents consist with chemical structure R (4-n)-Si-$(R´X)_n$ (n = 1,2) where R is alkoxy, X represents an organofunctionality, and R´ is an alkyl bridge (or alkyl spacer) connecting the silicon atom and the organofunctionality. These organofunctionalities of silanes are typically amino, mercapto, glycidoxy, vinyl, or methacryloxy groups (Xie, Hill, Xiao, Militz, & Mai, 2010). Many cotemporary researches have been discovered on role of silane as a coupling agent in the non-functionally active rubbers such as SBR and NR to improve the reinforcing efficiency of silica. (Sae-oui, Sirisinha, Thepsuwan, & Hatthapanit, 2006). Various silane structures have been tested for coupling of silica reinforcements and organic polymer matrices.

In this study, polymethacrylic acid (PMAA) homopolymer and polymethacrylic acid-ethyl hexyl acrylate (P(MAA-EHA)) copolymer have been used as synthetic surface modifiers.

To act as a coupling agent, surface modifiers should contain both hydrophilic and hydrophobic segments. According to the structure of PMAA: it consists both hydrophilic and hydrophobic segments where hydrophilic segments react with surface of silica particles and hydrophobic segments reacts with polymer matrix.

The same in true for the P(MAA-EHA) copolymer as a surface modifier.

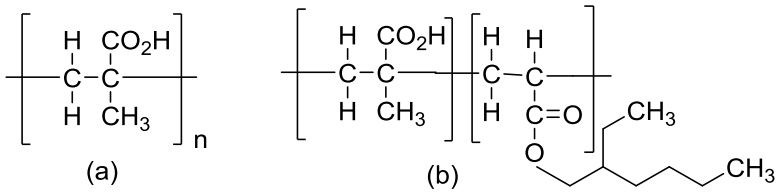

Figure 2.11: Structure of (a) PMAA homopolymer and (b) P(MAA-EHA) copolymer

2.4.2.2 NPs

NPs from renewable natural resources have become increasingly interesting because of their better biocompatibility, biodegradability, nontoxicity, readily availability and low cost of some natural polymers. NPs mainly can be classified as protein-origin polymers and polysaccharidic polymers. NPs such as gelatin, chitin, chitosan, cellulose are suitable candidates as surface modifiers for silica and they contain poly-functional groups which can react with hydroxyl groups on silica surface retarding the aggregation of silica particles (Malafaya, Silva, & Reis, 2007).

2.4.2.2.1 Protein-origin polymers

In this study, the consideration is directed in two protein-based polymers widely applied in research works for surface modification, namely collagen and gelatin. In a molecular perspective, proteins may be considered as polymer structures composed by 20 distinct amino acids linked by amide (or peptide) bonds (Malafaya et al., 2007).

Amino acids are the building blocks of polypeptides and proteins, which consist of a central carbon linked to an amine group, a carboxyl group, a hydrogen atom, and a side chain (R groups). R groups can be classified as non-polar groups, uncharged polar groups or charged polar groups, and their distribution along the protein backbone renders proteins with distinct characteristics (Malafaya et al., 2007).

The hydrophobicity/hydrophilicity ratio of the side-chains plays an important role in the physicochemical behavior of polypeptide chains as surface modifiers for silica and their folding into three-dimensional structures. The amino group in protein can react with surface silanol groups of nanosilica particles and can act as a terminator to inhibit further growth of particle size (See Figure 2.12). Hence protein constituents can employ as surface modifier for nanosilica particles which can play both roles: the capping agent as a chain terminator and the surfactant as a bridge between inorganic filler and organic matrix in rubber lattices. Collagen and gelatin were selected as suitable natural surface modifiers for silica.

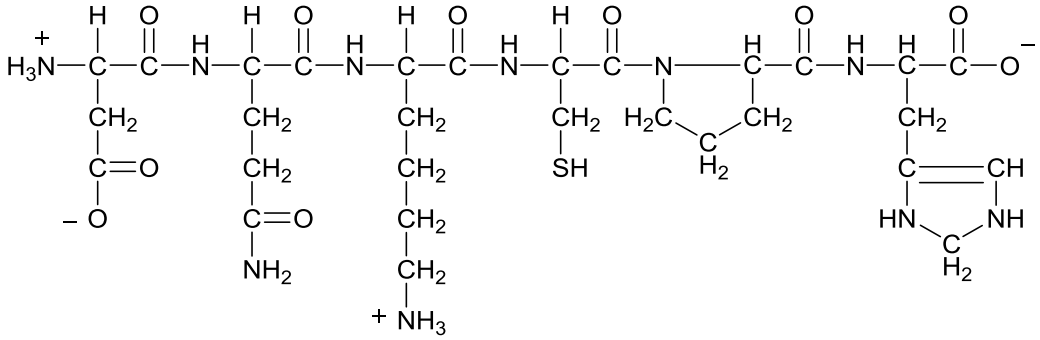

Figure 2.12: Structure of gelatin

2.4.2.2.2 Polysaccharide polymers

Polysaccharides are a class of biopolymers constituted by simple sugar monomers. The monomers (monosaccharides) are linked together by O-glycosidic bonds that can be made to any of the hydroxyl groups of a monosaccharide, conferring polysaccharides the ability to form both linear and branched polymers (Nishinari & Takahashi, 2003). Two types polysaccharide polymers; cellulose and chitosan were used in this study as surface modifiers (See Figures 2.13 and 2.14). Polysaccharide polymers can also play dual role as a surface modifier: as a capping agent at the stage

of nanoparticle synthesis and as a coupling agent between inorganic and organic faces at the stage of latex compounding.

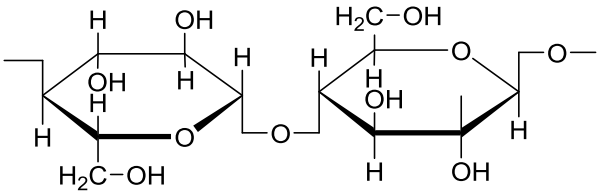

Figure 2.13: Structure of cellulose

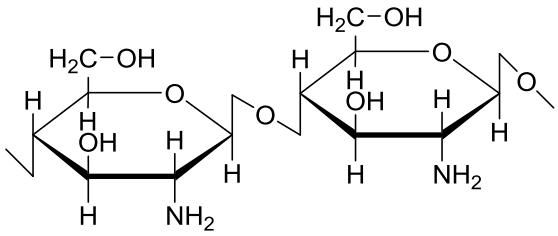

Figure 2.14: Structure of chitosan

2.4.3 Methods for silica surface modification

Two diverse approaches can be identified, filler pre-coating and the in situ process in which the matrix polymer is in essence used as the coating solvent and coating takes place during compounding. A comparison between two modification processes is given in Table 2.1.

Table 2.1: A comparison of the pre-coating and in situ methods of filler treatment (Rothon, 2002)

In-situ	Pre-coating
Usually less expensive, but may require higher additive levels	Expensive
Surface reaction is very much at the mercy of processing conditions, including competition from other additives	Surface reaction and coverage can be strictly controlled
Opportunity to treat fresh surface generated during compounding	Unable to treat fresh surface generated during compounding.
Superior formulation freedom	Limited flexibility for adjusting the formulation
Residual, unreacted, additive more	No interference from other compounding

likely to be present and may cause problems	additives
Better chance for coating/matrix interpenetration	Interpenetration of coating and matrix may be limited

In the present investigation the in-situ process for surface modification of nanosilica particles was followed.

2.5 Previous activities of synthesis of silica particles using metal alkoxides

A pioneering work for synthesis of spherical and monodispersed nanosilica done by Stöber *et al.* (1968) (Stöber, Fink, & Bohn, 1968), which continuously applied method to date. In this process, tetraethylorthosilicates (TEOS) are combined in a mixture of water, alcohol, and ammonia and agitated to form silica particles. The particle size depends on the concentration of the silicate additives and solvents. Without templates this method can be implemented to form solid particles.

The kinetics and characterization of Stöber process have been numerously investigated in order to precisely control particle shape, size, and uniformity. The simple synthesis is used in the formation of nanosilica particles through the hydrolysis of TEOS, in the presence of ammonia in ethanol.

Bogush *et al.* (1988) (Bogush et al., 1988) acquired monodispersed silica particles having sizes ranging from 40 nm to several micrometers by controlled hydrolysis of TEOS in alcohol medium, followed by condensation of silicic acid.

Pontoni *et al.* (2002) (Pontoni, Narayanan, & Rennie, 2002) carried out small angle X-ray scattering (SAXS) experiments and revealed that the most likely growth mechanism is coalescence which is diffusion controlled after the initial nucleation phase.

Green *et al.* (2003) (Green et al., 2003)carried out a study using dynamic light scattering, 29Si NMR and SAXS for the characterization of nanosilica particles. All of which confirmed that through the Stöber method there was continuous nucleation in conjunction with controlled aggregation of primary particles.

2.6 Synthesis of silica particles using sodium metasilicate

Das *et al.* (2009) (Das, Parida, & Mishra, 2009) reported a highly cost effective method for the preparation of mesoporous silica spheres with core shell structure. Sodium silicate used as the silica precursor together with cetyltrimethyl ammonium bromide (CTAB) and methanol as the surfactant and the co-surfactant respectively. Mesoporous silica spheres with core shell structure were isolated from the template by dissolutions or/and activation at higher temperature. The methanol to CTAB molar ratio of 8.5:1 were given the best results. Particles are spherical in nature and have very large surface area (~589–1044 m^2/g), pore volume (~0.98–1.41 cm^3/g), and ordered pore structure.

Sarawade *et al.* (2009) (Sarawade, Kim, Hilonga, & Kim, 2010) studied on preparation of hydrophobic mesoporous silica powder using sodium silicate as the silica precursor and trimethylchlorosilane (TMCS) as the surface modifier. The effects of the volume percentage of TMCS, on the physicochemical properties of the silica powder were investigated. Sodium silicate, sulfuric acid, TMCS and n-hexane were used.

Sadeghi *et al.* (2013) (Sadeghi, Dorodian, & Rezaei, 2013) investigated about the factors affecting on the precipitation process of amorphous silicon dioxide using sodium metasilicate aqueous solution and sulfuric acid. In this study authors investigated the effect of addition of sodium dodecyl sulfate-SDS (anionic surfactant) on particle size, size distribution and degree of agglomeration of the precipitated silica. The particle size of precipitated silica decreased with increasing of sodium metasilicate concentration at different concentrations of SDS. According to the results obtained, the effect of sodium metasilicate concentration on silica particle size is great. The average particle size of precipitated silica decreased from 1030 nm to 170 nm with increasing concentration of sodium metasilicate from 10 to 20 (wt%) at 100 ppm SDS, and from 850 nm to 74 nm at 200 ppm SDS. The particle size was changed with the nucleation and growth rates of silica particles. For instance, in this study increasing sodium metasilicate concentration; upsurge the nucleation rate resulting fine silica particles.

Rida *et al.* (2014) (Rida & Harb, 2014) worked on synthesis of nanosilica particles according to Stőber method using cost effective template. Sodium silicate as silica precursor, hydrochloric acid and cationic surfactants such as cetyltrimethylammonium bromide (CTAB) and dodecyltrimethylammonium bromide (DTAB) were used. The average particle size of nanosilica was finely tuned in the range 148–212 nm by altering the chain length of cationic surfactant. Amorphous nanosilica particles were prepared using aqueous sodium silicate as a cheap source of silica and HCl as a catalyst. The particle size of nanosilica was controlled using CTAB (148 nm) and DTAB (212 nm), as cationic surfactants. The particle size decreased as the chain length of the surfactants was increased. Both, sodium silicate and HCl materials are available in the market at reasonable price as compared to the other raw materials used for silica synthesis. The investigations performed in this work have indicated that there is a great scope for their exploitation as raw materials for the production of amorphous nanosilica powder on industrial scale.

2.7 Reinforcement of latex by organic/inorganic fillers

Jarnthong *et al.* (2010) (Jarnthong, Peng, Nakason, & Lopattananon, 2010) have reported reinforcement of Epoxidized natural rubber (ENR) with surface modified nanosilica particles (SiO_2). Nanosilica particles were pretreated with 3-aminopropyltriethoxysilane (APS) and 3-methacryloxypropyltrimethoxysilane (MPS). The dispersion of treated nanosilica in ENR matrix, was better than that of the untreated nanosilica in ENR matrix. Moreover, it was found that significant reinforcing effect in surface modified SiO_2 than the unmodified SiO_2. However, MPS modified nanosilica filled composites showed better interfacial interaction when compared with the APS modified nanosilica filled composites.

Ain *et al*. (2011) (Ain & Azura, 2011) studied the effects of different types of fillers and filler loadings on the properties of XNBR latex vulcanizates. They have found that silica, mica and carbon black (CB) had reinforcing effect on XNBR composites. They observed an increase of physical properties like tensile strength and tear strength up to silica filler loading of 15 phr followed by a decrease with higher filler loadings. They also observed homogeneous distributions of silica filler in rubber

matrix with certain degree of agglomeration of silica. According to the findings of this study, the best physical properties could be observed for CB. They proposed that higher interaction of filler-rubber is the result of high activity of CB and its oxidized surface. Carboxylic groups of the XNBR and reactive groups on the CB surface are believed to form chemical and physical bonds. Mica filler was also reported as a reinforcing filler for XNBR latex vulcanizates. However, the morphological observations reported by the researchers indicate that dispersion of the mica filler in the XNBR latex vulcanizates was very poor.

Luo *et al.* (2013) (Luo et al., 2013) studied about nanocomposite consists with poly(methyl methacrylate) modified core-shell nanosilica (SiO_2-PMMA) in PMMA-modified natural rubber matrix (NR-PMMA). The observations successfully confirmed that PMMA chains had properly grafted on the nanosilica surface, and better interaction between PMAA modified core-shell nanosilica and NR-PMMA latex. At low silica loading ($SiO_2 \leq$ 3 wt %) better distribution were observed through the NR matrix, while at high silica loading (5 wt% SiO_2), aggregation of nanosilica particles were observed. The final composite obtained improved ageing resistance compared with pure NR latex. Tensile strength of composite increased with increasing silica loading up to 0.5%wt. and then decrease with further addition of silica due the aggregation of silica particles.

Wang *et al.* (2014) (Wang et al., 2014) published a study on composite comprise with bacterial cellulose whisker (BCW) in XNBR latex matrix. Bacterial cellulose is naturally occurring substance from certain types of bacteria. At present, there are many novel methods to accelerate the growth of cellulose in laboratories as a large-scale. In this study, XNBR latex reinforced with BCW suspension. They proposed that BCW has rod-like nanofiber structure. Improved tensile strength, tear strength and Young's modulus were observed in BCW/XNBR vulcanizates compared with unfilled XNBR.

Nair *et al.* (2014) (Nair, Nair, & Joseph, 2014) reported same work on nanocomposite with varying amounts of nanokaolin in XNBR matrix. Sonication technique carried out to obtain homogenous dispersion of clay in rubber matrix.

Proper dispersion of nanoclay was obtained due to the partial exfoliation/intercalation of clay and better interaction of clay with the polar XNBR latex resulting nanokaolin as a good reinforcing filler in XNBR latex. Consequently, incorporating of nanokaolin enhanced the physical properties of the final nanocomposite.

Somaratne *et al.* (2014) (Somaratne, Liyanage, & Walpalage, 2014) studied surface modification of precipitated silica (Ultrasil VN_3) using hydrophilic polymers of which the hydrophilic groups interact with surface bound hydroxyl groups of silica. The modified silica was used to reinforce natural rubber latex. Uniform distribution of silica particles within rubber matrix was seen in films cast from modified silica incorporated natural rubber latex whereas a settled layer of filler was seen in unmodified filler added films. Influence of surface modification upon the reinforcement of natural rubber latex was confirmed by comparing the values of tensile and tear strengths of unmodified and modified filler added vulcanized films. Tear strength of all the films first increased, passed through a maximum and then decreased with the increase of filler loadings. The maximum values of both modified filler added films were nearly 50 % higher than that of unmodified filler in the range of 5-10 phr of filler loadings. The tensile strength of modified filler added films also showed a maximum at 5 phr of filler addition whilst that of unmodified filler added films was increased only slightly with the concentration of filler. However, the modified filler added films showed nearly 35 % increase at 5 phr compared that with the highest value of unmodified filler added films observed at 20 phr. It was suggested that uniform distribution of filler particles and the improvement in physical properties predict the better compatibility of modified silica with natural rubber latex via interfacial interactions.

Sala *et al.* (2014) (Sala et al., 2014) investigated the performance of surface modified nanosilica particles with 3-(trimethoxysilyl)propyl methacrylate(SiO_2-MPS) or enclosed with a polymeric shell obtained from reaction between divinylbenzene and styrene (SiO_2-Pol), in commercial XNBR. The hydrophobicity character of the modified nanosilica particles improved the interaction of nanosilica particles with XNBR macromolecules.

Ramasinghe *et al.* (2016) (Ramasinghe, Gannoruwa, & Liyanage, 2016) discovered suitability of NPs as coupling agents for silica filled XNBR latex vulcanizates. Cellulose, Gelatin Chitin and Chitosan were used as natural surface modifiers for this investigation. Surface modification of silica particles with natural polymers was carried out via in-situ surface modification process. Interactions between polar groups of silica and functional groups of natural polymers which obstruct the aggregation of silica particles were confirmed by FTIR spectroscopy. NPs like chitin and gelatin were found to be effective coupling agents for silica possibly, by discouraging filler/filler interactions while encouraging rubber/filler interactions.

CHAPTER 03

3 EXPERIMENTAL

3.1 Materials

A sample of XNBR latex (4% carboxylate content) obtained from Ansell Lanka (Pvt) Ltd. was used throughout the study. Nanosilica was obtained from Sigma Aldrich, USA. Sodium meta silicate (Research Lab, India), hydrochloric acid (37 %, Sigma Aldrich, USA), n-butanol (Research Lab, India), tetrahydrofuran (Research Lab, India), zinc oxide (Sigma Aldrich, USA), zinc diethyldithiocarbamate (ZDEC), potassium hydroxide (KOH), 35% (w/w) aqueous ammonia solution, antioxidant styrenated phenol, dispersing agent tamol (sodium salt of condensed naphthalene sulfonic acid), monomers; methacrylic acid and 2-ethylhexyl acrylate, a commercial grade of micro silica , gelatin, chitosan, collagen, & cellulose were obtained from local chemical suppliers and used without further purification. Deionized water was obtained from Thermo scientific smart2pure.

3.2 Methodology

3.2.1 Characterization of latex

3.2.1.1 pH of latex

pH of latex was measured at 28°C by using pH meter PL-700PV.

3.2.1.2 Dry rubber content of latex

A sample of latex was weighed accurately to three decimal points in a watch glass and dried in an oven maintained at 70 ° C until the weight of the residue became constant. Dry rubber content of latex was calculated as a percentage, according to the equation 9.

$$\text{Dry rubber content \%} = [(m_2-m_0)/(m_1-m_0)] \times 100 \quad (9)$$

Where, m_0 -weight of the empty watch glass

m_1 - weight of the watch glass with the latex sample

m_2 - weight of the watch glass with residue after drying

3.3 Synthesis of polymers

The homopolymer of methacrylic acid (PMAA) was synthesized by following the free radically initiated solution polymerization process. 0.25 g of dicumyl peroxide initiator and 25 g of methacrylic acid monomer were mixed together. 150 ml of xylene solvent was transferred to a five neck reaction flask and heated up to 110 °C in a heating mantle. The initiator and monomer mixture, added slowly over a period 20 min to the xylene in the reaction vessel at 110 °C while constantly stirring and bubbling nitrogen gas to the sealed vessel. The reaction was allowed to continue for 3 h under the same conditions and resultant polymer, which was separated as a precipitate was isolated by filtration followed by vacuum drying at 60 ºC for 10 h before use.

A copolymer of methacrylic acid (MAA) and 2-ethylhexyl acrylate (EHA) (P(MAA-EHA)) (60:40) was also synthesized by the same procedure using a mixture of 15 g of methacrylic acid and 10 g of 2-ethyl hexyl acrylate and the reaction was allowed to continue for 6 h under the same conditions as described above. Figure 3.1 shows a sketch diagram of assembled polymerization set up.

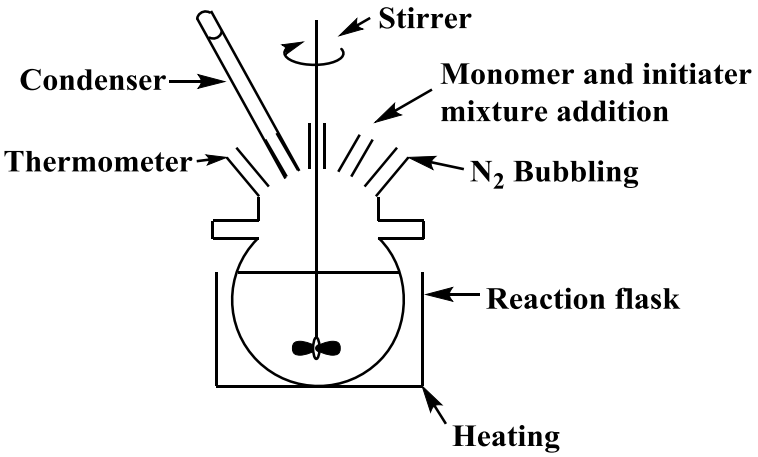

Figure 3.1: Diagram of polymerization setup

3.4 Synthesis of surface modified nanosilica particles

Synthesis of surface modified nanosilica particles is a condensation like polymerization in which the hydrolysis product of sodium metasilicate acts as monomer and PMAA and P(MAA-EHA) surface modifiers act as chain terminators.

Sodium metasilicate is hydrolyzed in the presence of hydrochloric acid to form silicic acid (See equation 10). Then the condensation like polymerization of silicic acid into three dimensional network occurs where Si and O are joined to each other to form the three-dimensional structures (See Figure 3.2). Large numbers of hydroxyls are left on the surface of silica particles. In the presence of a surface modifier, soon as particles are formed the hydroxyl groups on the silica surface react with the –OH group of the surface modifier. The surface modifier substitutes the portion of active group of nanosilica and prevents continuous growing and agglomerating of silica particles simultaneously (See Figure 3.3). These two reactions are competitive reactions. Acrylic polymer capped nanosilica particles can be obtained through the systematic monitoring of reaction parameters (Ostwald, 1900).

The following reaction scheme is proposed for the formation of nanosilica particles in the presence of PMAA;

The nanosilica particles are obtained via the following reactions:

$$Na_2SiO_3 + 2HCl \rightarrow SiO_2 + 2NaCl + H_2O \qquad (10)$$

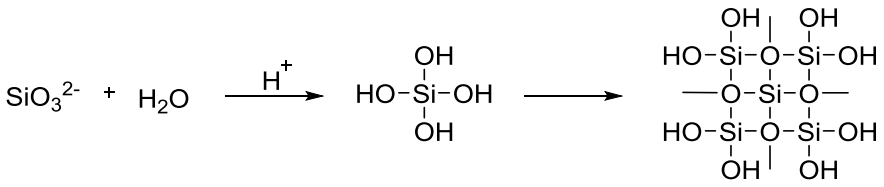

Figure 3.2: Hydrolysis reaction of sodium metasilicate

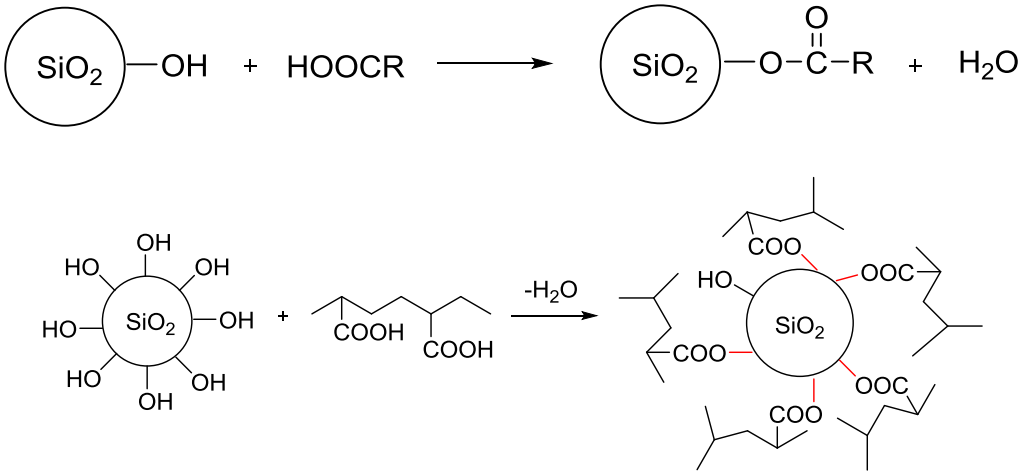

Figure 3.3: Reaction Scheme of anchored surface modifier on nanosilica particles

The acrylic polymer concentration, required for optimization of formation of nanosilica was investigated. The experiments were performed by varying its concentration from 0 to 2.5 wt. %, keeping all the other reaction parameters constant.

A range of modified nanosilica was synthesized using acrylic polymers as well as using NPs. These modified silica, a commercial sample of nanosilica and a sample of micro silica were used in present study. Each silica sample was given an identification code of modification so that their states of modification was immediately apparent i.e. Table 3.1.

Table 3.1: Details of identification codes of silica samples

Constituents									Code
PMAA	P(MAA-EHA)	CE	CO	CHO	GE	Synthesized nanosilica	Commercial nanosilica	Micro silica	
-	-	-	-	-	-	100	-	-	UMNS
-	-	-	-	-	-	-	100	-	*UMNS
-	-	-	-	-	-	-	-	100	VN_3
1	-	-	-	-	-	100	-	-	$MNS_{M\ 1}$
1.5	-	-	-	-	-	100	-	-	$MNS_{M\ 1.5}$
2	-	-	-	-	-	100	-	-	$MNS_{M\ 2}$
2.5	-	-	-	-	-	100	-	-	$MNS_{M\ 2.5}$
-	1	-	-	-	-	100	-	-	$MNS_{M/E\ 1}$
-	1.5	-	-	-	-	100	-	-	$MNS_{MA/E1.5}$
-	2	-	-	-	-	100	-	-	$MNS_{M/E2}$
-	2.5	-	-	-	-	100	-	-	$MNS_{M/E\ 2.5}$
2	-	-	-	-	-	-	100	-	$*MNS_{M\ 2}$
-	1.5	-	-	-	-	-	100	-	$*MNS_{M/E\ 1.5}$
-	-	2	-	-	-	-	100	-	$*MNS_{CE2}$
-	-	-	2	-	-	-	100	-	$*MNS_{CO2}$
-	-	-	-	2	-	-	100	-	$*MNS_{CHO2}$
-	-	-	-	-	2	-	100	-	$*MNS_{GE2}$
-	-	2	-	-	-	-	-	100	MMS_{CE2}
-	-	-	2	-	-	-	-	100	MMS_{CO2}
-	-	-	-	2	-	-	-	100	MMS_{CHO2}
-	-	-	-	-	2	-	-	100	MMS_{GE2}

* For commercial silica samples

PMAA	Homopolymer of methacrylic acid
P(MAA-EHA)	Copolymer of methacrylic acid and 2-ethylhexyl acrylate
CE	Cellulose
CO	Collagen
CHO	Chitosan
GE	Gelatin

3.4.1 Trial-01

Nanosilica particles were prepared by drop-wise addition (~2 drops/s) of 2.5 % (w/v) HCl into a diluted sodium metasilicate solution with constant stirring for 500 rpm at 60 °C until a cloudy, viscous gel was formed. Then silica gel was stirred continuously for 500 rpm at 60 °C with drop-wise addition (~2 drops/s) of 2 % (w/v) HF, until a clear solution obtained. The solution was then filtered using Whatman filter paper No.1. The filtrate was then evaporated to dryness, resultant white powder was thoroughly washed with deionized water and dried in an oven at 80 °C. The process was repeated for 4 to 5 times. The product was then dried in a vacuum oven at 120 °C for 24 h (Patel & Patel, 2014).

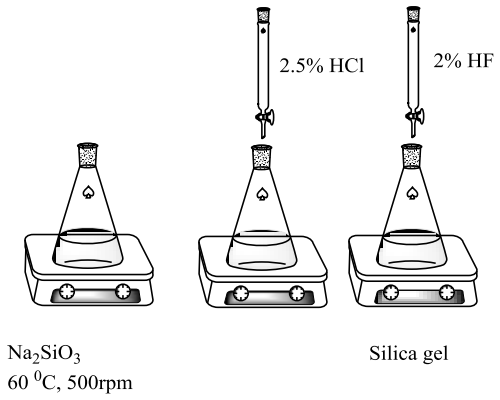

Figure 3.4: Schematic diagram of Trial-01

3.4.2 Trial-02

In the second method a mixture was prepared with 33 % (w/v) ammonia and 95 % (w/v) ethanol (A/E) in equal amounts, i.e., 30 ml each. 0.85 g of poly ethylene glycol

(PEG) solid was added to the A/E mixture with constant stirring at a speed of 500 rpm at 60 °C (Stanley & Nesaraj, 2014). As a precursor medium of silica, 0.5 ml sodium metasilicate aqueous solution (7 % w/w) was mixed with 7 ml of distilled water and added drop-wise to A/E/PEG mixture while maintaining the mixture temperature at 60 ° C. After aging for 1 h, the mixture was centrifuged (4000 rpm, 20 min) and the residue was washed with distilled water and finally dried in vacuum oven at 120 °C for 24 h to obtain nanosilica particles (Zulfiqar, Subhani, & Husain, 2016).

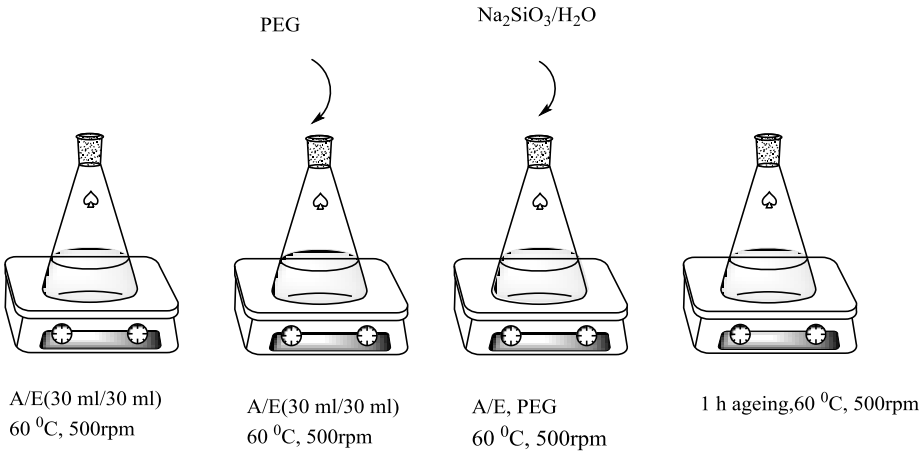

Figure 3.5: Schematic diagram of Trial-02

3.4.3 Trial-03

The procedure followed in Trial-02 was repeated for a mixture containing different amounts of ammonia and ethanol i.e. A-90 ml and E-30 ml, with 0.85 g of PEG solid (Zulfiqar et al., 2016).

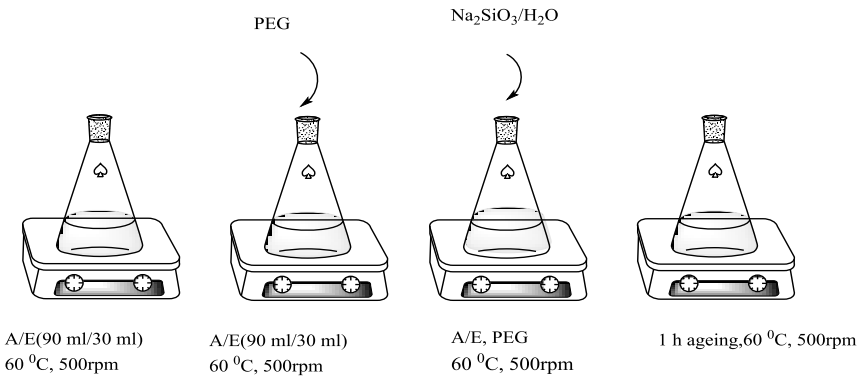

Figure 3.6: Schematic diagram of Trial-03

3.4.4 Trial-04

1.4 g of precipitated silica (VN_3) was dissolved in 50 ml of 2.0 M NaOH by continuous stirring for 2 h at 90 ° C on a magnetic stirrer. Then 2.5 % (w/v) HCl was added drop-wise to the solution to adjust the pH to 2 with stirring at a constant speed of 500 rpm at 60 °C until a cloudy, viscous gel was formed. Resultant silica gel was then washed repeatedly with warm deionized water until the filtrate became alkali free. The precipitate was separated by centrifugation (4000 rpm for 20 min). The residue was dried at 60 ºC in a vacuum oven for 24 h in order to obtain nanosilica.

3.4.5 Trial-05

1.4 g of precipitated silica was dissolved in 50 ml of 2.0 M NaOH by continuous stirring for 2 h at 90 °C on a magnetic stirrer. 0.6 g of poly ethylene glycol (PEG) solid was added to the solution with constant stirring at a speed of 500 rpm at 60 °C. Then 2.5 % (w/v) HCl was added drop-wise to the solution to adjust the pH to 2 with stirring at a constant speed of 500 rpm at 60 °C until a cloudy, viscous gel was formed. Resultant silica gel was then washed repeatedly with warm deionized water until the filtrate became alkali free. The precipitate was separated by centrifugation (4000 rpm for 20 min). The residue was dried at 60 ºC in a vacuum oven for 24 h in order to obtain nanosilica.

3.4.6 Trial-06

An acrylic type modifier (1, 1.5, 2, 2.5 wt.% of sodium metasilicate) was dissolved in the sodium metasilicate solution (7%w/w). Subsequently, 1 M HCl solution was added with constant stirring into the solution in order to initiate the hydrolysis-condensation reaction at 500 rpm and at 60 °C until a cloudy, viscous gel was formed at pH 1-2. The resultant gel mixture was stirred continuously at a speed of 500 rpm for a period of 2 h and the temperature was maintained at 70 °C. After completion of the reaction, the resultant slurry was kept at room temperature for 24 h. From this point onwards the extraction procedure for homopolymer modified silica was different from that of copolymer modified silica. The homopolymer modified

nanosilica particles were extracted into n-butanol with the aid of a separating funnel (See Figure 3.8). Subsequently isolation of surface modified silica particles from the solvent was done by drying in a vacuum oven at 120 °C for 8 h. The extraction of copolymer surface modified silica particles was performed using tetrahydrofuran as the extraction medium (See Figure 3.9) and the isolation of modified silica from the solvent was done by drying at 70 °C under vacuum for 8 h (Rafiee, Shahebrahimi, Feyzi, & Shaterzadeh, 2012).

The above described Trials 01-05 were not successful in producing nanosilica. Trial 06 was found to be successful in producing modified nanosilica. Hence the synthesis of surface modified nanosilica were continued using the method described in Trial-06 after optimizing process parameters.

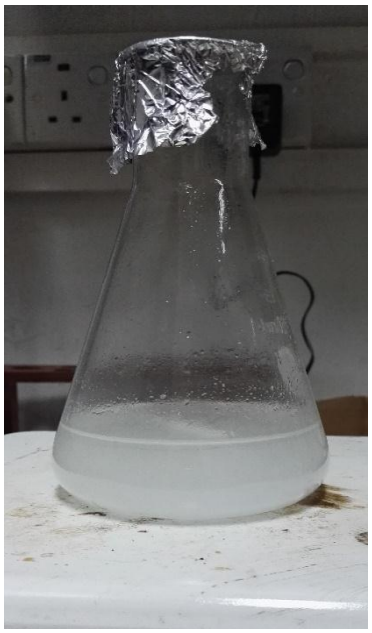

Figure 3.7: Photograph of a dispersion of nanosilica particles

The unmodified nanosilica was synthesized using the sodium metasilicate solution (7%w/w). 1 M HCl solution was added with constant stirring into the solution in order to initiate the hydrolysis-condensation reaction at 500 rpm and at 60 °C until a cloudy, viscous gel was formed at pH 1-2. The resultant gel mixture was stirred continuously at a speed of 500 rpm for a period of 2 h and the temperature was

maintained at 70 °C. After completion of the reaction, the resultant slurry was kept at room temperature for 24 h. Then the precipitate was separated by centrifugation (4000 rpm for 20 min). The residue was dried at 60 ºC in a vacuum oven for 24 h in order to obtain nanosilica.

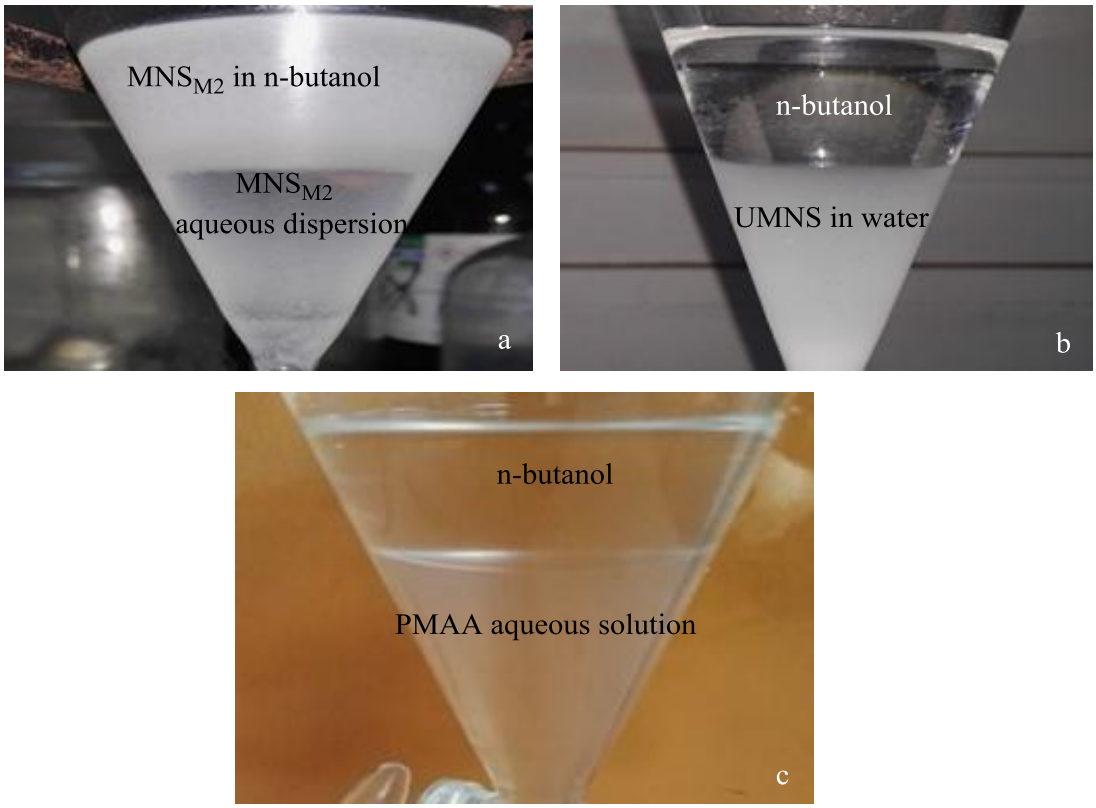

Figure 3.8: Extraction of PMAA modified nanosilica particles (a) MNS$_{M2}$ in n-butanol and MNS$_{M2}$ aqueous dispersion, (b) n-butanol solvent layer and UMNS in water, (c) n-butanol solvent layer and PMAA aqueous solution

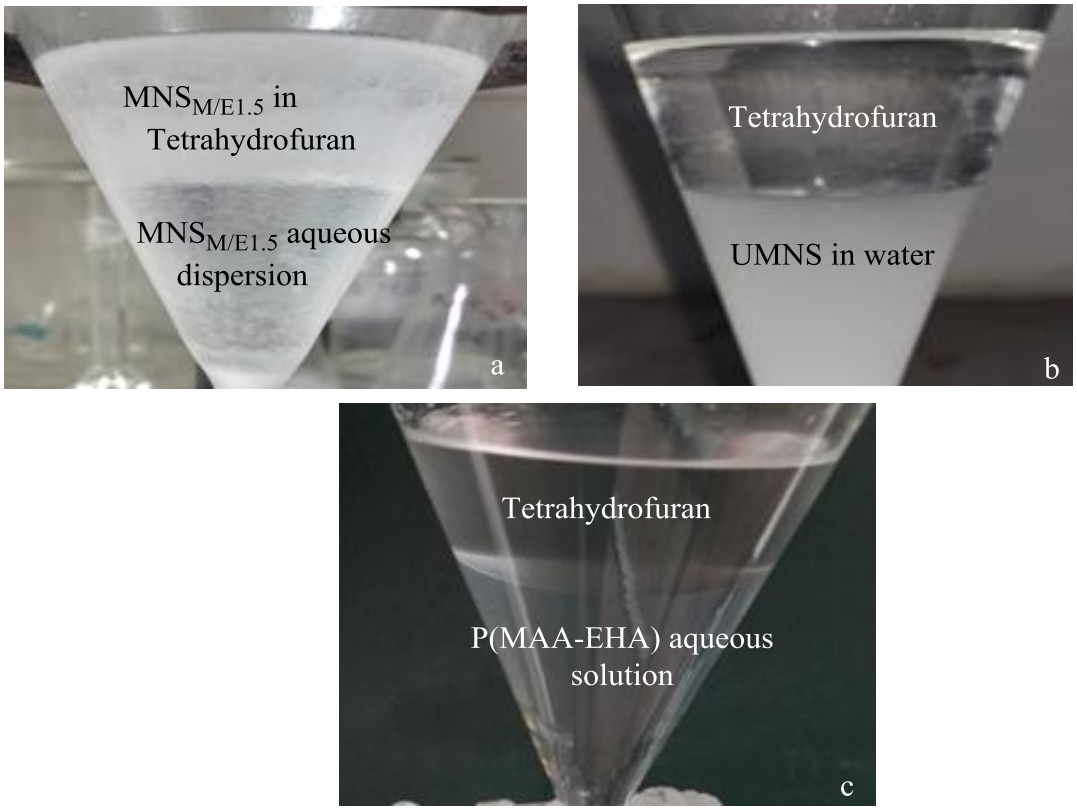

Figure 3.9: Extraction of P(MAA-EHA) copolymer modified nanosilica particles (a) $MNS_{M/E1.5}$ in tetrahydrofuran and $MNS_{M/E1.5}$ aqueous dispersion, (b) tetrahydrofuran solvent layer and UMNS in water, (c) tetrahydrofuran solvent layer and P(MAA-EHA) copolymer aqueous solution

3.5 Characterization of synthesized unmodified and acrylic polymer modified nanosilica

3.5.1 Fourier transform infrared (FTIR) spectroscopy

FTIR spectra of KBr pellets prepared for the unmodified and acrylic modified silica particles were carried out using ALPHA FTIR spectrophotometer in 500-4000 cm^{-1} wave number range to confirm the chemical and physical interactions between the rubber segments and filler segments.

3.5.2 Thermogravimetry analysis (TGA)

TGA of unmodified and modified silica samples were carried out using SDT Q600 TA instrument under a nitrogen purge with heating to 500 °C at a rate of 10 °C/min.

3.5.3 Powder X-ray diffraction analysis (XRD)

Powder X-ray diffraction analysis of unmodified and modified silica samples were performed at room temperature using Advance D8 BRUKER using Cu-Kα radiation.

3.5.4 Scanning Electron Microscopy (SEM)

Morphological attributes of nanosilica were observed using scanning electron microscope (EVO|18 Research, Carl Zeiss Microscopy) at an accelerating voltage of 10 kV. The samples were analyzed under high vacuum (HV) mode with gold-palladium coating so as to improve the image quality. The samples were placed on a sample holder with a double stick conducting carbon tape.

3.6 Preparation of silica dispersions

3.6.1 Preparation of dispersions of unmodified and acrylic polymer modified nanosilica

15 % nanosilica dispersions were prepared using pestle and mortar in small quantities. In this method requisite amounts of synthesized surface modified nanosilica, Tamol and deionized water (See Table 3.2) were mixed together and dispersed thoroughly and homogenously using pestle and mortar for 20 min. MNS_{M2} and $MNS_{M/E1.5}$ were used for preparation of dispersions.

Table 3.2: Formulation used for the preparation of 15 % unmodified and acrylic polymer modified nanosilica dispersions

Ingredients	Weight (g)		
UMNS	15	-	-
MNS_{M2}	-	15	-
$MNS_{M/E1.5}$	-	-	15
Tamol	1	1	1
Deionized water	84	84	84
Total	100	100	100

3.6.2 Preparation of dispersions of nanosilica modified with acrylic and NPs

The surface modification was carried out with PMAA at 2% level of modification, P(MAA-EHA) at 1.5% level of modification (See Table 3.3) and NPs at 2% level of modification (See Table 3.4). 15% silica dispersions were prepared with the aid of pestle and mortar in small quantities according to the formulation given in Table 3.3 and 3.4. In this method requisite amounts of commercial (Sigma Aldrich, USA) nanosilica, polymer, Tamol and deionized water were mixed together and dispersed thoroughly using pestle and mortar for 20 min. Cellulose, collagen, chitosan and gelatin were used as natural surface modifiers.

3.6.3 Preparation of dispersions of micro silica modified with NPs

In this method requisite amounts of precipitated silica, NPs, Tamol and deionized water were mixed together and dispersed thoroughly with the aid of a ball mill for 8 hours according to the formulation given in Table 3.4. The surface modification of micro silica with NPs was done at 2% level of modification. Cellulose, collagen, chitosan and gelatin were used as natural surface modifiers for silica filler.

Table 3.3: Formulation used for 15% acrylic polymers modified silica dispersions

Ingredients	Weight (g)	Weight (g)
Commercial nanosilica	15	15
PMAA	0.3	-
P(MAA-EHA)	-	0.225
Tamol	1	1
Deionized water	83.7	83.775
Total	100	100

Table 3.4: Formulation used for 15% NPs modified silica dispersions

Ingredients	Weight (g)
Commercial nanosilica/microsilica	15
Natural polymer	0.3
Tamol	1
Deionized water	83.7
Total	100

3.7 Characterization of NPs modified commercial nanosilica dispersions

Surface modification conferred on nanosilica by NPs was confirmed via FTIR and TGA tests performed as described in section 3.5.

3.8 Preparation of dispersions of compounding ingredients

33% (w/w) ZnO aqueous dispersion, 25% (w/w) ZDC aqueous dispersion and 10% (w/w) KOH aqueous solution are compounding ingredients required for XNBR latex compounding. KOH was added as an aqueous solution. ZnO and ZDC were added as aqueous dispersions. The formulations used in the preparation of the aqueous dispersions are given in Tables 3.5 and 3.6 respectively. The milling time was 8 h for both dispersions. The total solid content of the ZnO aqueous dispersion and ZDC aqueous dispersion were 33 % and 25 % respectively.

Table 3.5: Formulation used for preparation of 33 % (w/w) ZnO dispersion

Ingredients	Weight (g)
ZnO	33
Tamol	1
Deoinized water	66
Total	100

Table 3.6: Formulation used for preparation of 25 % (w/w) ZDC dispersion

Ingredients	Weight (g)
ZDC	25
Tamol	1
Deoinized water	74
Total	100

3.9 Latex compounding, film casting, drying and vulcanization

The XNBR latex compounding was done as per the formulation given in the Table 3.7.

Table 3.7: Formulation for XNBR latex compounding

Ingredient	Dry Weight (g)
XNBR latex	100
10% (w/w) KOH solution	1
25% (w/w) ZDC aqueous dispersion	0.2
33% (w/w) ZnO aqueous dispersion	10
30% (w/w) SP aqueous emulsion	0.5
15% (w/w) Silica aqueous dispersion	10

Latex films were prepared as follows;

-The latex and other compounding ingredients were added according the sequence of the ingredients mentioned in Table 3.7, subsequently gently hand mixed for 15 min to obtain a homogenous mixture.

-The mixture was kept for 24 h at room temperature for maturation.
-Latex films were prepared via casting method using 15 cm diameter glass petri dishes as casting molds.
-Casting molds were kept on a leveled table to avoid the occurrence of variation of film thickness.
-Maturated latex compound was gently mixed and poured into the molds carefully avoiding the formation of air bubbles in latex films.
-Latex in molds were kept at room temperature for drying without any external disturbances (See Figure 3.10).
-Then, the films were removed from the molds carefully and hanged in air for further drying of both sides of the films (See Figure 3.11). For air drying square shape steel structures were used to avoid the shrinkage of films during drying.
-Completely dried latex films were vulcanized by heating at 70 ºC for 10 min in a well-ventilated oven.

Figure 3.10: Latex film casting

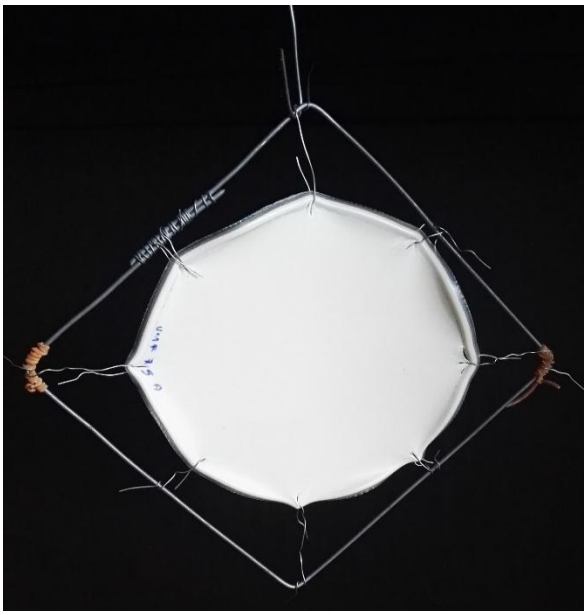

Figure 3.11: Latex film air drying

3.10 Evaluation of vulcanizate properties

3.10.1 Measurement of physical properties of vulcanized latex films

The overall influence of the surface modification of silica in enhancing the physical properties of latex is expected to be due to discouragement of filler-filler interactions and ensuring uniform distribution of the filler throughout the rubber matrix and encouragement of rubber-filler interactions.

The suitability of the selected surface modifiers which help to promote the rubber-filler interactions could be investigated by performing tests for tensile, tearing, modulus at 300% elongation and elongation at break.

Dumbbell shaped tensile test pieces were cut from vulcanized latex films (See Figure 3.12). Tensile strength (TS), elongation at break (EB %) and modulus at 300% elongation (M300) of the vulcanizates were measured using Houndsfield H10KT tensile testing machine under conditions given in Table 3.8. The test was carried out according to the ISO 37, 2011 standard.

Test pieces for tear resistance testing were cut from vulcanized latex films (See Figure 3.13). Tear strength (TRS) of the vulcanizate was measured using

Houndsfield H10KT tensile testing machine under conditions given in Table 3.9.The test was carried out according to the ISO 34-1, 2010 standard.

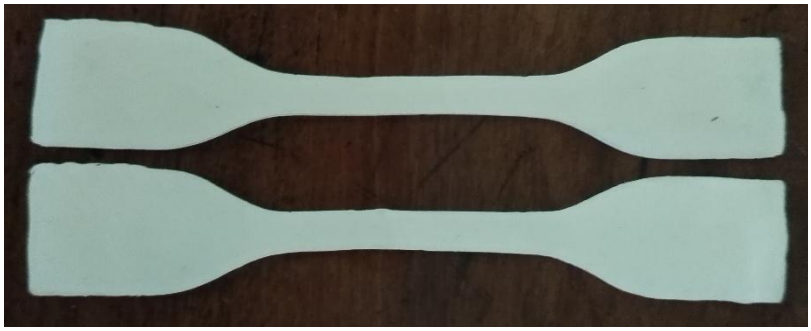

Figure 3.12: Tensile test samples

Figure 3.13: Tear resistance test sample

Table 3.8: Operating conditions for tensile testing

Load range	0-50 N
Extension range	0-1000 mm
Test speed	300 mm/min
Gauge length	25 mm

Table 3.9: Operating conditions for tear resistance testing

Load range	0- 50 N
Extension range	0-1000 mm

Test speed	300 mm/min
Gauge length	25 mm

Test speed for both tensile and tear tests was used as 300 mm/min due to overcome the slipping of sample while testing.

3.10.2 Swelling properties of vulcanized latex films

The swelling properties of vulcanized films were determined by immersing pre-weighted 1cm x 1cm size test sample in methylethyl ketone (MEK) and permitting to absorb solvent till the equilibrium was reached. Test samples of vulcanized latex cast films swollen in MEK were dried in an oven at 60 ºC until a constant weight was achieved. The following weight measurements were taken for each samples;

W_0 – Weight of the test piece before swelling

W_s –Weight of the swollen test piece, at equilibrium

W_d– weight of dried specimen after swelling

The crosslink density of the film was determined by Flory-Rehner equation (Flory, 1950).

The swelling % was calculated using the equation 12.

$$\text{Swelling \%} = (W_s - W_0) \text{ X } 100/W_0 \qquad (12)$$

It is possible to estimate the concentration of physically effective cross-links in the rubber network from the values of equilibrium swelling. The crosslink density is usually determined by using the modified Flory Rehner equation.

$$Vc = \{-\ln(1-Vr)-Vr-\mu(Vr)^2\}/ \{Vs\ (Vr^{1/3} - Vr\ /2)\} \qquad (13)$$

Where; Vc –crosslink density

Vr–volume fraction of the polymer in the swollen network

Vs– molar volume of the solvent

μ – polymer solvent interaction parameter

The volume fraction of the XNBR latex films in the swollen films (Vr) was calculated using the following equation 14.

$$Vr = (W_2/d_2) / \{(W_1/d_1) + (W_2/d_2)\} \quad (14)$$

$$W_2 = W_d - FW_0 \quad (15)$$

Where; W_1 – weight of solvent (MEK) absorbed

d_1 –density of MEK

d_2 –density of rubber

F – weight fraction of insoluble (filler) component

Rubber-filler interaction was determined from the swelling parameters using Park and Lorenze equation.

$$Q = (W_s - W_d) / W_2 \quad (16)$$

Q – weight of solvent absorbed per gram of rubber at equilibrium

The higher extent of the interaction between the filler and the matrix is shown by the lower value of Q_f/Q_g ratios.

f , g – subscripts refer to filled and gum vulcanizates

3.10.3 Morphology of vulcanized latex films

Cross sectional microstructures of films cast from XNBR latex vulcanizates filled with 10 phr of either unmodified or modified filler were examined through a metallurgical microscope (MEIJI, Mx7100).

CHAPTER 04

4 RESULTS AND DISCUSSION

4.1 Surface modification of nanosilica particles using acrylic surface modifiers

The surface functionalization of silica particles is important for tuning the overall properties of particles to fit targeted applications. At present, there is a high tendency of surface modification of inorganic nanoparticles with organic materials. Surface modification with acrylic polymers can play dual role. The problem of agglomeration of particles with high surface energy can be overcome by the surface modification of silica nanoparticles and it is expected that the introduction of acrylic polymers on the nanosilica surface will increase the surface hydrophobicity.

4.1.1 Yield extracted from synthesis of surface modified nanosilica particles

Table 4.1 and 4.2 illustrate the effect of concentrations of surface modifier on the yield of isolated PMAA and P(MAA-EHA) surface modified nanosilica particles respectively. The best isolated yield could be observed for MNS_{M2} and $MNS_{M/E1.5}$.

Table 4.1: Extracted yield (%) of PMAA modified nanosilica

Types of silica nanoparticles	Extracted yield (%)
MNS_{M1}	6.11
$MNS_{M1.5}$	7.02
MNS_{M2}	13.52
$MNS_{M2.5}$	5.21

Table 4.2: Extracted yield (%) of P(MAA-EHA) modified nanosilica

Types of silica nanoparticles	Extracted

	yield (%)
$MNS_{M/E1}$	7.17
$MNS_{M/E1.5}$	12.8
$MNS_{M/E2}$	8.5
$MNS_{M/E2.5}$	No yield obtained

4.1.2 Characteristics of synthesized unmodified and acrylic polymer modified nanosilica

4.1.2.1 Results of FTIR analysis of unmodified and acrylic polymer modified nanosilica

Figures 4.1 and 4.2 show the FTIR spectra of UMNS, PMAA homopolymer and PMAA modified nanosilica at different concentrations of surface modifier (1, 1.5, 2, 2.5 % wt) and those of P(MAA-EHA) (60:40) copolymer, P(MAA-EHA) modified nanosilica at different concentrations of surface modifier (1, 1.5, 2 % wt) respectively.

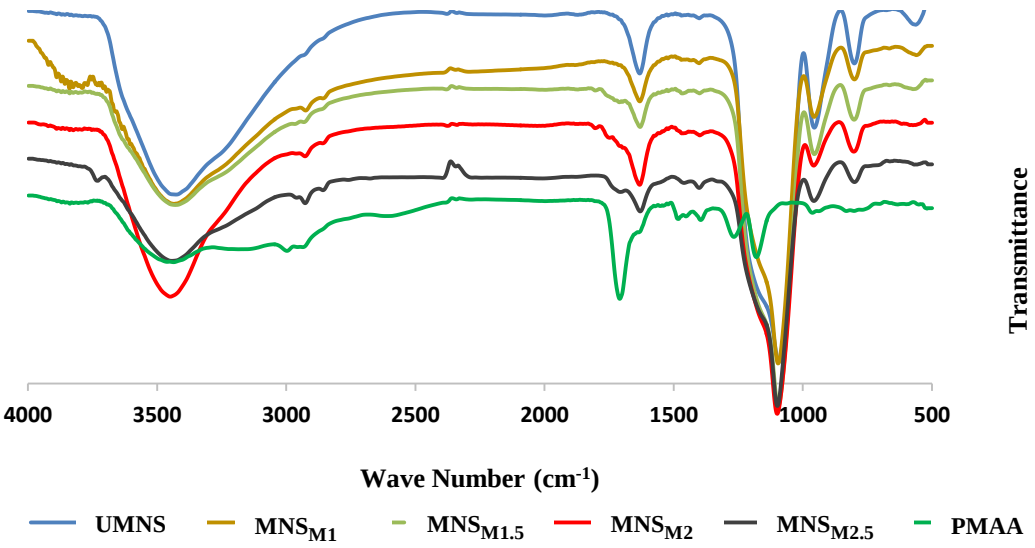

Figure 4.1: FTIR spectra of UMNS, PMAA homopolymer and PMAA modified nanosilica at different concentrations of PMAA

Table 4.3: Characteristic group frequencies of silica

Wave number (cm^{-1})	Assignment
3470-3450	O-H stretching of H_2O molecular & Si-OH stretching of surface silanols
1653-1634	H_2O bending
1095-1089	Si-O-Si asymmetric stretching
960	Si-O inplane stretching of silanols
800	Si-O-Si symmetric stretching

Generally nanosilica are more hydrophilic than micro silica due to the presence of surface silanol groups. The carbonyl functional group of carboxylic groups shows an IR peak in the range of 1725-1700 cm^{-1} while peaks relevant to carbonyl functional groups of esters can be observed in the range of 1750-1730 cm^{-1} (Pavia et al., 2008). In Figure 4.1, the appearance of a small peak at around 1730cm^{-1} in spectra of modified silica confirms the formation of ester bonds between carboxylic groups of PMAA and -OH groups of silica. The strong peak at 1706 cm^{-1} of the spectrum of PMAA, corresponds to the carbonyl group of carboxylic acid group (Pavia et al., 2008). The sharp absorption bands observed at 2,924 and 2,853 of pure PMAA spectra and all modified silica spectra are due to the bending vibrations of $–CH_2$ groups of surface modifier. All the modified FTIR spectra show the absorption band due to bending vibration of C-H at around 2924 cm^{-1} and 2853 cm^{-1}, clearly indicating the modification of the nanoparticle surfaces by organic molecules. Figure 4.1 clearly shows the modification via the formation of ester bonds with surface silanol and enhancement of peak with the level of modification while no such peak can be found in spectrum of UMNS. Figure 4.1 shows the presence of intense silicon-oxygen covalent bonds vibrations due to the formation of dense silica.

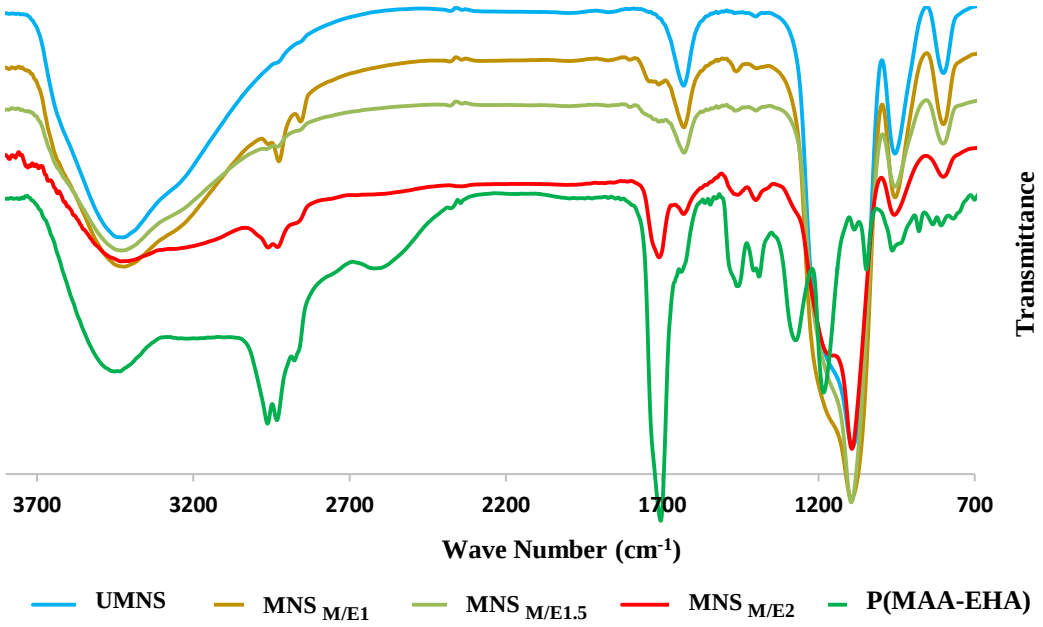

Figure 4.2: FTIR spectra of UMNS, PMAA –EHA copolymer and P(MAA-EHA) modified nanosilica at different concentrations of P(MAA-EHA)

Copolymer modified nanoparticles are more likely to be soluble in tetrahydrofuran. In Figure 4.2 the appearance of a small peak at around 1730 cm^{-1} confirms the formation of ester bonds between carboxylic groups of MAA repeat units of the copolymer and -OH groups of silica while copolymer showed a strong intense peak at 1708 cm^{-1} with shoulder at 1730 cm^{-1} which correspond to the carbonyl groups of carboxylic acid and ester respectively. All the P(MAA-EHA) modified nanosilica FTIR spectra contain peaks corresponding to C-H bonds at around 2924 cm^{-1} and 2853 cm^{-1}, clearly indicating the modification of the nanoparticle surfaces by organic molecules. Figure 4.2 clearly shows the modification via the formation of ester bond with surface silanol and enhancement of peak with the level of modification while no such peak can be found in the spectrum of UMNS. Figure 4.2 shows the presence of intense silicon-oxygen covalent bonds vibrations due to the presence of dense silica in all surface modified nanosilica extracted.

4.1.2.2 Results of TGA of unmodified and acrylic polymer modified nanosilica

The thermal stability of nanosilica particles is altered by the modification of silica particles. Hence, the study of the thermal behaviors of unmodified and surface modified nanosilica particles are imperative. Figure 4.3 shows the TGA curves of UMNS, VN_3, PMAA modified nanosilica, PMAA homopolymer in an atmosphere of nitrogen and the corresponding curves for P(MAA-EHA) copolymer modified silica are shown in Figure 4.4.

Two distinct mass loss steps could be observed for UMNS and VN_3 (See Figure 4.3). The first mass loss occurred below 150 ° C is due to the removal of physisorbed water molecules from the silica surface. The second mass loss is broader and responsible for slow condensation of silanol groups. It is noticeably observed that, higher weight loss % for UMNS compared to VN_3 up to 150 ° C (See Table 4.4). This is due to the presence of high number of silanol groups of UMNS, which permits higher number of water molecules to be attached when compared with VN_3. As for the second weight loss, higher weight loss could be observed in UMNS than in VN_3, again due to the presence of higher number of surface silanols, allowing more condensation of UMNS (See Table 4.4).

All PMAA modified nanosilica show three steps of mass losses. First mass loss is due to the removal of water molecules from the silica surface while second and third mass losses are due to the decomposition of PMAA polymer chains attached to the nanosilica particles as described below;

Pure PMAA decomposes in three steps: in the first step, removal of physisorbed water molecules; in the second step, formation of poly (methacrylic anhydride)

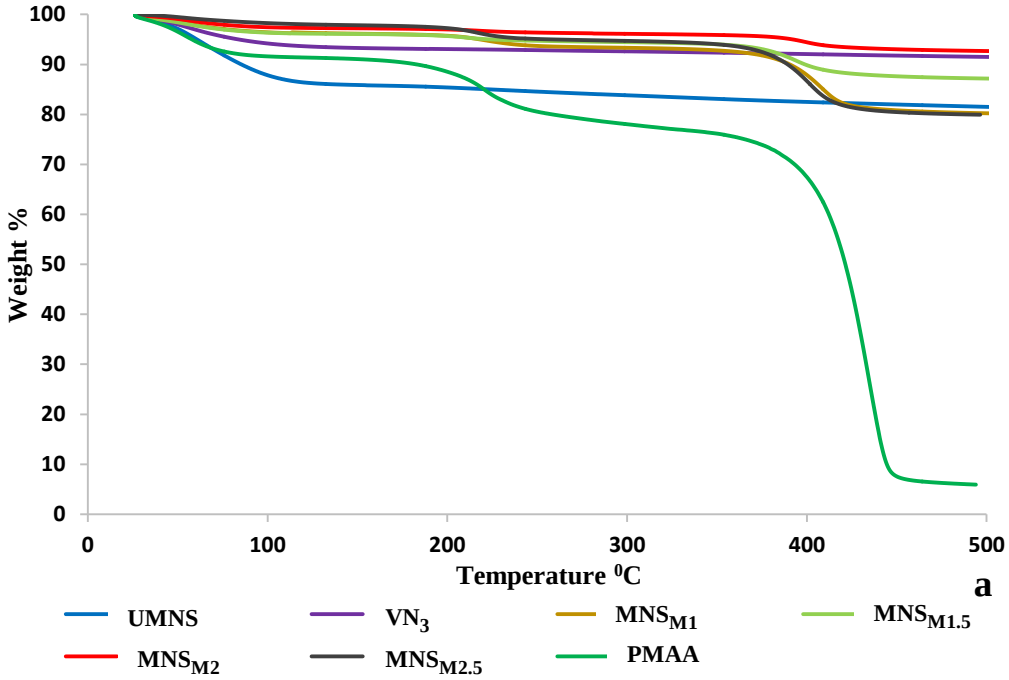

(PMAN) comprising six-membered glutaric anhydride-type rings; at elevated temperatures further decomposition and charring happens as a magnitude of fragmentation of these rings. In the third step decomposition peaks represented the formation of carbon monoxide, carbon dioxide, propane and isobutylene as products of the fragmentation of the anhydride rings (Rida & Harb, 2014).

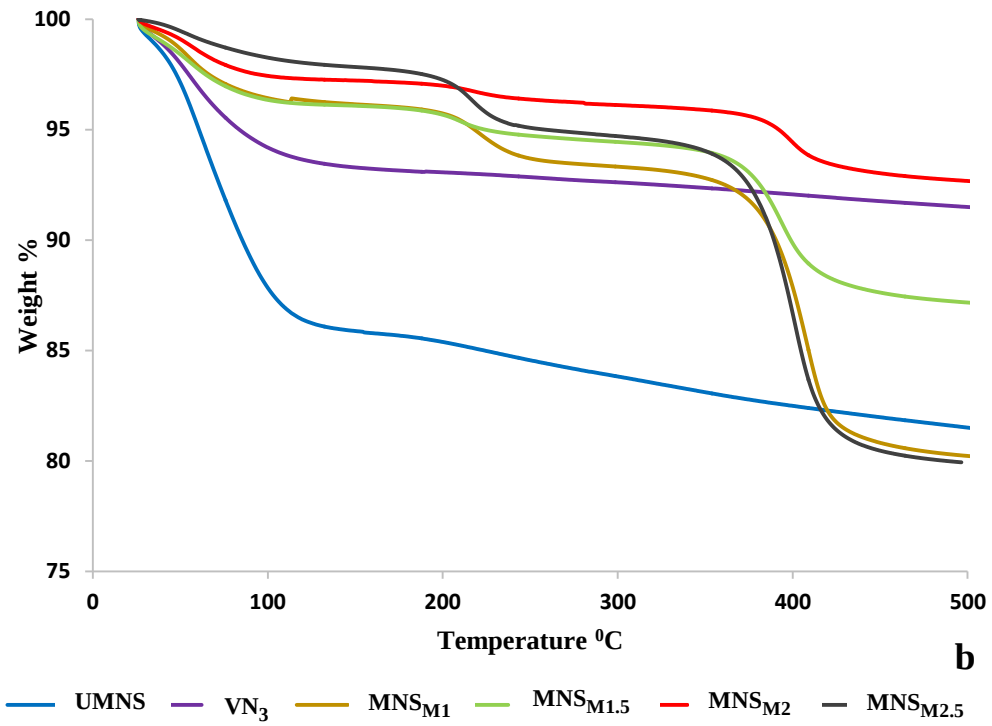

Figure 4.3: (a) TGA curves of UMNS, VN_3, MNS_{M1}, $MNS_{M1.5}$, MNS_{M2}, $MNS_{M2.5}$ and PMAA homopolymer, (b) Enlarged version of (a) except PMAA curve

Degradation of polymeric modifiers in surface modified silica commenced at significantly higher temperatures compared with the pure polymers indicating success of the modification reaction. Temperature corresponding to the second weight loss of PMAA attached to modified silica was about 40 °C higher than that of the pure polymer (See Table 4.5). However, this trend was not observed for the third weight loss. Slight reduction of degradation temperatures for PMAA modified nanosilica were noticeably observed (See Table 4.5).

Table 4.4: Weight loss % of UMNS, VN_3 and PMAA modified nanosilica at different levels of modification

Type of silica	Weight loss (%) below 150 ° C	Weight loss (%) between 150-500 ° C
UMNS	14	5
VN_3	7	2

MNS_{M1}	4	17
$MNS_{M1.5}$	4	9
MNS_{M2}	3	4
$MNS_{M2.5}$	2	18

Table 4.5: Degradation temperatures of PMAA and PMAA modified nanosilica at different levels of modification

Type of silica	Second weight loss starts at (° C)	Third weight loss starts at (°C)
PMAA	124	350
MNS_{M1}	179	325
$MNS_{M1.5}$	159	315
MNS_{M2}	170	347
$MNS_{M2.5}$	148	331

Copolymer P(MAA-EHA) (60:40) showed a thermal behavior which appeared to be as a combination of MAA and EHA. Here again, surface modified nanosilica show higher thermal stability comparing with UMNS. Further, thermal degradation temperatures were enhanced with increasing the surface modifier concentration from 1% to 2% wt (See Figure 4.4).

As for TGA curves of UMNS and VN_3, lower weight loss could be observed for VN_3 (See Table 4.4). This is because of the presence of lower amount silanols on silica surface as the surface area of micro silica is lower than that of nanosilica.

Second weight loss of P(MAA-EHA) attached silica occurred at a temperature which is about 50 °C higher than that of the pure copolymer (See Table 4.7). But, this was not so for the third weight loss. Instead, slight reduction of third weight loss temperatures for P(MAA-EHA) modified nanosilica was noticeably observed (See Table 4.7).

In both modification procedures, weight losses corresponding to the loss of physically absorbed water, were lower compared with UMNS nanoparticles. Therefore, TGA results show that acrylic polymer modified nanoparticles absorb less amount of water than UMNS (See Tables 4.4 and 4.6). This is due to the functionalization of polymers with surface silanol groups of nanosilica via formation of ester bonds with surface modifiers, conferring a hydrophobic character to the surface of nanosilica. But there may still be some hydroxyl groups available which are not modified by polymers. Therefore, water molecules can be attached to those polymer free areas and give low percentage of weight losses.

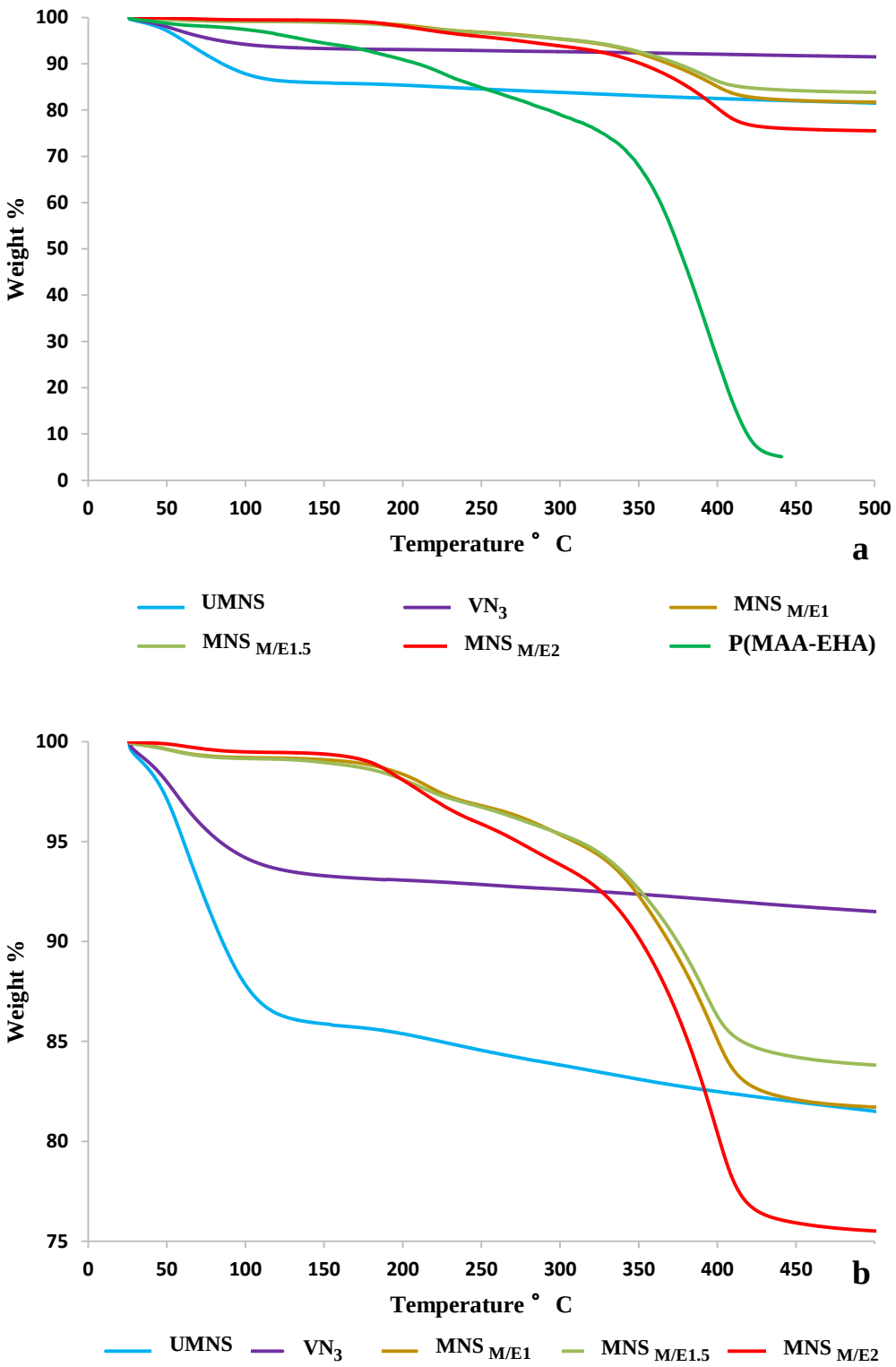

Figure 4.4: (a) TGA curves of UMNS, VN_3, $MNS_{M/E1}$, $MNS_{M/E1.5}$, $MNS_{M/E2}$ and P(MAA-EHA), (b) Enlarged version of (a) except P(MAA-EHA) curve

Table 4.6: Weight loss (%) UMNS, VN_3 and P(MAA-EHA) modified nanosilica at different levels of modification

Type of silica	Weight loss (%) below 150 ° C	Weight loss (%) between 150-500 °C
UMNS	14	5
VN_3	7	2
$MNS_{M/E1}$	0.9	18
$MNS_{M/E1.5}$	1	13
$MNS_{M/E2}$	0.6	24

Table 4.7: Degradation temperatures of P(MAA-EHA) and P(MAA-EHA) modified nanosilica at different levels of modification

Type	Second weight loss starts at (° C)	Third weight loss starts at (°C)
P(MAA-EHA)	124	299
$MNS_{M/E1}$	179	291
$MNS_{M/E1.5}$	159	293
$MNS_{M/E2}$	170	292

Typically, the weight loss (%) and the yield (%) of PMAA modified nanosilica should increase in the order of 1%, 1.5%, 2% and 2.5%. But here, the weight loss gradually decreased in the order of 1%, 1.5%, 2% and then increased at 2.5% whereas the pattern of variation of extracted yield % was in an exactly opposite manner to that of weight loss (See Table 4.8). In other words, the highest yield is observed when the weight loss is at its minimum (2%) (See Figure 4.5).

Table 4.8: Variation of weight loss (%) and yield (%) with PMAA level of modification of nanosilica

Surface modification level (%)	Weight loss (%) between 150-500 °C	Extracted yield (%)
1	17	6.11
1.5	9	7.02
2	4	13.52
2.5	18	5.21

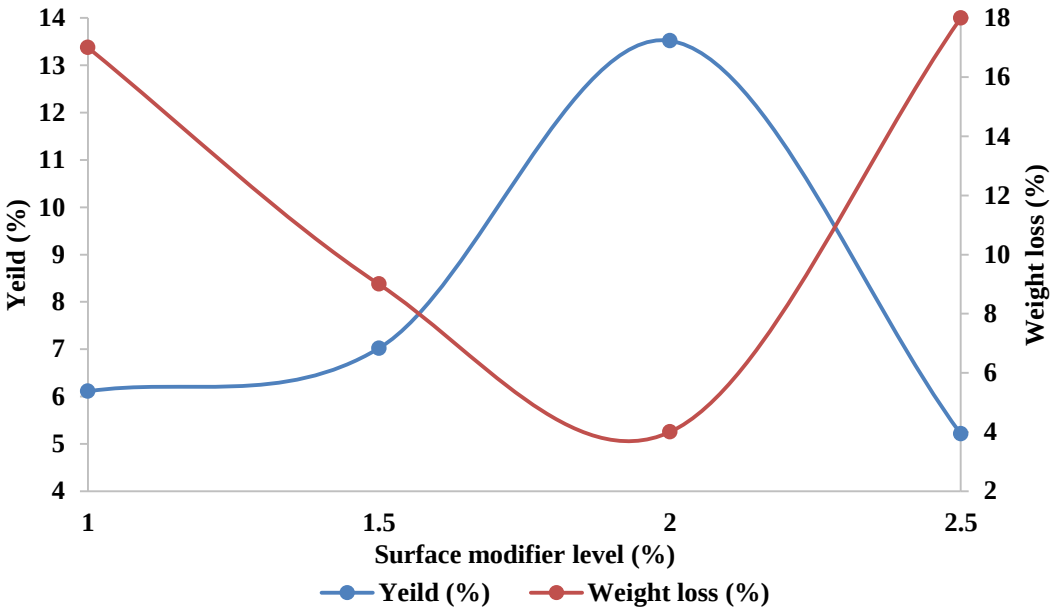

Figure 4.5: Variation of extracted yield (%) and weight loss (%) with level of surface modifier PMAA homopolymer

The same pattern is revealed in P(MAA-EHA) modified nanosilica as well. In which, the weight loss decreased as per 1%, 1.5% and increased at 2% while the yield behaved in an exactly opposite manner (See Figure 4.6). Here, the highest yield is observed at the minimum weight loss of 1.5% (See Table 4.9).

The lowest weight loss depicts low thermal decomposition. Low thermal decomposition depicts better thermal stability of the structure; which illustrates, surface modifiers are strictly adhered to the nanosilica surface during the synthesis, thus making it more stable. On both the occasions highest yield category produced

lowest weight loss %. This explains that the surface modification techniques at MNS_{M2} and $MNS_{M/E1.5}$ is distinctive. In this synthesis method, better surface modification is not achieved at higher surface modifier levels. It could be due the fact that at $MNS_{M2.5}$ and $MNS_{M/E2}$, high number of surface modifiers are not bonded with nanosilica or they are loosely bonded with the nanosilica surface than their optimum modification level.

Table 4.9: Variation of weight loss (%) and extracted yield (%) with P(MAA-EHA) level of modification of nanosilica

Surface modification level (%)	Weight loss (%) between 150-500 °C	Extracted yield (%)
1	18	7.17
1.5	13	12.8
2	24	8.5
2.5	-	Negligible yield

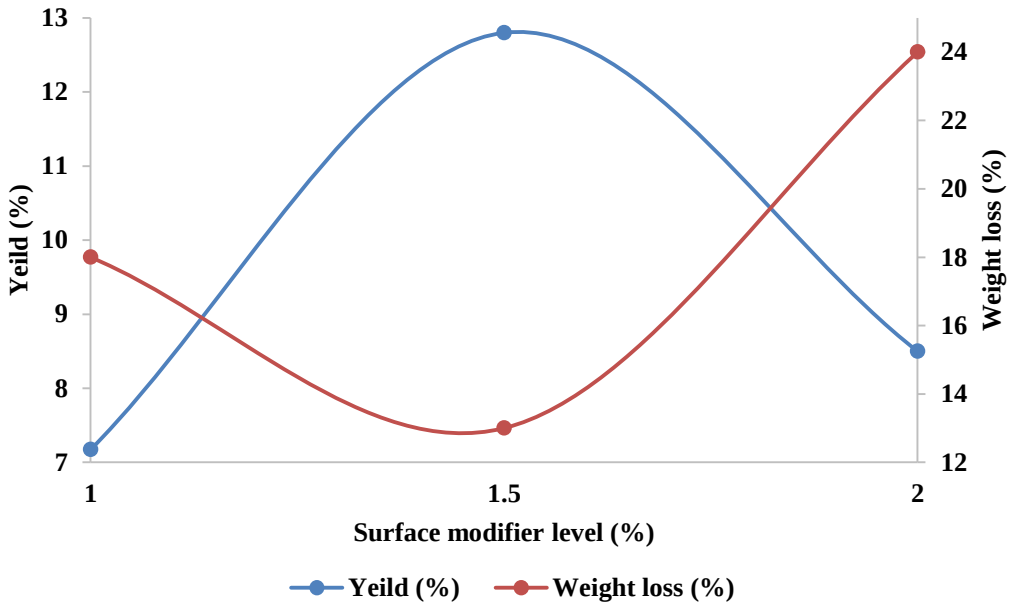

Figure 4.6: Variation of extracted yield (%) and weight loss (%) with level of surface modifier P(MAA-EHA)

4.1.2.3 Results of XRD analysis of unmodified and acrylic polymer modified nanosilica

Figures 4.7 to 4.9 illustrate XRD diffractograms of UMNS, PMAA homopolymer and MNS_{M2} respectively. The UMNS spectrum appears as a broad band with the equivalent Bragg angle at 2θ=23°, which indicates that the material is amorphous (Rafiee et al., 2012). Clearly observed broader peak for pure PMMA indicates the amorphous nature of PMMA (Mahipal, Agrawal, Hanisah, Arshed, & Ramesh; Ying Zhang, Fang, Wang, & Lin, 2004). Here, both nanosilica particles and surface modifier are amorphous in nature. XRD of MNS_{M2} shows a broad peak, and the broad upsurge centered at 2θ angle of about 22.9º (See Figure 4.9).

The size of the particles was estimated by the half width of the peak (β) using Scherer's formula (Rafiee et al., 2012).

$$D=K\lambda/(\beta \cos\theta)$$

with K = 0.9 nm as a constant, λ = 1.542 Å as wavelength of Cu-Kα, and β in radian. By manual evaluation of the XRD chart, the particle size of MNS_{M2} was found to be about 200 nm.

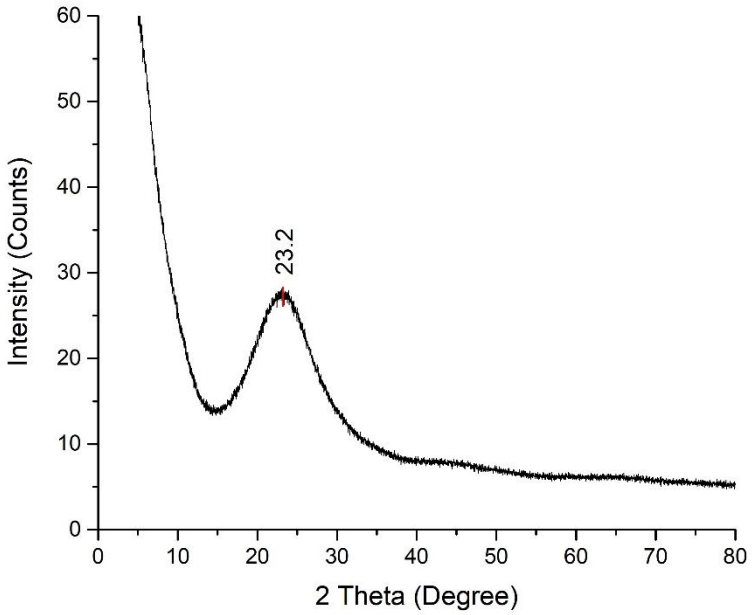

Figure 4.7: XRD of UMNS

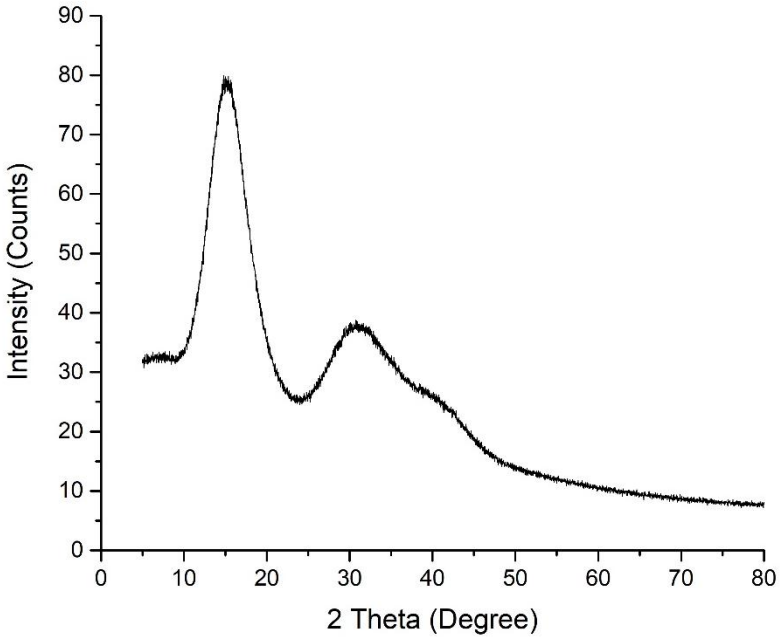

Figure 4.8: XRD of PMAA polymer

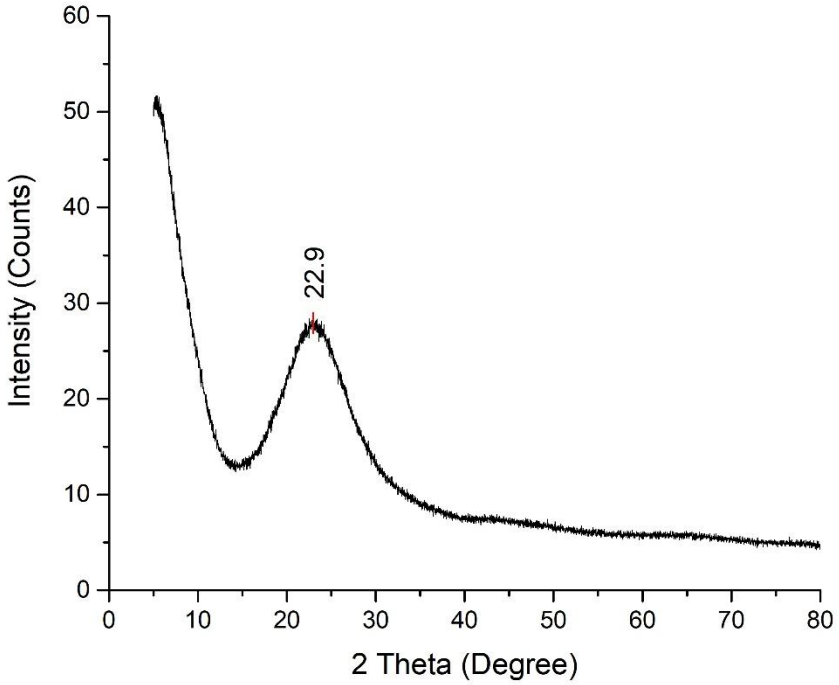

Figure 4.9: XRD of MNS_{M2}

Figure 4.10 exemplify the XRD of $MNS_{M/E1.5}$. It is noticed that the modified nanosilica is also amorphous in nature. As can be seen, the pattern shows a broad

peak, and the broad rise centered at 2θ angle of about 23.6° which is a known typical characteristic of silica (Rafiee et al., 2012). The particle size of $MNS_{M/E1.5}$ was calculated to be about 195nm.

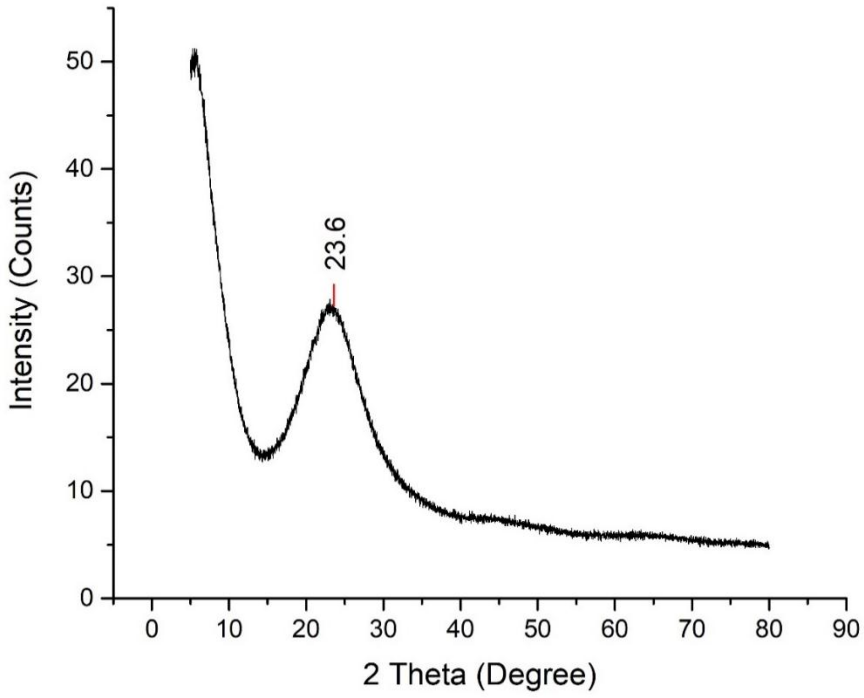

Figure 4.10: XRD of $MNS_{M/E1.5}$

4.1.2.4 Morphology and particle size distribution of unmodified and acrylic polymer modified nanosilica

Figures 4.11 to 4.16 elucidate the SEM of micro silica, UMNS and PMAA modified nanosilica at several modification levels. SEM of VN_3 shows the giant aggregation of silica particles. According to the particle size analysis results (See Figure 4.20), the average particle size of UMNS was about 310 nm. But, it was found that UMNS particles showed a big tendency to agglomerate than surface modified nanosilica. SEM micrograph of UMNS does not show particles with spherical shapes. It was observed that UMNS particles bridge with each other and form a particle network unlike spherical separate particles in surface modified particles.

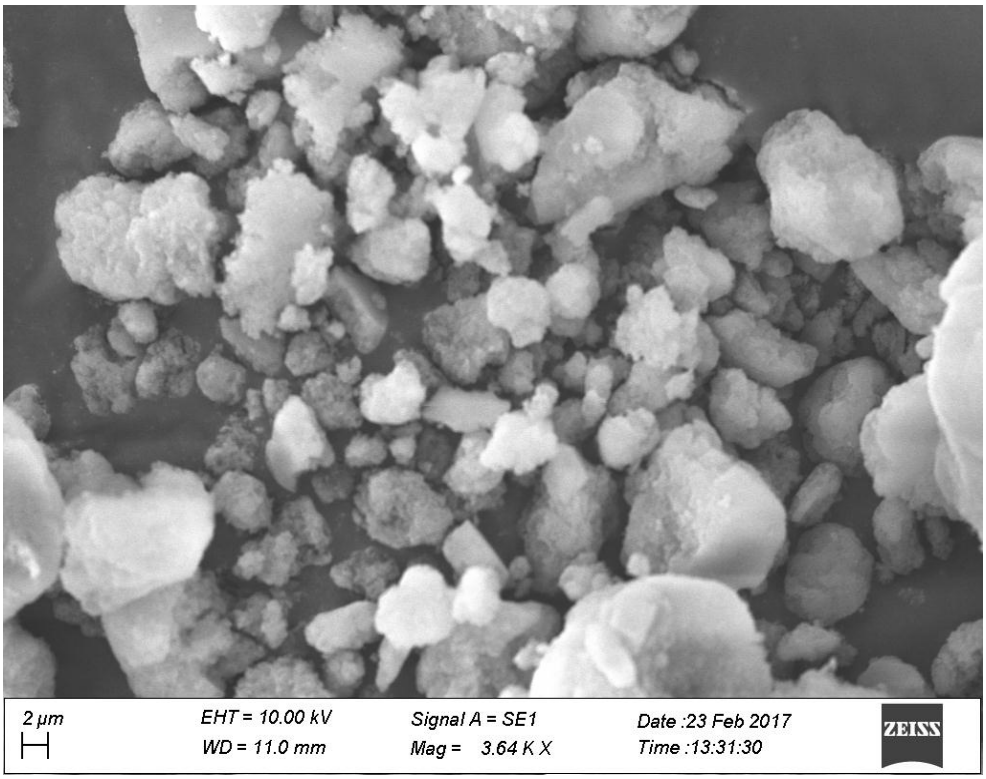

Figure 4.11: SEM of micro silica

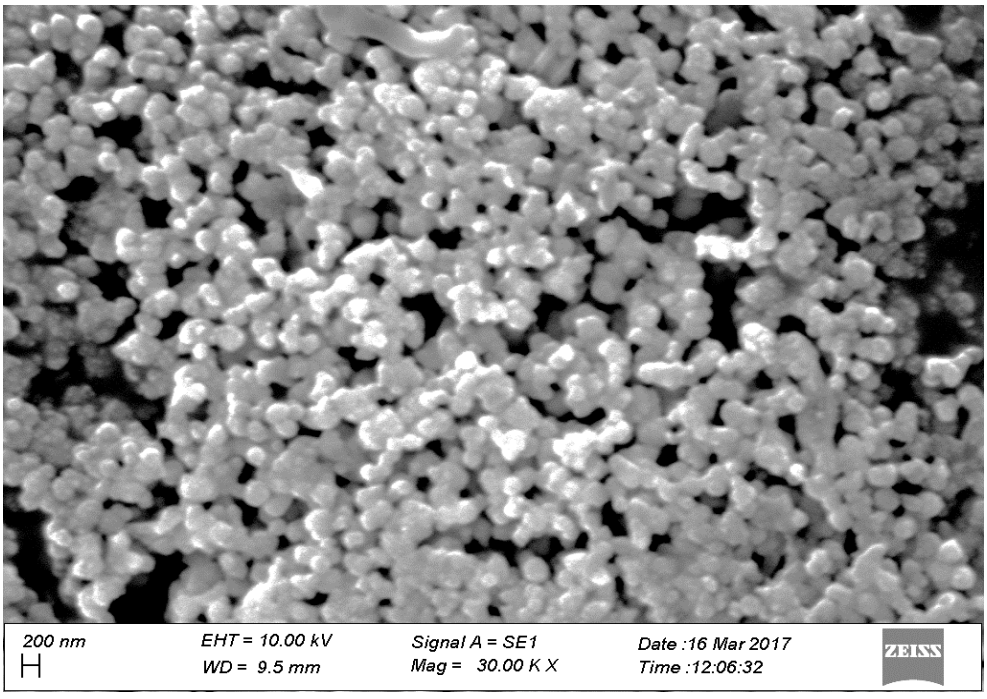

Figure 4.12: SEM of UMNS

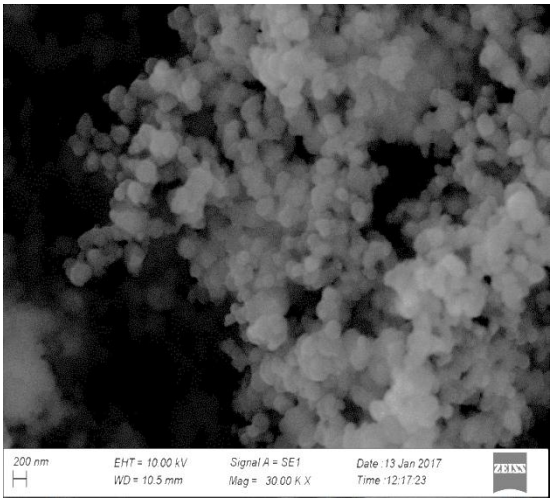

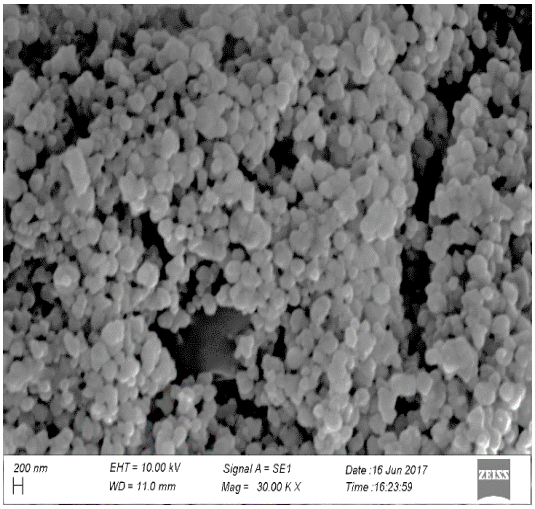

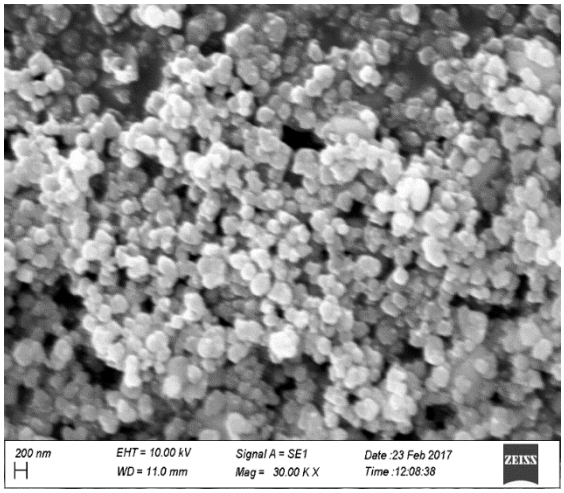

Figure 4.13: SEM of MNS_{M1}

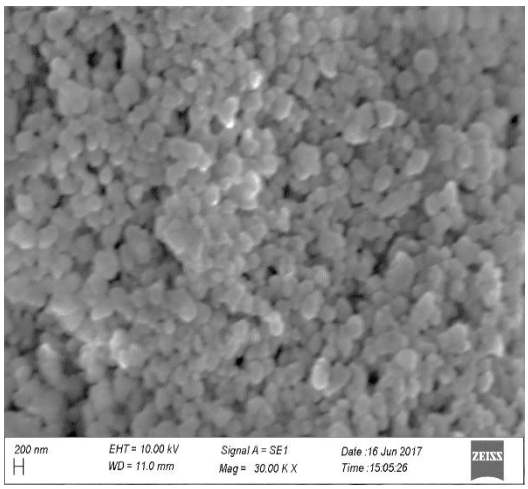

Figure 4.14: SEM of $MNS_{M1.5}$

Figure 4.15: SEM of MNS_{M2}

Figure 4.16: SEM of $MNS_{M2.5}$

Synthesis of modified nanosilica were performed by varying surface modifier concentration from 1 to 2.5% of total mass of silica, keeping all the other parameters constant. It was observed that the particle size of modified nanosilica would be considerably affected by the concentration of surface modifier (Rafiee et al., 2012). Albeit, surface modifier concentration noticeably affected the extracted yield of surface modified nanosilica as mentioned in Table 4.10. Further, surface modification level significantly affected the particle aggregation. It appears that 2% PMAA is the best surface modifier concentration to protect the surface of silica, making combination of silica and PMAA dispersed completely in the n-butanol solvent.

Figures 4.17 to 4.19 illustrate the SEM of P(MAA-EHA) modified nanosilica containing different concentrations of copolymer from 1 to 2% of total mass of silica. A similar phenomena could be observed in P(MAA-EHA) modified nanosilica as described above. The variation of surface modifier concentration considerably affected the particle size, and it prominently affected the extent of particle aggregation and the extracted yield of nanosilica into tetrahydrofuran solvent (Rafiee et al., 2012). This microstructural analysis confirms that less aggregation could be observed for $MNS_{M/E1.5}$, further ratifying the results obtained for yield calculation values.

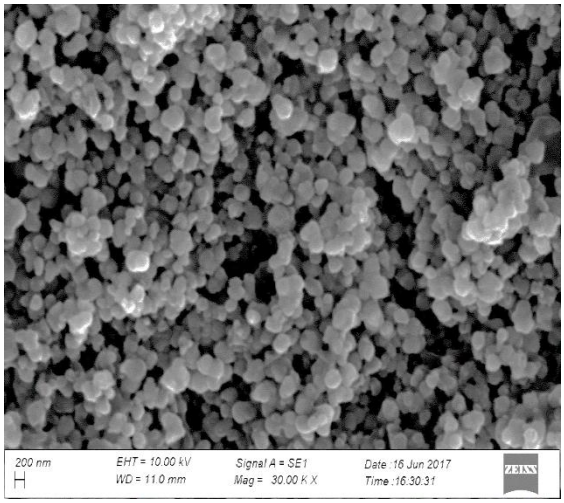

Figure 4.17: SEM of $MNS_{M/E1}$

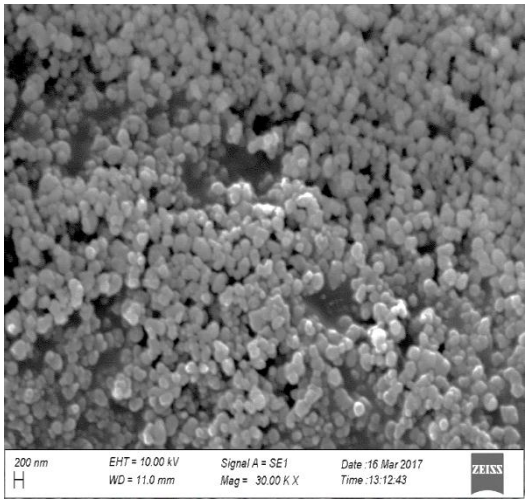

Figure 4.18: SEM of $MNS_{M/E1.5}$

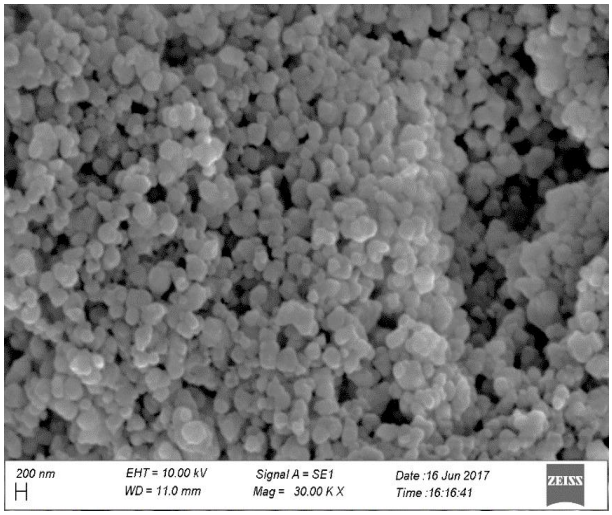

Figure 4.19: SEM of $MNS_{M/E2}$

The particle size distributions of the UMNS, MNS_{M1}, $MNS_{M1.5}$, MNS_{M2} and $MNS_{M2.5}$ used in this work are given in Figure 4.20. Particle size distributions of the $MNS_{M/E1}$, $MNS_{M/E1.5}$ and $MNS_{M/E2}$ were elucidated from Figure 4.22. The average particle size of the synthesized MNS_{M1}, $MNS_{M1.5}$, MNS_{M2}, $MNS_{M2.5}$, $MNS_{M/E1}$, $MNS_{M/E1.5}$ and $MNS_{M/E2}$ in this study are given in Tables 4.10 and 4.11.

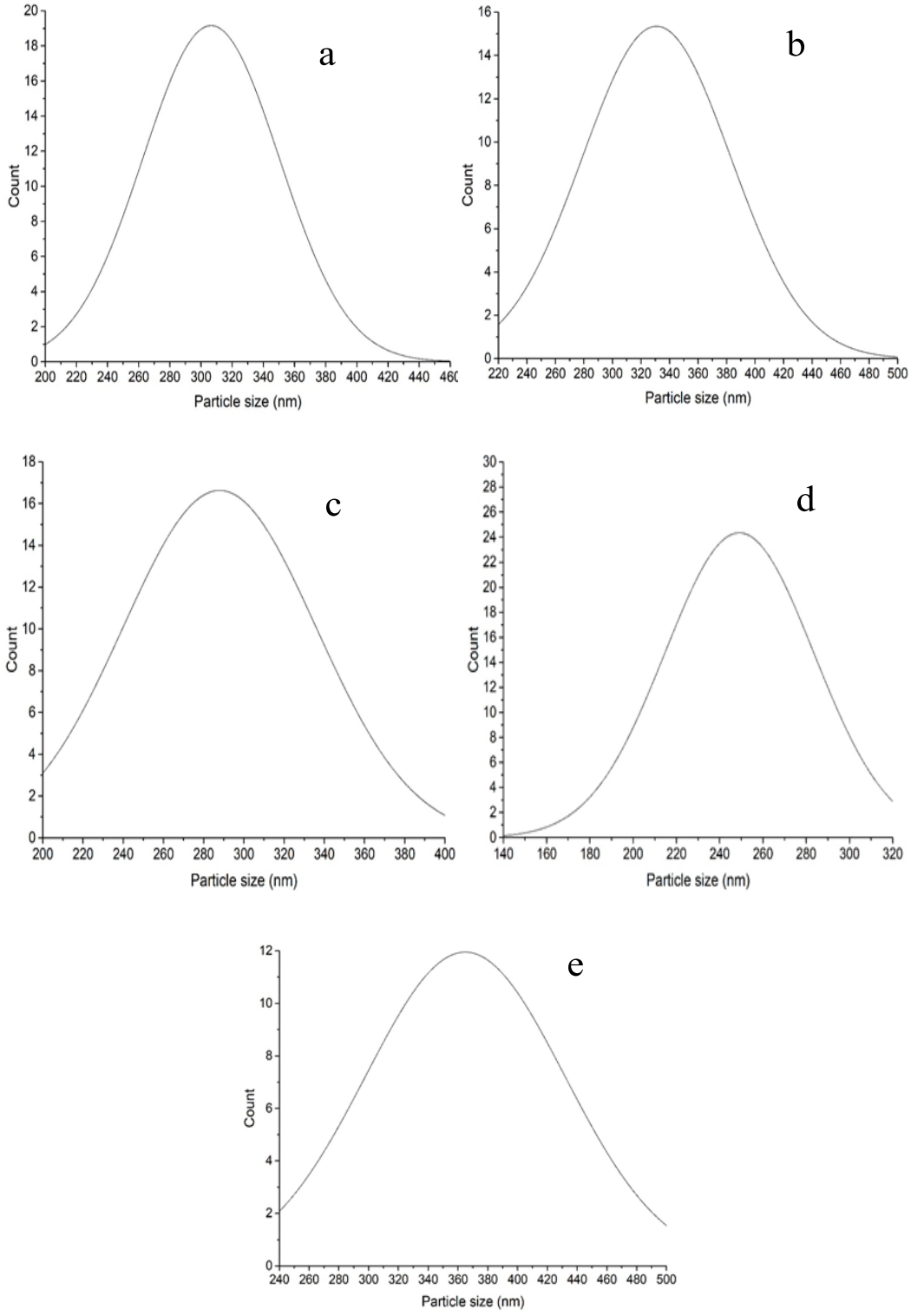

Figure 4.20: Particle size distribution of (a) UMNS, (b) MNS_{M1}, (c) $MNS_{M1.5}$, (d) MNS_{M2} and (e) $MNS_{M2.5}$

Table 4.10: Variation of weight loss (%), extracted yield (%) and average particle size with PMAA level of modification of nanosilica

Surface modification level (%)	Weight loss (%) between 150-500 °C	Extracted yield (%)	Average particle size (nm)
1	17	6.11	330
1.5	9	7.02	288
2	4	13.52	235
2.5	18	5.21	364

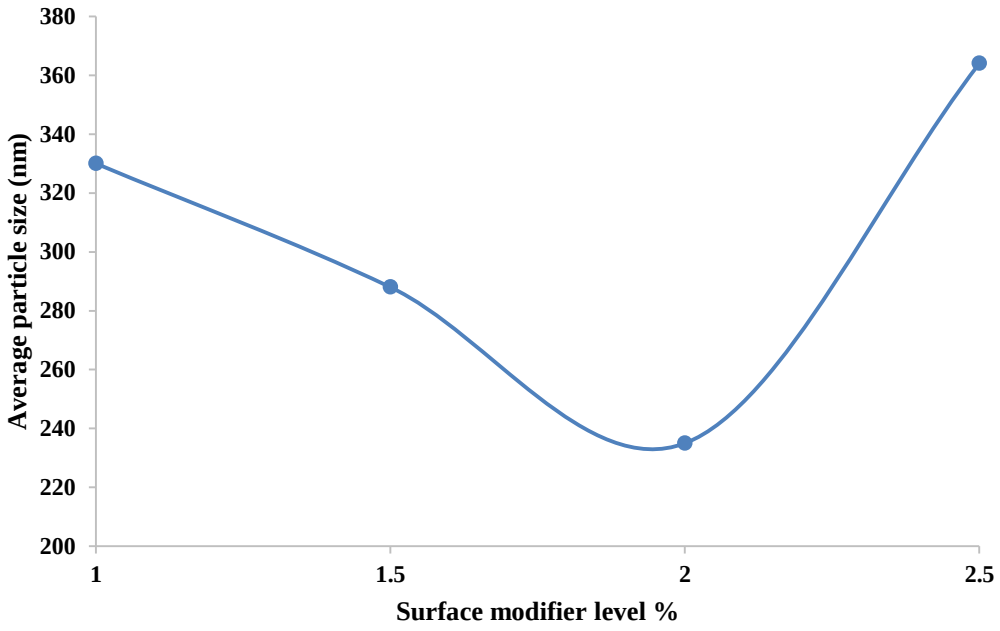

Figure 4.21: Variation of average particle size with level of surface modifier PMAA

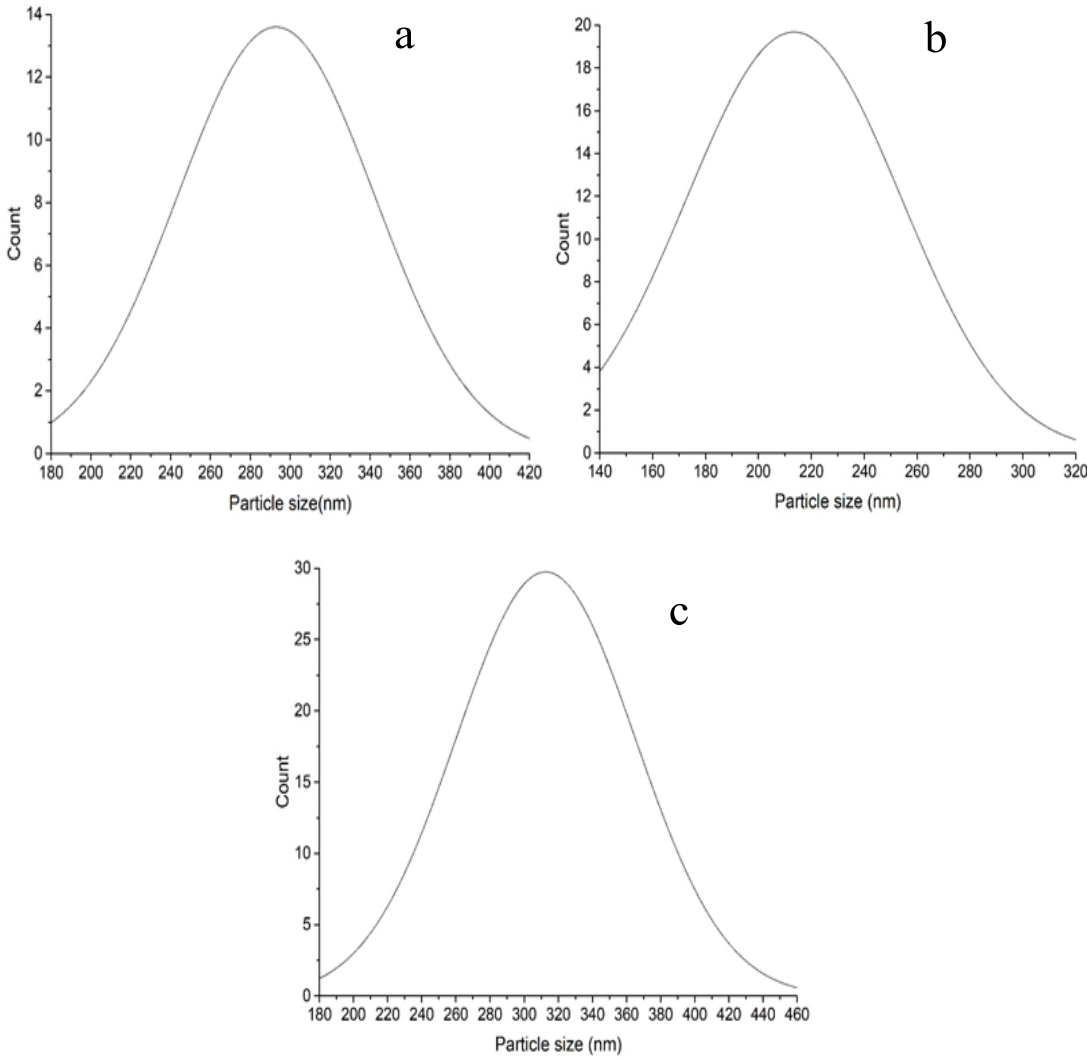

Figure 4.22: Particle size distributions of (a) $MNS_{M/E1}$, (b) $MNS_{M/E1.5}$ and (c) $MNS_{M/E2}$

Table 4.11: Variation of weight loss (%), extracted yield (%) and average particle size with P(MAA-EHA) level of modification of nanosilica

Surface modification level (%)	Weight loss (%) between 150-500 °C	Extracted yield (%)	Average particle size (nm)
1	18	7.17	292
1.5	13	12.8	213
2	24	8.5	312
2.5	-	No yield obtained	-

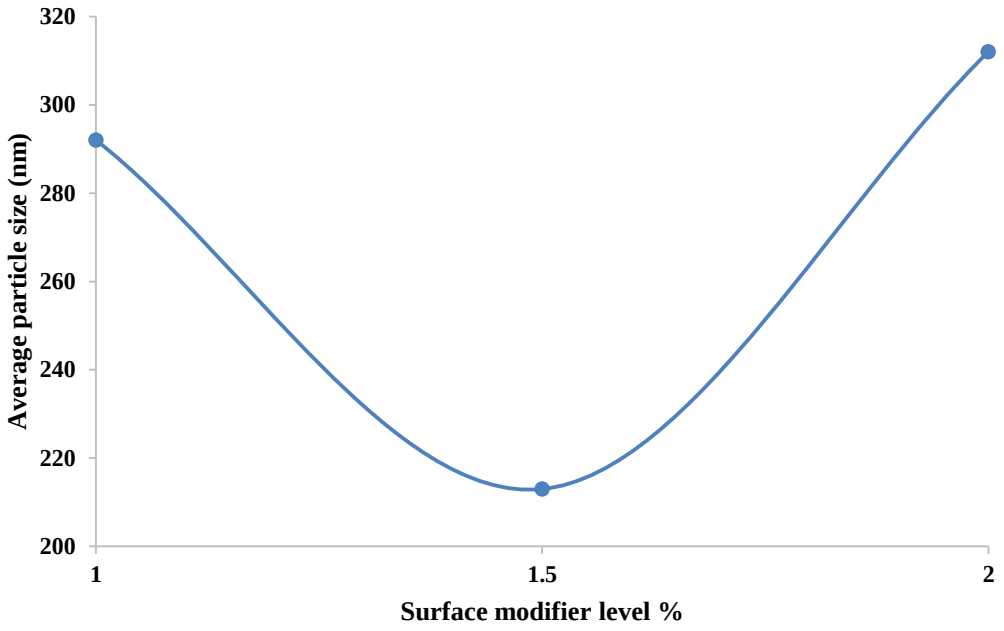

Figure 4.23: Variation of average particle size with level of surface modifier P(MAA-EHA)

The particle size distribution results showed that the samples have well-defined size range and narrow size distribution. The average particle size distribution values of PMAA modified nanosilica reveal that the average particle size gradually decreased in the order of 1%, 1.5%, 2% and increased at 2.5% PMAA modified nanosilica (See Figure 4.21). In short, minimum particle size could be observed at MNS_{M2} (See Table 4.10). The same scenario could be observed in P(MAA-EHA) modified nanosilica as well. In which, the average particle size decreased in the order of 1% & 1.5% and then increased at 2% P(MAA-EHA) modified nanosilica (See Table 4.11). Here, the minimum particle size could be observed at 1.5% (See Figure 4.23) where the lowest weight loss (%) and highest extracted yield (%) could also be observed. As mentioned earlier, this remarks that the surface modification technique at MNS_{M2} and $MNS_{M/E1.5}$ is unique. The average particle size decreased with increasing surface modifier level up to 2% and then increased in PMAA modified nanosilica (See Figure 4.21). Similarly, the average particle size decreased with increasing surface modifier level up to 1.5% and then increased in P(MAA-EHA) modified nanosilica (See Figure 4.23) (Thuc & Thuc, 2013).

Above observations indicate that; 2% for PMAA surface modifier and 1.5% for P(MAA-EHA) surface modifier are the best surface modification levels for nanosilica. Therefore, MNS_{M2} and $MNS_{M/E1.5}$ together with UMNS and VN_3 were used for the reinforcement of XNBR latex vulcanizates throughout this study.

4.1.3 Properties of XNBR latex vulcanizates filled with acrylic polymer modified nanosilica

4.1.3.1 Results of FTIR analysis of XNBR latex vulcanizates

The chemical environments of the filler-rubber interaction within the films were explored via FTIR spectroscopy. In this study, 10 phr level of filler loading was selected to investigate the effect of filler on the properties of the XNBR latex vulcanizates.

Figure 4.24 shows the FTIR spectrum of the unfilled XNBR latex vulcanizates, and Table 4.12 shows the characteristic group frequencies for the unfilled XNBR latex vulcanizates. In the spectrum of unfilled XNBR indicate peaks in the range 1600–1800 cm^{-1} appeared due to the presence of carboxylic groups in polymer chain. A peak located at about 2236 cm^{-1} was obtained due to the triple bond of nitrile group. The other designated peaks positioned at 921, 970, 1446, 1703, 2854, and 2923 cm^{-1} are due to the presence of hydrocarbon moieties of the XNBR structure (Ain & Azura, 2011). The O-H stretching frequency of the acid dimer appeared as a broad band centered at about 3495cm^{-1}. The spectrum of the nanosilica filled XNBR latex vulcanizate in Figure 4.25 shows pronounced bands appearing at 1080 cm^{-1} and 815 cm^{-1}. These bands are responsible for the vibration absorption of the silane group (Si-O-C) present in the elastomer network, which usually presents within the ranges 800–850 and 1100–1200 cm^{-1} (Jing, Lee, & Choi, 2002). The presence of these bands confirm the presence of interactions between silica and rubber chains.

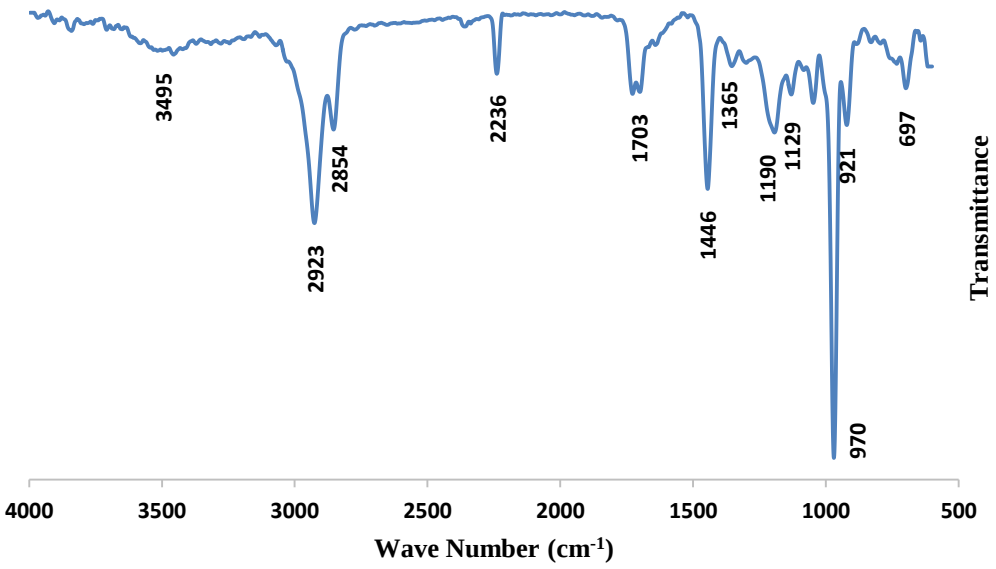

Figure 4.24: FTIR spectrum of unfilled XNBR latex vulcanizate

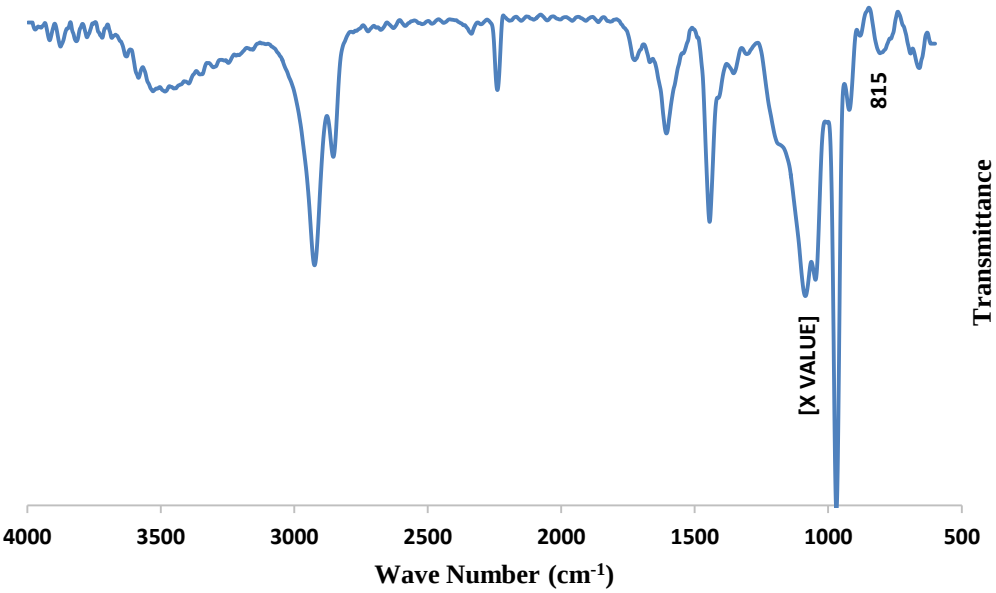

Figure 4.25: FTIR spectrum of UMNS filled XNBR latex vulcanizate

Table 4.12: Characteristic Group Frequencies of the unfilled XNBR latex vulcanizate (Ain & Azura, 2011)

Wave number (cm^{-1})	Assignment
921	Out-of-plane vibration of the methylene hydrogen atom of the vinyl group
970	Out-of-plane vibration of the hydrogen atom of the 1,4-trans component
1446	In-plane deformation of the methylene group
1703	Carbonyl stretching of monocarboxylic acid
2236	Stretching of nitrile triple bonds
2923	Symmetric stretching of the methylene group
3495	O-H stretching of the acid dimer

4.1.3.2 Results of physical properties of XNBR latex vulcanizates filled with acrylic polymer modified nanosilica

Possible interactions could be occur within the unmodified and modified silica filled vulcanizates as follows;

Filler-filler interactions (F/F): According to numerous studies, there is high interactions could be observed for silica due to the formation of silica due to the silanol groups (Si-OH) on the outer surface of silica particles(i.e. Figure 4.26). Therefore, there is a high tendency to agglomerate silica particles forming hydrogen bonds between surface silanol groups creating strong silica agglomerates. Consequently, enhancement of silica loading would be lead to the enhancement of silica–silica interaction and, hence, to decrease filler–rubber interactions.

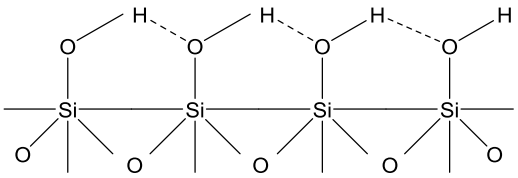

Figure 4.26: F/F interactions

Filler-rubber interactions (F/R): F/R interaction intensely influences on the reinforcing property in rubber compounds. The large number of silanol and siloxane

groups of the silica surface can be characterized by the surface energy. The surface energy be influenced by van der Waals forces, dipole-dipole interactions, van der Waals forces, electrostatic interactions and hydrogen bonding. The surface energy of a filler can be defined by the following equation, which is consists with two distinctive components (Mihara, 2009):

$$\gamma^{s} = \gamma^{d}_{s} + \gamma^{sp}_{s}$$

Dispersive component (γ^{d}_{s}), represent the degree of adhesion of inorganic fillers to an organic matrices such as a rubber polymer, and polar component (γ^{sp}_{s}) , represent the degree of intra molecular interactions of filler-filler particles. The γ^{sp}_{s} component is relatively high for silica filler compared to that of carbon black filler because of the large number of polar groups on the silica surface. The γ^{d}_{s} component, responsible for the degree of wetting of fillers by rubber, depends on the dissimilarity of the solubility parameters. According to the solubility parameters, the compatibility of silica with XNBR is better compared to that with natural rubber due to the presence of polar constituents in XNBR molecules (i.e. Figure 4.27).

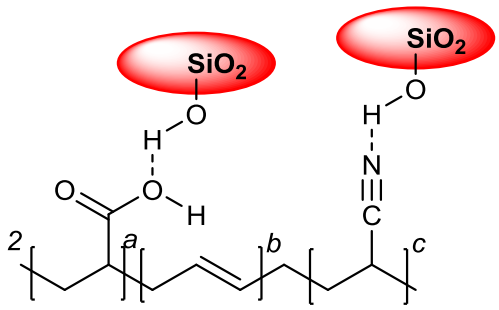

Figure 4.27: F/R interactions

Filler-surface modifier interactions (F/M): To decrease the above mentioned F/F interactions and enhance F/R interactions, surface modifiers are introduced on silica surface to improve the compatibility between rubber matrix and filler matrix. Therefore, it is important to employ the surface modifiers which may have ability to form bridge between both filler and rubber. Hydrophilic groups of surface modifiers may form hydrogen bonds between surface silanol groups silica as shown in Figure 4.28.

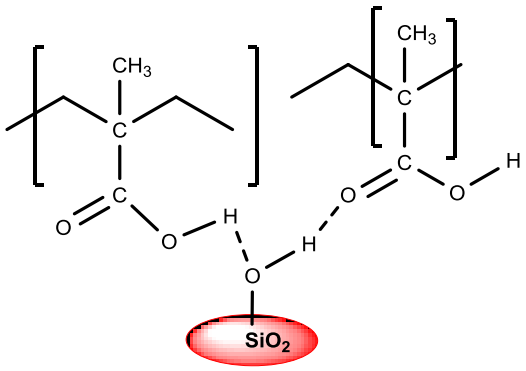

Figure 4.28: F/M interactions

Surface modifier-rubber interactions (M/R): Carboxylic groups present in modifier may form hydrogen bonds with carboxylic groups existing in XNBR (i.e. Figure 4.29). There may be a tendency to form van der Waals bonds between hydrophobic moieties presence in both rubber and surface modifier, as well.

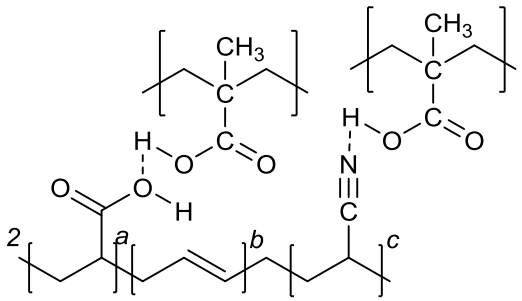

Figure 4.29: M/R interactions

Rubber/vulcanization agent interactions (R/V): XNBR can be cross-linked by conventional sulphur and accelerator system and several other methods. Through the remaining C=C double bonds of the butadiene units of the XNBR, covalent crosslinking sites are available making the thermal curing with either peroxides or sulfur in the presence of accelerators feasible. Moreover, the carboxylic groups introduced both ionic and covalent crosslink sites bonds into the XNBR network. The physical properties of XNBR articles are mainly governed by ionic bonds that are formed between the carboxylic moieties in the presence of salts and oxides of multivalent metals (e.g., ZnO and MgO). The tensile and modulus values increased, while the extension tended to be lower and tear strength poorer. In the present study,

the conventional thermal curing with ZnO is employed to generate ionic crosslinks with the rubber matrix. (See Figure 4.30)

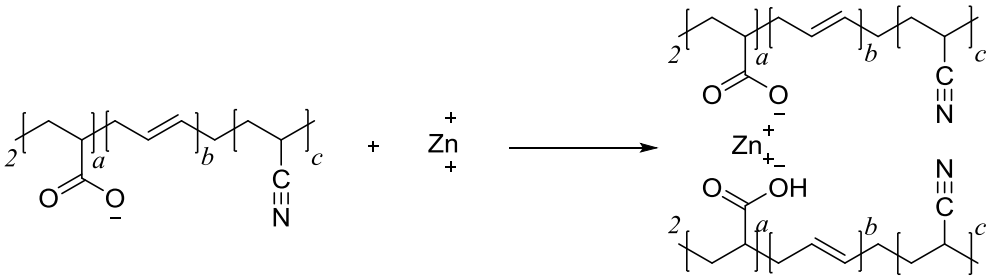

Figure 4.30: R/V interactions

Surface modifier-vulcanization agent interactions (M/V): As mentioned in rubber/vulcanization agent interactions, ZnO vulcanizing agent has the ability to form ionic crosslinks with carboxylic moieties. Hence, there is a tendency to form ionic crosslinks between ZnO and carboxylic groups present in surface modifiers (PMAA and P(MAA-EHA)) (See Figure 4.31). These interactions are also responsible for high tensile & modulus and low elongation & tear values.

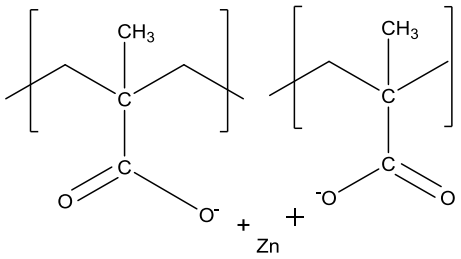

Figure 4.31: M/V interactions

Bound rubber model of silica filled rubber

Due to the presence of number of chemical involved during compounding, numerous chemical reactions could be take place during processing of filler filled elastomers. Hence, a novel model has been introduced to describe the behavior of fillers in rubber matrix. According to this model there are two components can be introduced: one is occluded rubber in the silica aggregates and cross-linked polymer due to recoupling and polymer chain scission [Mihara, 2009].

Luginsland et al. proposed a simple model of silica/silane reinforcement based on the hydrodynamic-occlusion-interaction theory as proposed by Medalia [Luginsland, 2002]. A schematic representation of the model is shown in Figure 4.32. This model can be applied to this study to discuss silica/ acrylic polymer reinforcement.

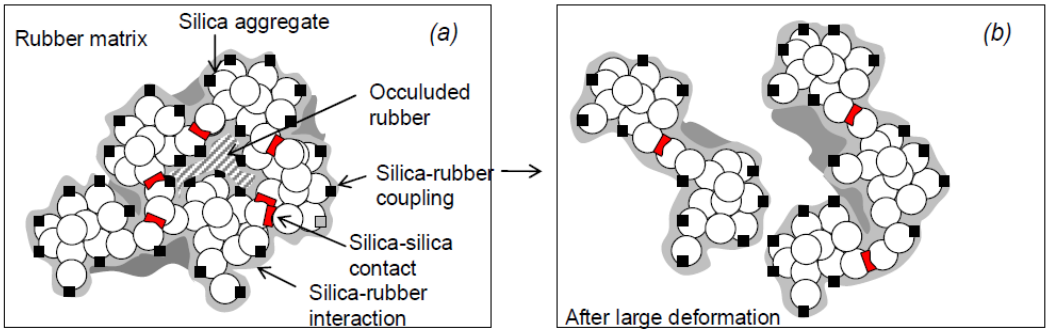

Figure 4.32: Bound rubber model [Mihara, 2009]

Due to the large polarity differences between silica and rubber, the filler-filler network can simply arrange and as a result, part of the rubber matrix is occluded in this filler network. Therefore, chemically and physically immobilized occluded rubber could be formed within the filler network. When, high deformations take place on the rubber- filler network, this filler network could be partly breaks open. Surface modified filler filled vulcanizates encourage the less giant filler-filler network resulting less formation of occluded rubber in the matrix. Therefore, in surface modified silica filled matrix comprises with less immobilized rubber which is contribute to the modulus property [Mihara, 2009].

Figures 4.33 to 4.36 illustrate the variation of TS, EB (%), M300 and TRS of XNBR vulcanizates filled with different levels of MNS_{M2} and $MNS_{M/E1.5}$ separately. The TS, EB (%), M300 and TRS of equivalent films containing VN_3 and UMNS are also plotted for comparison.

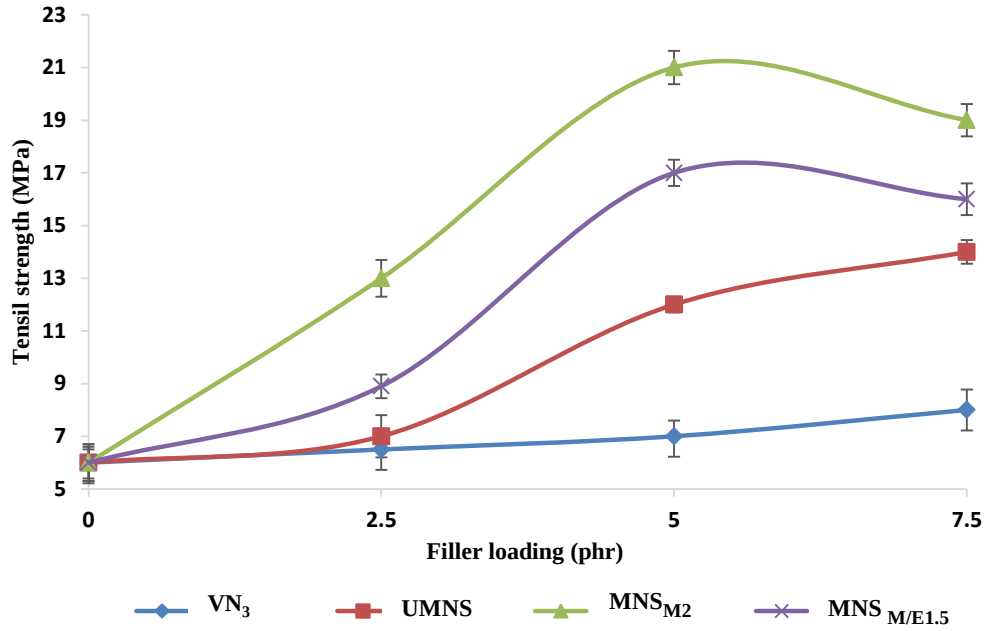

Figure 4.33: Variation of TS of XNBR latex vulcanizates with MNS_{M2} and $MNS_{M/E1.5}$ at different levels of filler loading

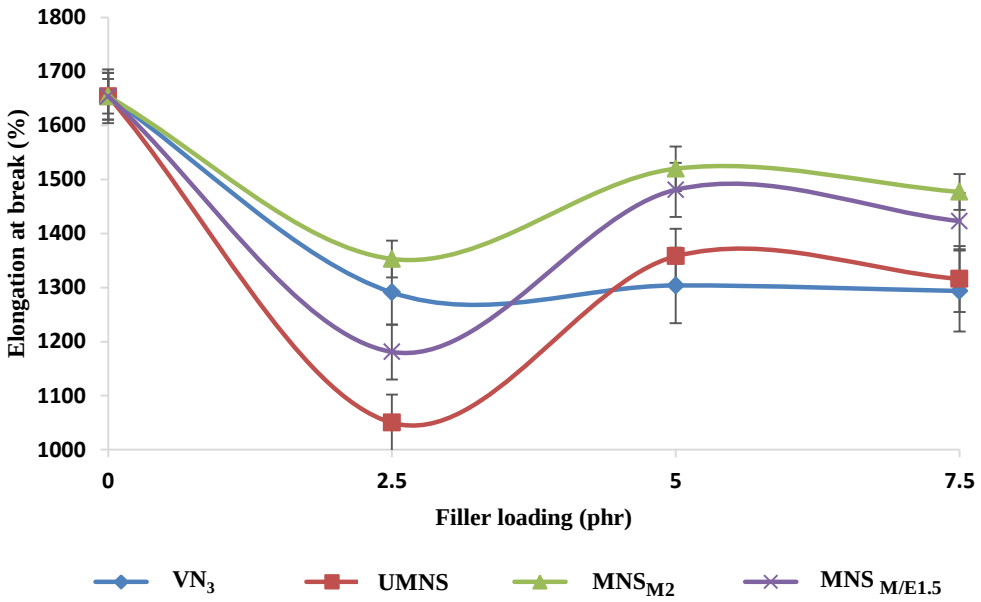

Figure 4.34: Variation of EB of XNBR latex vulcanizates with MNS_{M2} and $MNS_{M/E1.5}$ at different levels of filler loading

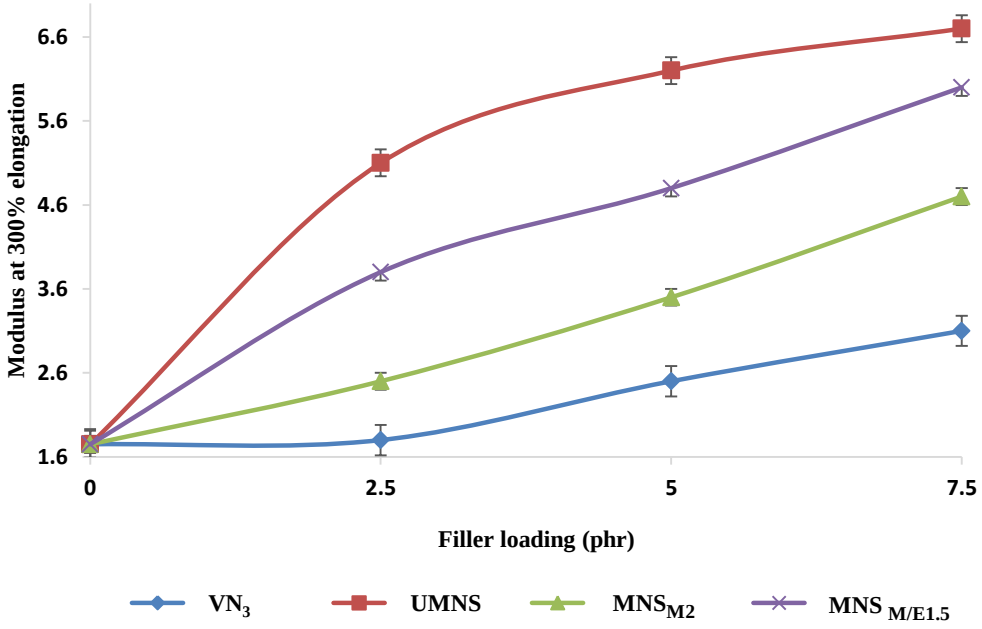

Figure 4.35: Variation of M300 of XNBR latex vulcanizates with MNS_{M2} and $MNS_{M/E1.5}$ at different levels of filler loading

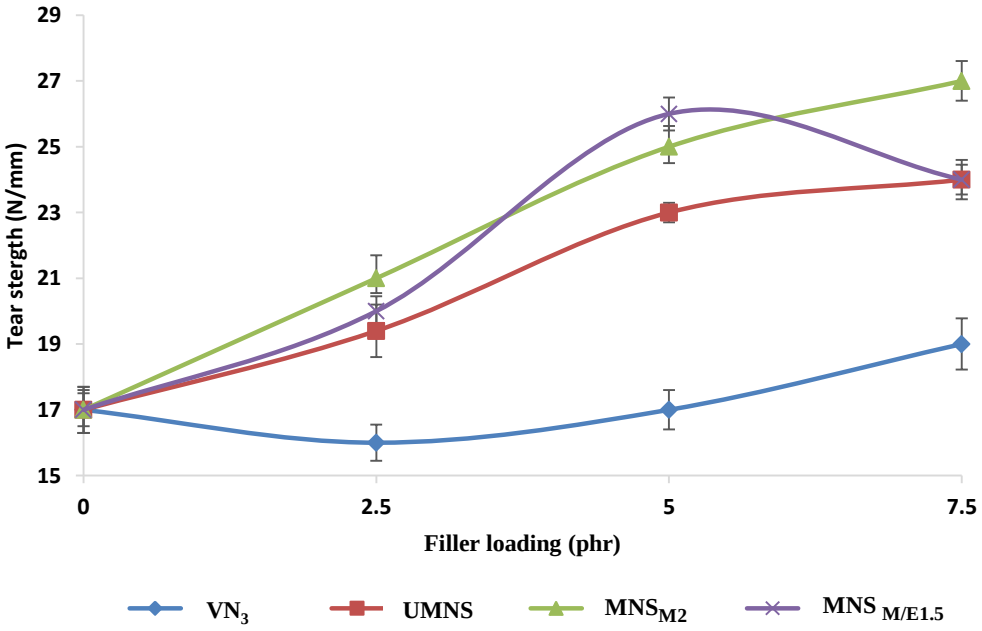

Figure 4.36: Variation of TRS of XNBR latex vulcanizates with MNS_{M2} and $MNS_{M/E1.5}$ at different levels of filler loading

In films filled with of VN_3 or UMNS, only F/F, F/R and R/V interactions are possible within the vulcanizate. To inherent the good physical properties, it is important to have high physical and chemical interactions between rubber and filler phases, transferring the mechanical forces from rubber matrix to filler particles efficiently. Thus, when surface modifiers are applied, additional F/M and M/R interactions may be formed, resulting better F/R interactions compared to unmodified situations. Therefore, homopolymer and copolymer modified silica filled vulcanizates may consist of less F/F interactions and high F/R, F/M and M/V interactions. Variation of filler loadings may affect the F/F, F/R interactions in unmodified filler filled vulcanizates, while that in modified filler filled vulcanizates F/F, F/R, F/M, M/R and M/V interactions get affected.

Tensile properties are one of the most significant criteria to gauge the usefulness of rubber articles for glove manufacturing. As expected, TS of filled vulcanizates is higher than that of unfilled vulcanizates. This is because, XNBR synthetic polymers are not inherent with self-reinforcing ability like natural rubber. Therefore, it is indispensable to use reinforcing fillers in XNBR to induce better physical properties.

TS of the latex films containing MNS_{M2} was found to be highest over all the levels of filler addition. And also the TS of UMNS filled latex films was higher at the all levels of filler addition than VN_3 filled latex films. High surface area of nanosilica imparts the ability to form better F/R interactions leading to the improved physical properties of latex vulcanizates. TS of VN_3 filled latex vulcanizates at 7.5 phr level of filler addition can be obtained from UMNS filled latex vulcanizates at 2.5 phr level of filler addition. In surface modified latex vulcanizates, the TS increases gradually with the level of filler addition, reaching a maximum and then slightly decreases with the increase of the filler level. Surface modified latex vulcanizates always show better tensile properties within the all levels of filler addition than unmodified filler filled vulcanizates. Both MNS_{M2} and $MNS_{M/E1.5}$ filler filled latex vulcanizates show their maximum TS at 5 phr filler level. The maximum TS observed for MNS_{M2} filled vulcanizates at 5 phr was found to be increased by 200% of that of VN_3 filled vulcanizates while for $MNS_{M/E1.5}$ filled vulcanizates was about 143%. At this filler loading, the TS increment by UMNS filled vulcanizates was

about 72% of that VN_3 filled vulcanizates. In other words, TS of MNS_{M2} filled vulcanizates was about three times of that of UMNS filled vulcanizates.

Meanwhile, $MNS_{M/E1.5}$ filled vulcanizates also exhibit better performance compared with UMNS, again confirming the improved F/R interactions. In case of 7.5 phr level of filler addition, UMNS show higher TS value than 5 phr level. In contrast, MNS_{M2} and $MNS_{M/E1.5}$ show slightly lower TS value at 7.5 phr than 5 phr level. This is because, high filler loading increase the F/F interactions. This is a prominent phenomenon especially for nanosilica particles due to its high surface area.

EB expresses the capability of a latex film to resist changes of shape without crack formation, which is significant in glove production. According to the elongation results depicted by Figure 4.34, sudden reduction could be observed with the addition of fillers. This is because the rubber is likely to stretch more when unfilled and then if very fine particles are introduced and fill the spaces, it will restrict the movements of polymer chains and decrease elongation property as described in bound rubber model before.

In the case of VN_3 filled vulcanizates it is observed that the change of EB is only marginal. Nevertheless, in UMNS, MNS_{M2} and $MNS_{M/E1.5}$ filled vulcanizates EB was found to increase gradually when the filler content was incremental from 2.5 phr to 5 phr. This is due to the diffusion of very fine nanosilica through the rubber chains and support the rubber chains while enhancing stretching, which is reflected by elongation. However, it was also found that EB of acrylic polymer modified silica filled vulcanizates was higher than that of UMNS filled vulacanizates. This could be described by bound rubber model. Immobilized occluded rubber is formed due to the F/F interactions in latter case. In modified silica, formation of occluded rubber is less due to the surface modification of silica surface leading to less F/F interactions.

Glove manufacturers must carefully balance strength with stretch and comfort. Too high TS will make a glove stiff or difficult to donning. Therefore, elongation is important to the performance of the glove. High elongation supports the glove material to stretch instead of tear when snagged. A glove with good elongation will stretch and conform to the hand, improving comfort and performance. MNS_{M2} filled

vulcanizates showed the best performance at 5 phr level of filler addition with balanced strength and stretch.

It was observed that M300 in all types of vulcanizates was increased continuously with the level of filler addition. It can also be seen that the moduli of all the filled vulcanizates were higher than those of the unfilled vulcanizates. The increase in moduli is due to the stiffening effect caused by the interaction between silica particles with the rubber matrix.

M300 is an important property in predicting the stiffness of the glove, for its performance and durability during the donning of the glove. M300 of all the unmodified and modified nanofiller filled vulcanizates were higher than those of VN_3 filled vulcanizates. This is a consequence of high surface area of nanofiller which helps to form better F/R interaction in comparison with the micro filler. The fineness of silica particles also makes it easy to distribute between rubber chains, increasing the modulus of elasticity. UMNS filled vulcanizates showed the highest M300 over all levels of filler addition than the homopolymer and copolymer modified nanosilica filled vulcanizates. This observation could be explained through the bound rubber model. UMNS filled vulcanizates contained high amount of F/F interactions than modified filler filled vulcanizates. Hence, UMNS filled vulcanizates may contain more occluded rubber and the rubber on the silica surface remain grossly immobilized, and therefore still contribute to the high modulus. Meanwhile, MNS_{M2} and $MNS_{M/E1.5}$ consists with low F/F interactions compared to UMNS, resulting less occluded rubber causing low modulus at small deformations.

However, modified nanofiller filled vulcanizates show lower stiffness values retaining the other properties as well. This observation together with the results of TS and EB indicates that MNS_{M2} filled vulcanizates are more viable for glove production with balanced strength, stretch and stiffness.

As for TRS, the TRS increased in all XNBR vulcanizates with the level of filler addition because XNBR do not achieve self-reinforcing effect and are thus of inherently low strength.

As shown in Figure 4.36, the TRS of unmodified and modified nanosilica filled vulcanizates were higher than that of VN_3 filled vulcanizates at all the levels of filler addition due to the fine dispersion of filler resulting in good adhesion at the rubber-filler interface, which is the basic requirement for attaining optimum reinforcement. High surface area of the nanosilica when compared to micro silica leads to better rubber-filler interactions. TRS of VN_3 filled vulcanizates at 7.5 phr of filler addition could be obtained by UMNS filled vulcanizates at 5 phr of filler addition. The surface modified nanosilica filled films showed slightly higher TRS than UMNS filled films. Generally, high TRS can be observed for MNS_{M2} filled films whilst the highest value was at 7.5 phr level of filler addition. The maximum TRS observed for MNS_{M2} filled vulcanizates at 7.5 phr was about 35% of that of VN_3 filled vulcanizates whereas the corresponding increase was about 20% for $MNS_{M/E1.5}$ filled vulcanizates. Similarly, the increase for UMNS filled vulcanizates was about 20%. The TRS of MNS_{M2} filled vulcanizates at 5 phr was increased by about 32% of that of VN_3 filled vulcanizates while corresponding increase was about 37% for $MNS_{M/E1.5}$ filled vulcanizates and about 35% for UMNS filled vulcanizates respectively.

Figures 4.37 to 4.40 illustrate the variation of TS, EB, M300 and TRS of XNBR vulcanizates filled with $*MNS_{M2}$ and $*MNS_{M/E1.5}$ at different levels of filler addition respectively. The TS, EB, M300 and TRS of equivalent films containing VN_3 and UMNS are also plotted for comparison. These are almost an extended version of Figures 4.33 to 4.36 respectively.

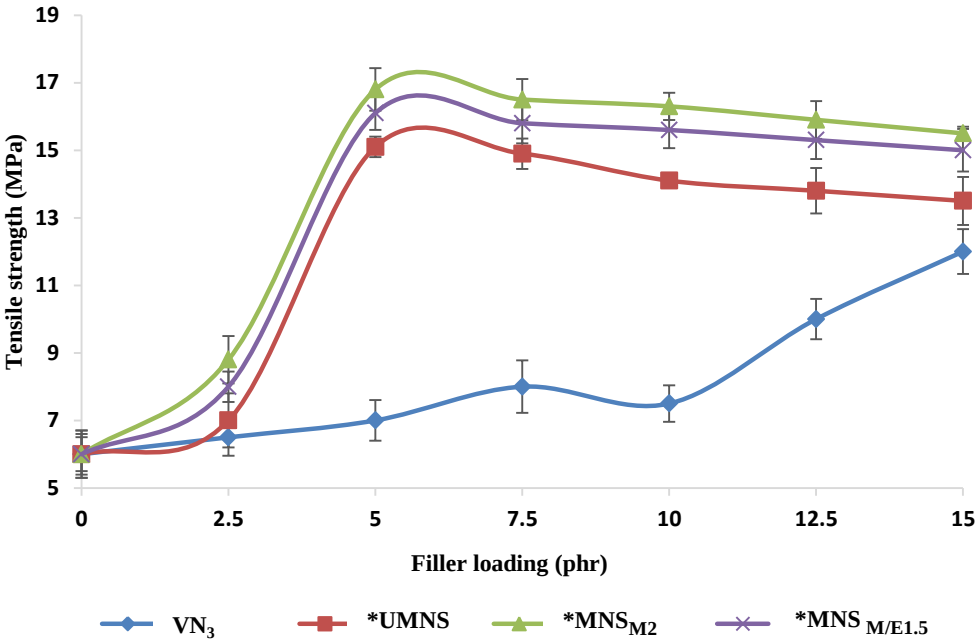

Figure 4.37: Variation of TS of XNBR latex vulcanizates with *MNS_{M2} and *$MNS_{M/E1.5}$ at different levels of filler loading

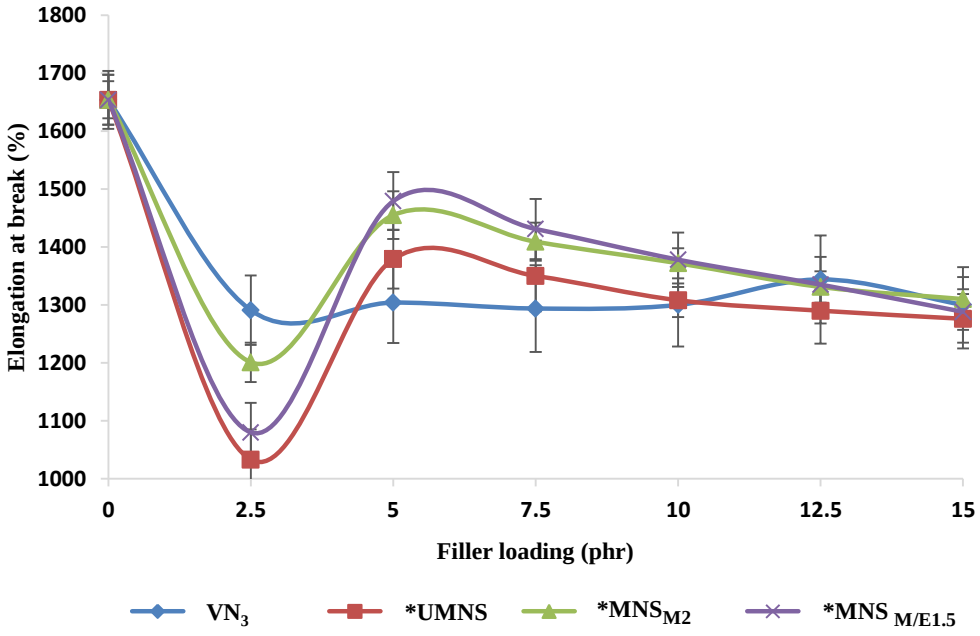

Figure 4.38: Variation of EB of XNBR latex vulcanizates with *MNS_{M2} and *$MNS_{M/E1.5}$ at different levels of filler loading

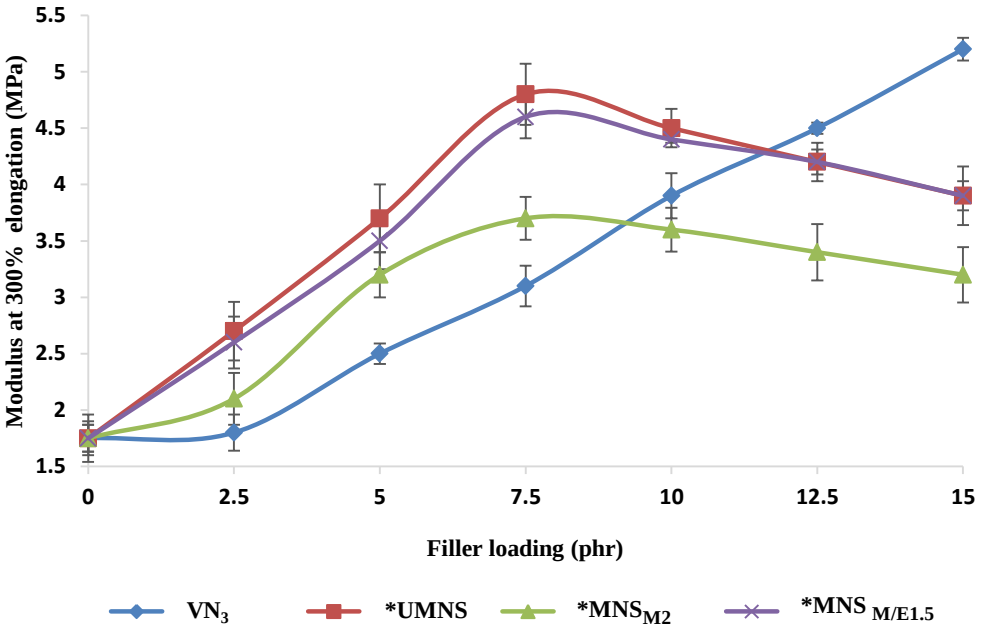

Figure 4.39: Variation of M300 of XNBR latex vulcanizates with *MNS_{M2} and *$MNS_{M/E1.5}$ at different levels of filler loading

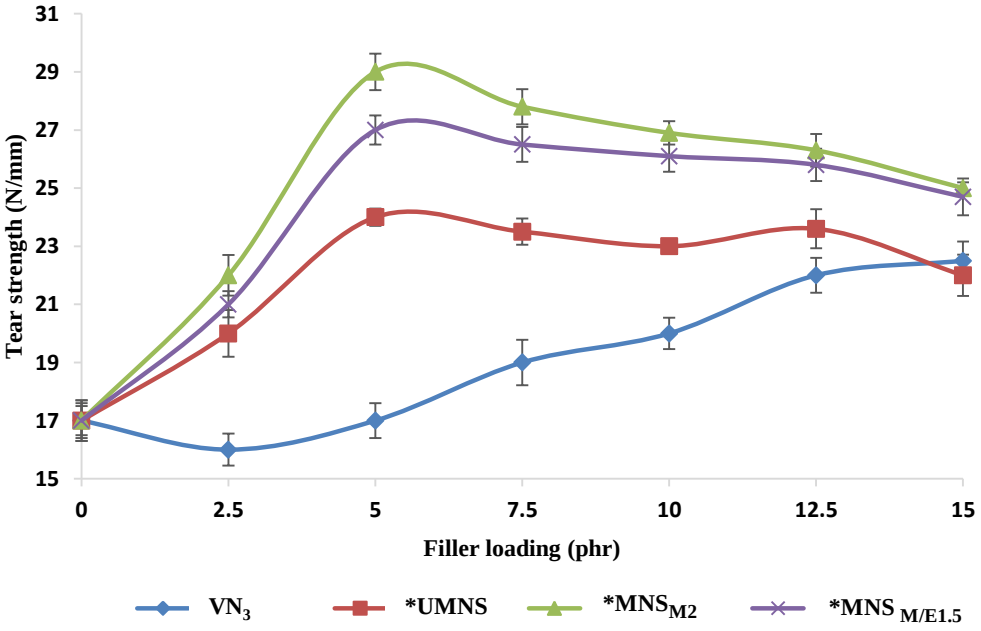

Figure 4.40: Variation of TRS of XNBR latex vulcanizates with *MNS_{M2} and *$MNS_{M/E1.5}$ at different levels of filler loading

According to the Figures 4.37 and 4.40, TS increases when amount of nanosilica increases up to 5 phr, and then, TS decreases with addition of nanosilica from 5 phr to 15 phr. Such a behavior can be explained by stating that, in the case of addition of small quantities, particles will fill the spaces between rubber chains, thus give a rigid structure with better TS, and in the case of addition of higher quantities, particle aggregation could occur in rubber matrix, thus weakening the bond between chains and decreasing TS. This results suggest that poor dispersion of nanosilica filler in the elastomeric network contributed to the trend observed. In contrast, addition of VN_3 from 0 phr to 15 phr, gradually increases the TS. This is because, enhancement of reinforcing filler region, clues to the improved physical properties.

According to the Figure 4.38 elongation property increases within 2.5 phr to 5 phr and then decreases continuously up to 15 phr of nanofiller filled vulcanizates. Consequently, this evidently proves that the best EB could be observed for $*MNS_{M2}$ and $*MNS_{M/E1.5}$ filled vulcanizates at 5 phr level of addition.

M300 of nanofiller filled vulcanizates in increased and emanate to its pinnacle point at 7.5 phr level of filler addition and then decrease continuously up to 15 phr (See Figure 4.39). This reduction is due to the heterogeneous distribution of unmodified and modified nanosilica leading to the agglomeration of particles at high filler concentrations. Although that M300 of VN_3 filled vulcanizates show increasing trend with the increasing of filler level, it could be explained by the results together with TS and crosslink density. In the state of VN_3 filled vulcanizates addition of filler continuously expresses the reinforcement capability, disparate to the state of nanosilica addition.

As shown by Figure 4.40, TRS reaches a maximum at 5 phr of nanosilica for the same reason as mentioned previously in the case of tensile property, that the particles will fill the spaces between rubber chains and make cross-links between each other and this leads to better tear resistance. In case, when addition of nanofiller level increases from the maximum of 5 to 15 phr, TRS will decrease. This may be due to the irregular distribution of nanosilica particles in rubber matrix and aggregation between nanoparticles.

4.1.3.3 Swelling properties

The swelling test gives an idea about the extent of dissolution of cross-linked polymers in different liquids. Solvent absorption into the cross-linked networks is highly depends on the molecular weight of the solvent, temperature, extend of crosslinking and rubber/solvent interactions, besides the ingredients added. Crosslinking density highly depends on the R/V interactions in unmodified filler filled vulcanizates while, in modified vulcanizates, both R/V and M/V interactions are important. Solvents are filled to the voids on rubber-filler interface. If the F/R interactions are more powerful, the tendency to remain voids on the rubber-filler interface is very less, leading to low solvent absorption to the vulcanizate.

At the beginning, the swelling rate is very high, and then reaches to its equilibrium state with the time. The observed high swelling rate may be due to the high solvent stress and large concentration gradient of the polymer network. Lastly, at equilibrium, the concentration gradient becomes zero. The vulcanizate has the maximum MEK uptake at equilibrium swelling, screening that there is no constraint for solvent penetration. Swelling rate decreased with the increase in filler loading. This is because of, the enhancement of F/R interactions of the compounds. This interaction clues to an increase in the effective degree of cross-linking and can be assessed by equilibrium swelling and by measurements of chain orientation. Due to the carboxylate groups and the carbon-carbon double bonds in the XNBR latex films, other two types of crosslinks were expected, namely the ionic crosslink from ZnO interacting with carboxylate groups and the sulphur crosslink from the electrophilic reaction of the butadiene groups. Assuming that ZnO and sulphur crosslinks are constant due to constant content and by varying only the filler levels in the study, it was hypothesized that any further increase of crosslinks should be due to the F/R crosslinks (Lim, Vivayganathan, & Amir-Hashim, 2012).

Figures 4.41 to 4.43 illustrate the variation of swelling %, crosslink density and rubber filler interactions respectively of XNBR latex films containing VN_3 and UMNS at different levels of addition together with those of equivalent films containing MNS_{M2} and $MNS_{M/E1.5}$.

The swelling % decreases with increasing filler loading in both unmodified and modified fillers filled vulcanizates as shown in Figure 4.41. The maximum solvent uptake could be observed for VN_3 filled vulcanizates. The nanosilica filled vulcnizates show lower solvent uptake comparing with VN_3 due to the high F/R interactions impart from the high surface area of nanosilica than micro silica. In the case of modified filler filled vulcanizates, they consists additional F/M and M/V interactions compared to unmodified filler filled latex vulcanizates. Therefore, these interactions may help to form better compatibility between rubber and filler phases, thus the voids between these interfaces are reduced. As expected, the lowest swelling % observed for MNS_{M2} filled vulcanizates. Swelling % of modified filler filled vulcanizates reduces from 2.5 to 5 phr and then increased. Reduction of swelling % could be due to the reduced F/F interactions while enhancement of F/R, F/M and M/V interactions in vulcanizates. The crosslink density is inversely proportional to the swelling %. The highest crosslink density could be observed for MNS_{M2} filled vulcanizates which obtained the lowest swelling % at all levels of filler loadings. Crosslink density of modified nanosilica filled vulcanizates reaches to its maximum values at 5 phr level of filler addition and then decreases.

The F/R interaction values further confirm the solvent uptake % and crosslink density values. The lowest Qf/Qg values could be observed at 5 phr level of filler addition for modified filler filled XNBR latex vulcanizates. Lower the Qf/Qg means higher the F/R interactions as mentioned in Chapter 03.

This swelling properties further confirm the pattern of the physical properties. The lowest swelling % and the highest crosslink density could be observed for MNS_{M2} filled vulcanizate at 5 phr filler addition which showed the highest TS.

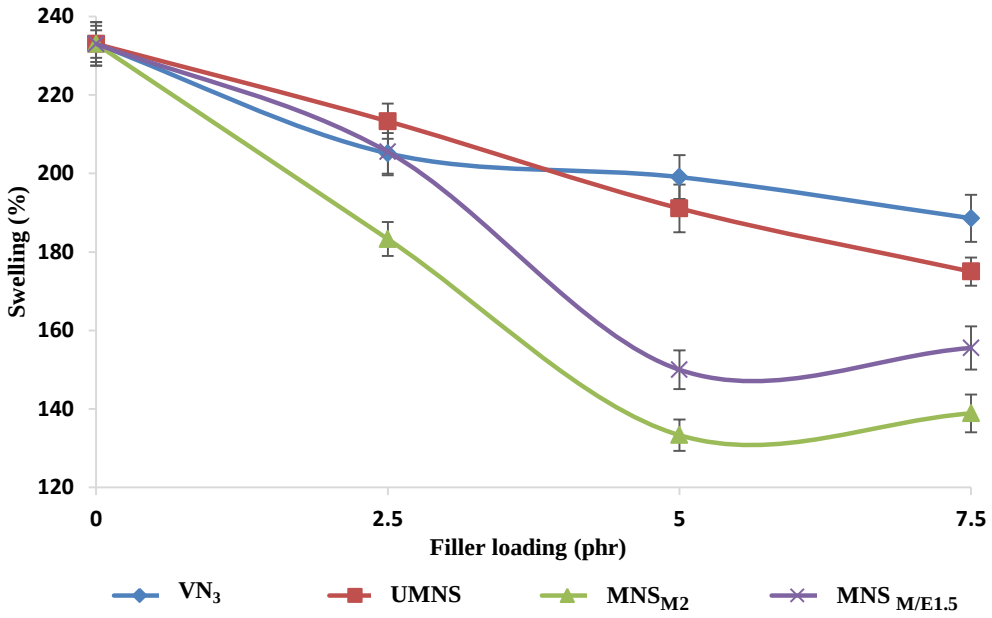

Figure 4.41: Variation of Swelling (%) of XNBR latex vulcanizates with MNS_{M2} and $MNS_{M/E1.5}$ at different levels of filler loading

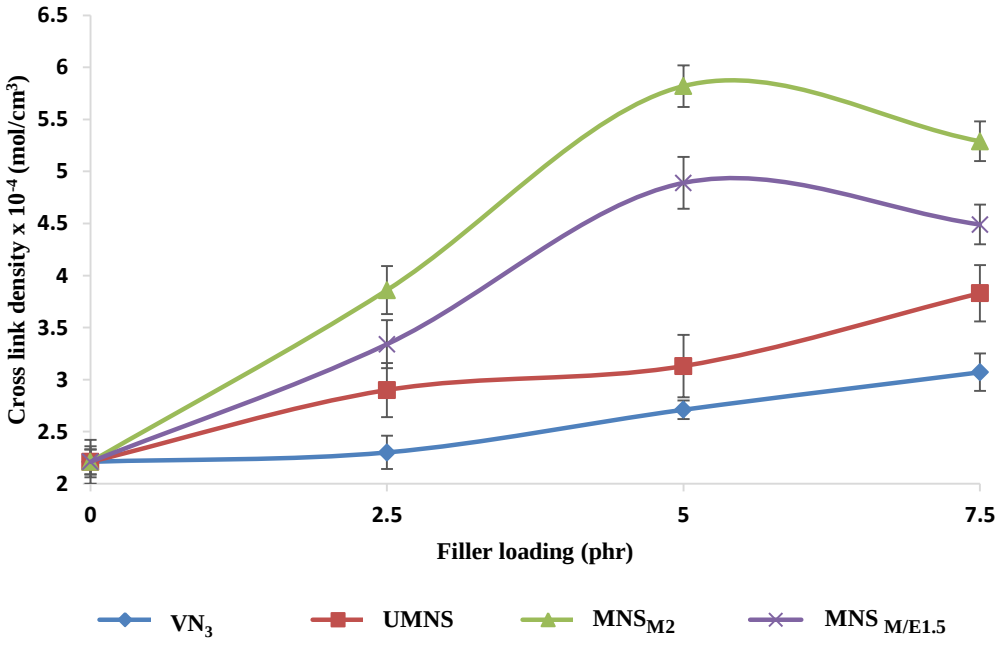

Figure 4.42: Variation of Crosslink density of XNBR latex vulcanizates with MNS_{M2} and $MNS_{M/E1.5}$ at different levels of filler loading

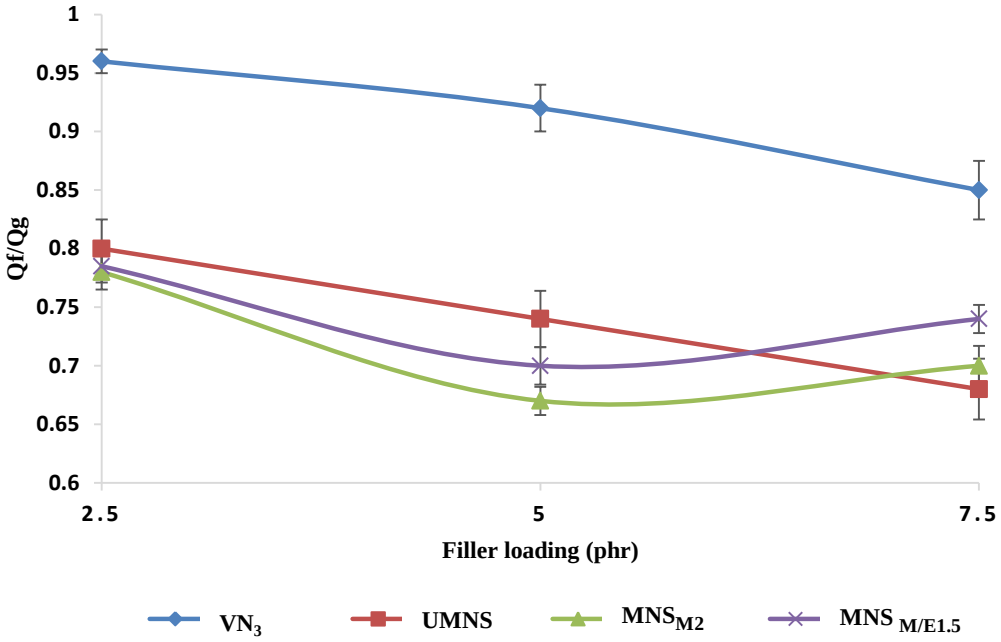

Figure 4.43: Variation of Rubber filler interactions of XNBR latex vulcanizates with MNS_{M2} and $MNS_{M/E1.5}$ at different levels of filler loading

Figures 4.44 to 4.46 illustrate the variation of swelling %, cross-link density and rubber filler interactions respectively of XNBR latex vulcanizates filled with *MNS_{M2} and *$MNS_{M/E1.5}$ at different levels of filler addition respectively. The swelling %, cross-link density and rubber filler interactions of equivalent films containing VN_3 and UMNS are also plotted for comparison. These are almost an extended versions of Figures 4.41 to 4.43 respectively.

The lowest swelling % could be observed for *MNS_{M2} filled vulcanizates. Figure 4.44 confirms the results observed in Figure 4.41. The lowest swelling % could be observed at 5 phr filler level and then again it increases continuously. But it was found that at 7.5 phr the solvent uptake was more than that at 5 phr loading. This might be due to the severe aggregation of nanosilica at the high concentrations. And also reduced pattern of crosslink density was observed after 5 phr of nanosilica filled unmodified and modified vulcanizates due to the same reason as mentioned above. Similarly, rubber filler interaction values also confirm that the best interactions at 5 phr level of filler addition for both *MNS_{M2} and *$MNS_{M/E1.5}$ filled vulcanizates (See Figure 4.46).

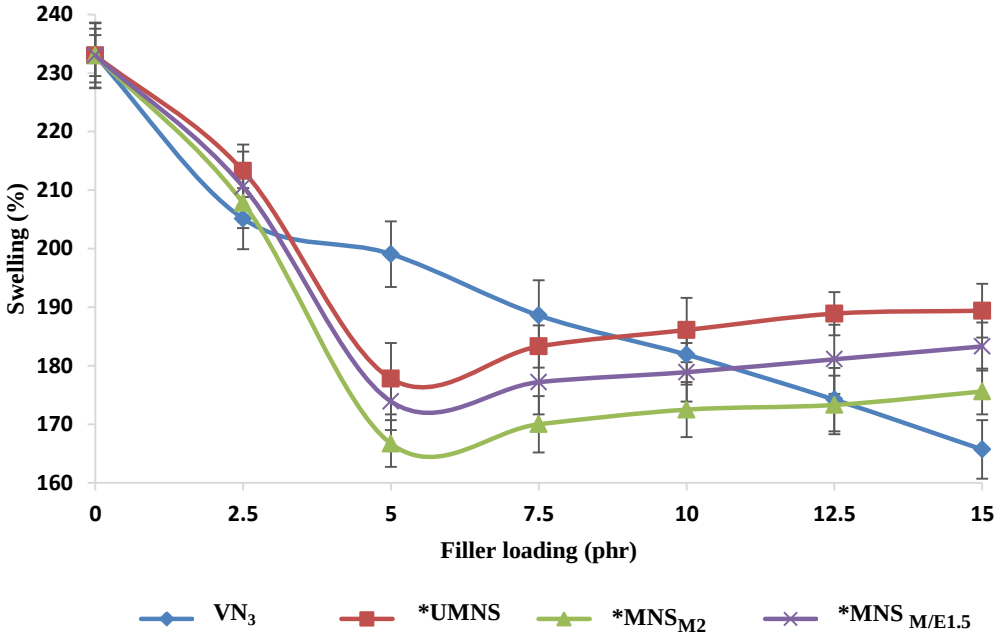

Figure 4.44: Variation of Swelling (%) of XNBR latex vulcanizates with *MNS_{M2} and *$MNS_{M/E1.5}$ at different levels of filler loading

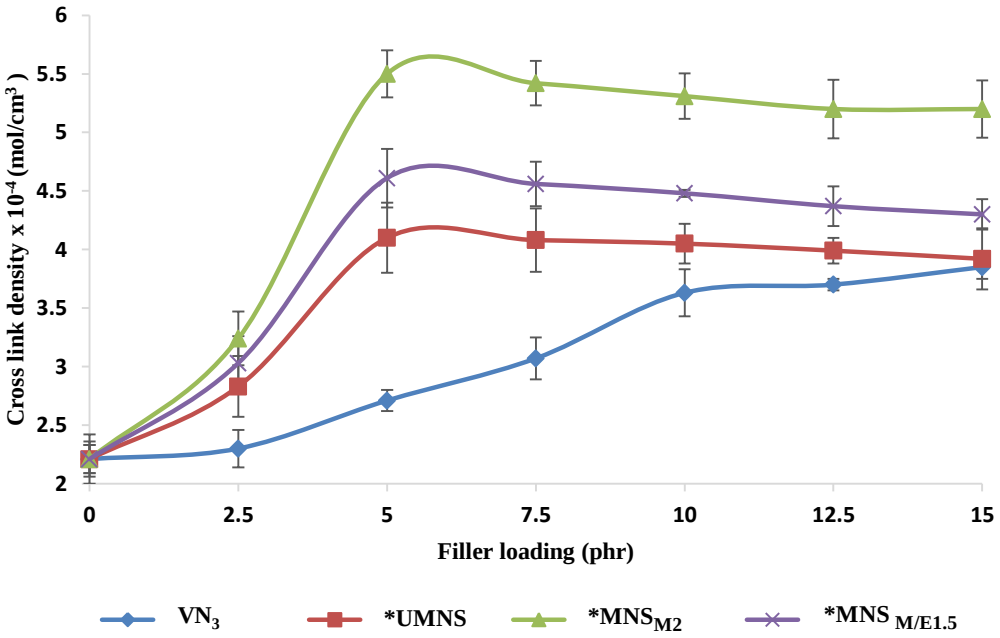

Figure 4.45: Variation of Crosslink density of XNBR latex vulcanizates with *MNS_{M2} and *$MNS_{M/E1.5}$ at different levels of filler loading

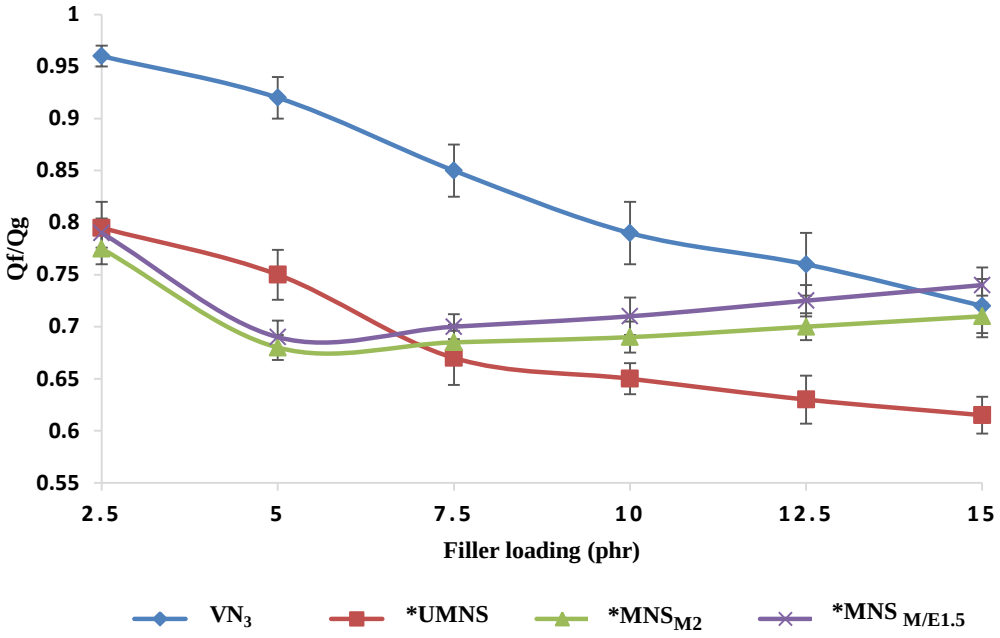

Figure 4.46: Variation of Rubber filler interactions of XNBR latex vulcanizates with *MNS_{M2} and *$MNS_{M/E1.5}$ at different levels of filler loading

4.1.4 Characterization of unmodified and NPs modified nanosilica

4.1.4.1 Surface modification of silica particles using NPs as surface modifiers

The NPs such as cellulose, collagen, chitosan and gelatin have been successfully used as suitable candidates for surface modification of silica particles especially due to their poly-functional properties. This surface modification can overcome the problem of agglomeration of silica particles and it is expected that the introduction of NPs on to the silica surface will increase the surface hydrophobicity. Alteration of the nature of the silica surface will help to reduce the F/F interactions preventing filler agglomerations and enhance F/R interactions yielding better physical properties to the final product.

4.1.4.2 Results of FTIR analysis of NPs modified nanosilica

Figure 4.47 shows the FTIR spectra of UMNS, *MNS_{CE2} and CE. The broad band in the 3660-3100 cm^{-1} region, which is due to the OH-stretching vibration, gives considerable information concerning the hydrogen bonds. The presence of the band

at 2900 cm^{-1}, corresponds to the C–H stretching vibration. In addition, the FTIR band at 1430 cm^{-1}, represents symmetric CH_2 bending vibration (Ciolacu, Ciolacu, & Popa, 2011). In *MNS_{CE2} spectra, all the characteristic peaks related to the nanosilica as described in section 4.1.2.1 can be seen.

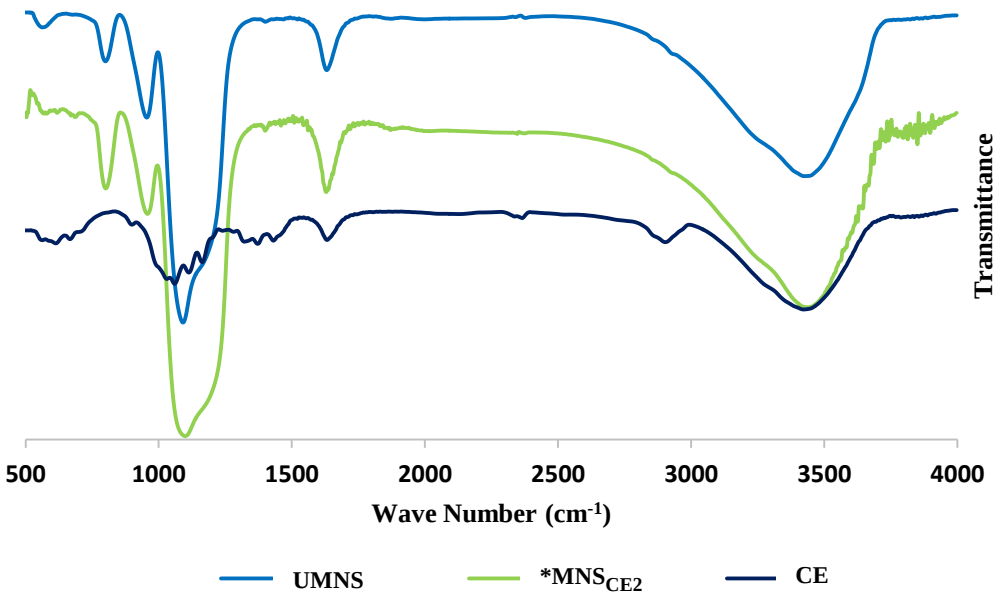

Figure 4.47: FTIR spectra of UMNS, *MNS_{CE2} and CE

Equivalent set of spectra for *MNS_{CO2}, *MNS_{CHO2} and *MNS_{GE2} are shown in Figures 4.48 to 4.50 respectively. In all the NPs modified nanosilica spectra additional peaks could be seen compared to UMNS, which are present in NP spectra.

Peaks located at in the range of 3600-3200 cm^{-1} of FTIR spectrum of the pure GE and CO were due to N–H stretching of secondary amide. C=O stretching at 1640 cm^{-1}, N–H bending between 1550 and 1500 cm^{-1}, N–H out of plane wagging at 670 cm^{-1} and C–H stretching at 2940, 2850 and 1040 cm^{-1} can also be seen in GE and CO spectra (Bhowmik et al., 2017). In both *MNS_{CO2} and *MNS_{GE2} spectra all the characteristic peaks of nanosilica: 3600-3200 cm^{-1} for O-H stretching vibration, 1200-1100 cm^{-1} for Si-O-Si asymmetric stretching vibration, 960 cm^{-1} for Si-OH stretching vibration and 800cm^{-1} for symmetric stretching vibration of Si-O-Si are present (Al-Oweini & El-Rassy, 2009). In both modified FTIR spectra show the C-H

stretching peaks at around 2924 and 2853 cm^{-1}, clearly indicating the organic modification of the nanoparticle surface with CO and GE.

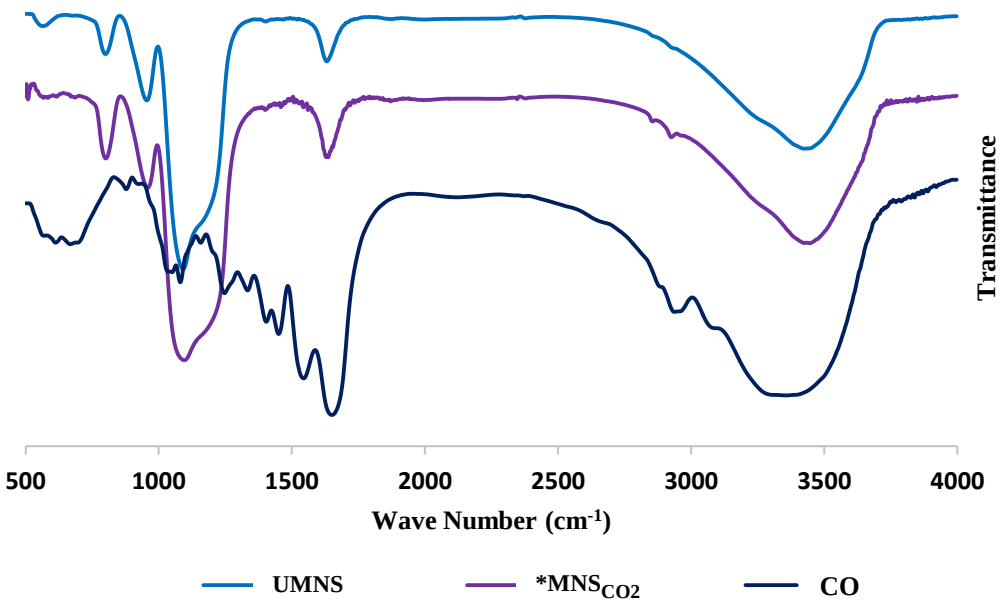

Figure 4.48: FTIR spectra of UMNS, $*MNS_{CO2}$ and CO

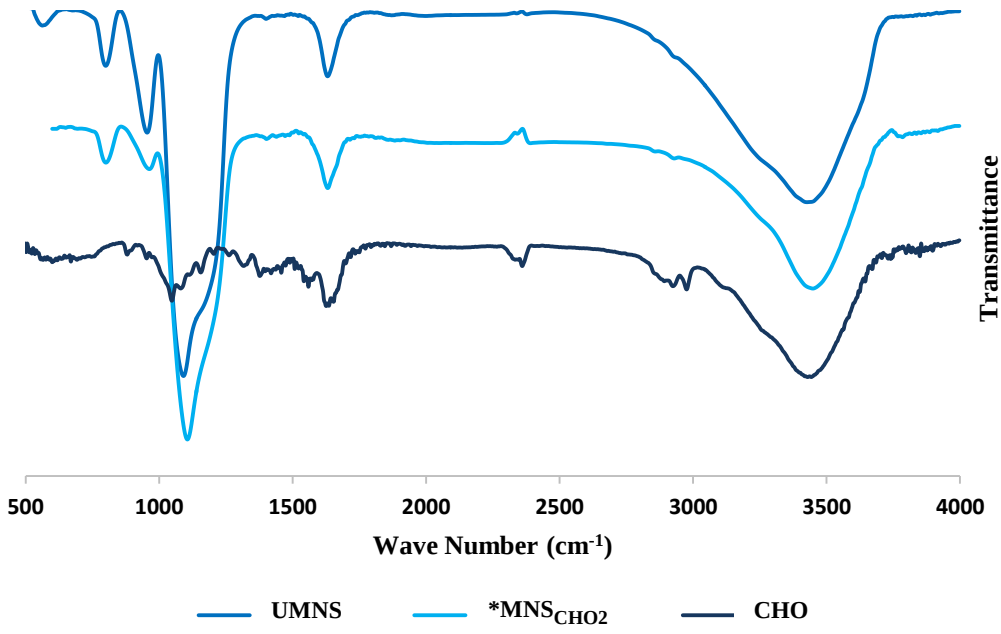

Figure 4.49: FTIR spectra of UMNS, $*MNS_{CHO2}$ and CHO

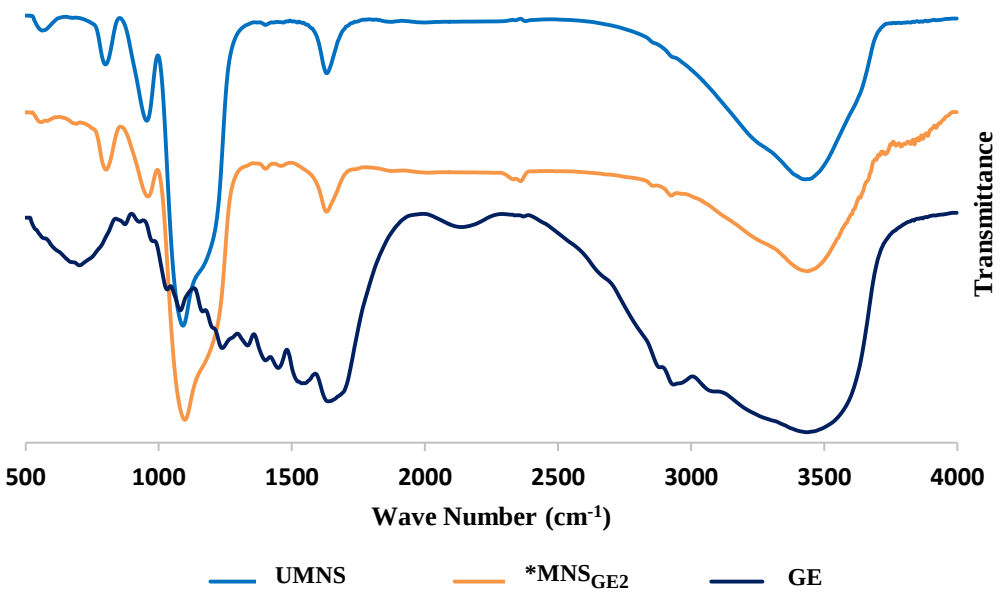

Figure 4.50: FTIR spectra of UMNS, *MNS_{GE2} and GE

4.1.4.3 Results of TGA of NPs modified nanosilica

Figures 4.51 to 4.54 illustrate the TGA of *MNS $_{CE2}$, *MNS_{CO2}, *MNS_{CHO2} and *MNS_{GE2} respectively. They noticeably show that in all types of natural surface modifier modified nanosilica, weight losses corresponding to the loss of physically absorbed water, were lower compared with UMNS. This is a very significant scenario, to express the hydrophobic nature of the NPs modified nanosilica. TGA results show that natural polymer modified nanoparticles absorb less amount of water than *UMNS (See Table 4.13). These results confirm the formation of bond between NP and surface silanol groups of nanosilica, conferring the hydrophobic character to the surface of nanosilica, although there are still some available free hydroxyl groups on silica surface to which water molecules can get attached and give a low percentage of weight loss reduction compared to UMNS.

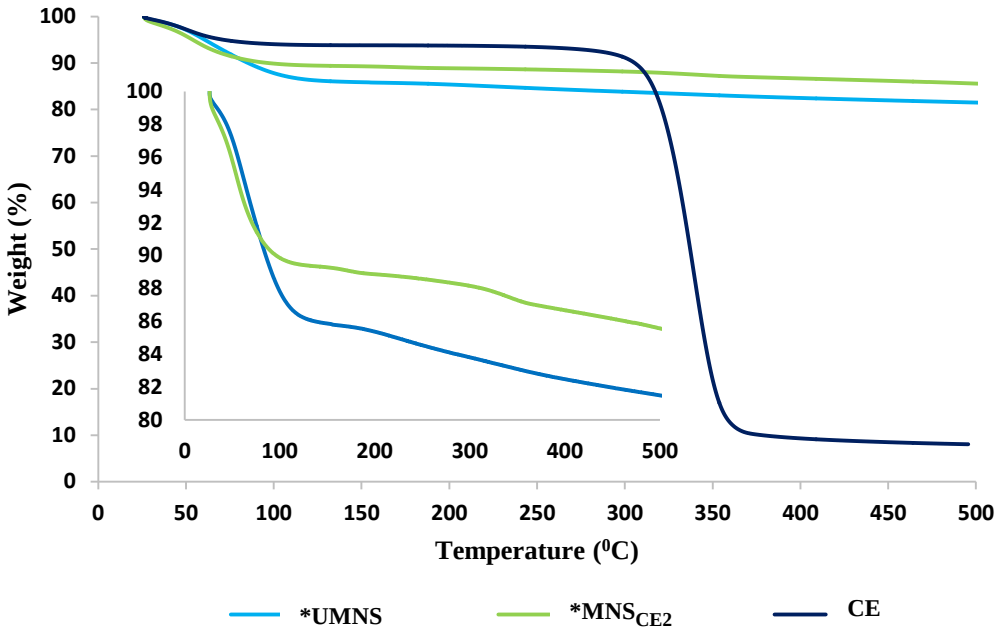

Figure 4.51: TGA of *UMNS, *MNS$_{CE2}$ and CE

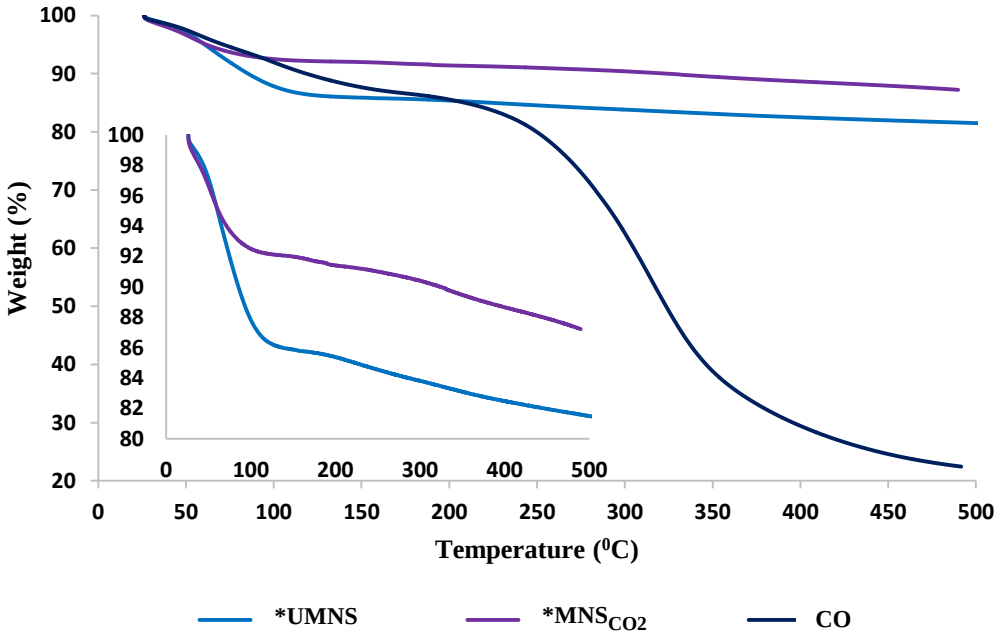

Figure 4.52: TGA of *UMNS, *MNS$_{CO2}$ and CO

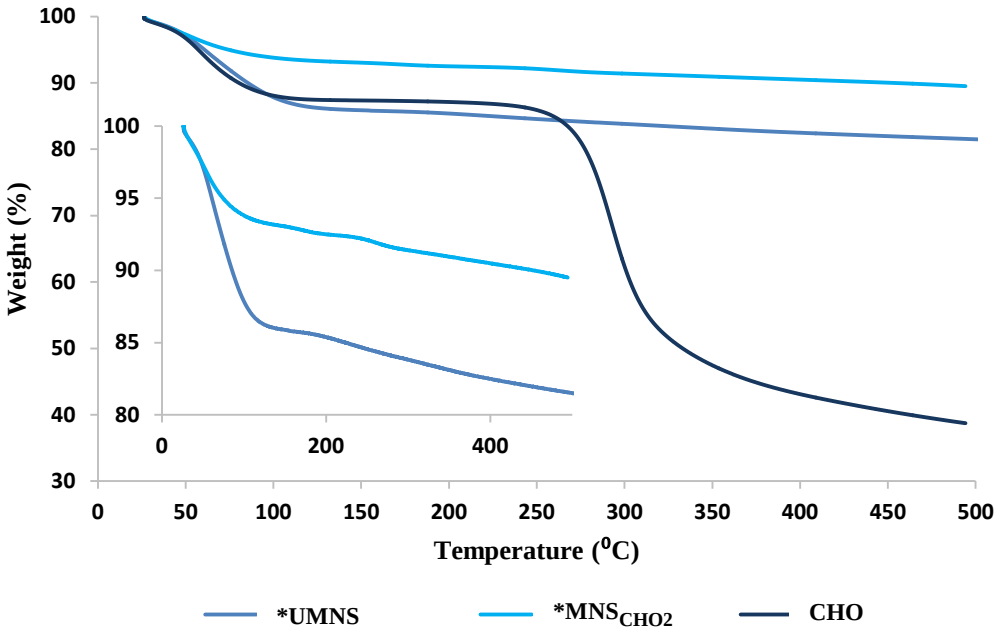

Figure 4.53: TGA of *UMNS, *MNS$_{CHO2}$ and CHO

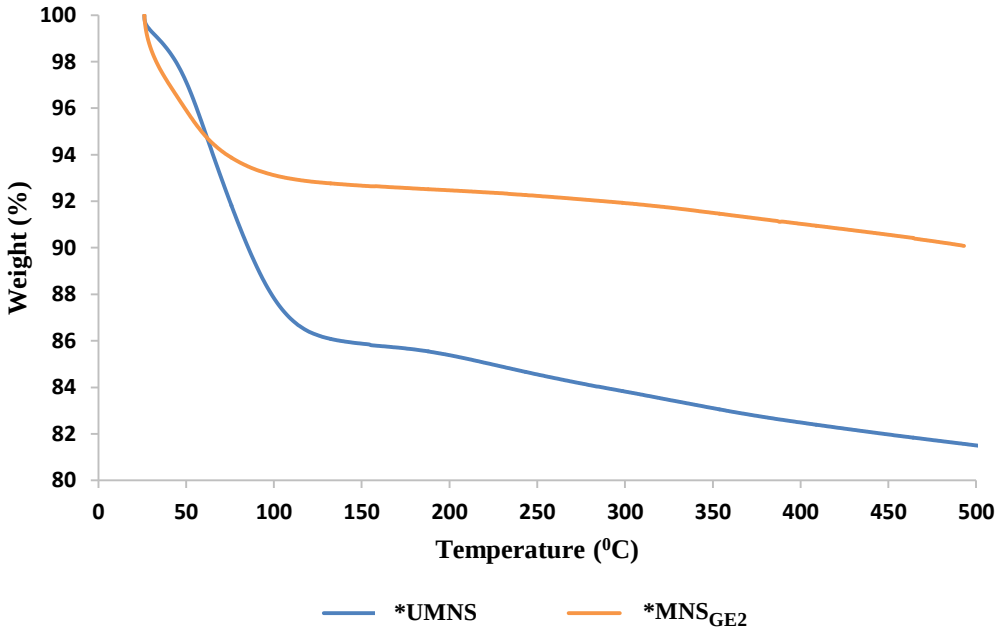

Figure 4.54: TGA of *UMNS and *MNS$_{GE2}$

Table 4.13: Weight loss (%) less than 150° C of UMNS and NPs modified nanosilica

Type	Weight loss (%) 150° C
UMNS	14
*MNS_{CE2}	11
*MNS_{CO2}	8
*MNS_{CHO2}	6
*MNS_{GE2}	7

4.1.5 Properties of XNBR latex vulcanizates filled with NPs modified nanosilica

4.1.5.1 Results of physical properties of XNBR latex vulcanizates filled with NPs modified nanosilica

Figures 4.55 and 4.56 illustrate the variation of TS of XNBR vulcanizates containing micro silica and nanosilica modified with NPs at different levels of addition respectively.

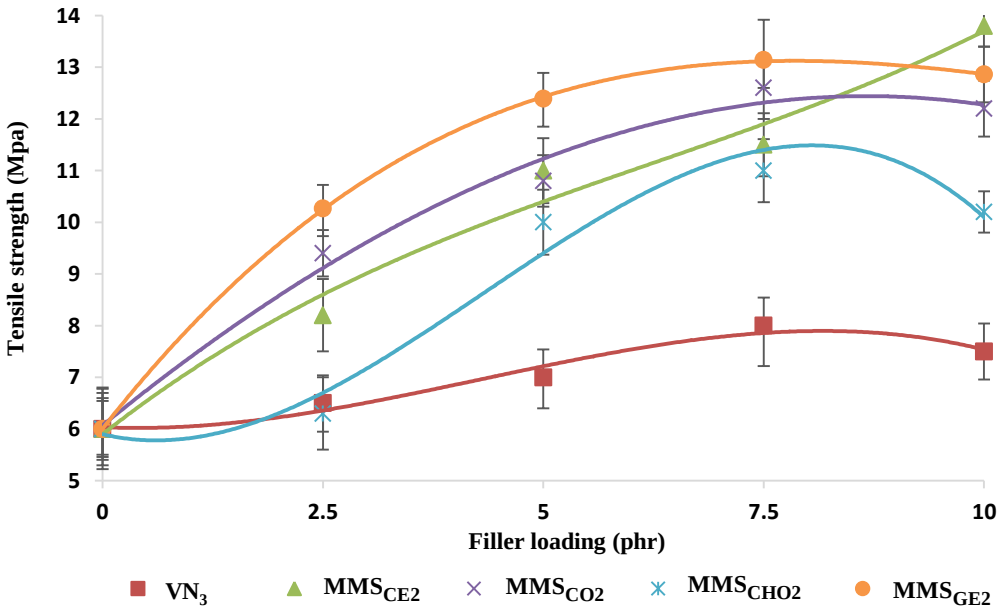

Figure 4.55: Variation of TS of XNBR latex vulcanizates filled with VN_3, MMS_{CE2}, MMS_{CO2}, MMS_{CHO2} and MMS_{GE2} at different levels of filler loading

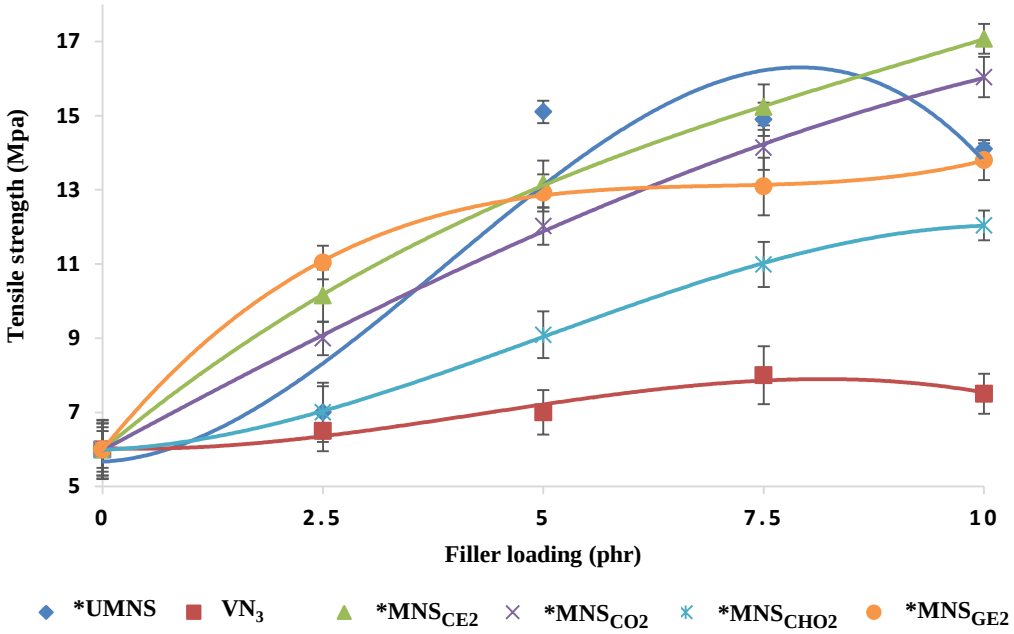

Figure 4.56: Variation of TS of XNBR latex vulcanizates filled with *UMNS, VN_3, *MNS_{CE2}, *MNS_{CO2}, *MNS_{CHO2} and *MNS_{GE2} at different levels of filler loading

TS of filled films at all the filler levels are higher than those of unfilled films. TS values of all the films filled with modified silica were higher than those of VN_3 filled XNBR latex vulcanizates at each level of filler additions. This may be due to the better F/R interaction of surface modified silica filled vulcanizates compared with unmodified silica filled vulcanizates. All the films filled with modified silica show increasing pattern of TS with increasing filler loading up to 7.5 phr level of filler addition and then unexpected slight reduction could be observed for all types of filler addition except for MMS_{CE2} filled vulcanizates. Generally, highest TS could be observed for MMS_{GE2} filled XNBR vulcanizates at all levels of filler addition except at 10 phr. And second highest TS could be observed for MMS_{CO2} filled vulcanizates.

Here, *MNS_{CE2} filled vulcanizates at all levels of filler addition display at least 20% higher TS value compared to MMS_{CE2} filled XNBR vulcanizates (See Table 4.14). Moreover, other NPs modified nanosilica filled vulcanizates also show higher TS compared to each NPs modified micro silica filled XNBR vulcanizates (See Table

4.14) except some arbitrary results. It evidently confirms that the high surface area of nanosilica leads to the formation of more interactions with rubber matrix than micro silica. Here, all types of modified nanofiller filled vulcanizates show an increasing pattern of TS, with increasing filler loading in vulcanizates. The highest TS could be observed in *MNS_{CE2} filled vulcanizates at 10 phr level of filler addition. It is witnessed that the variation of TS noticeably display a similar pattern in Figure 4.55 for surface modified microsilica and Figure 4.56 for surface modified nanosilica. However, in both cases the highest TS is observed at 10 phr level of filler addition.

Table 4.14: Increase in TS of vulcanizates filled with surface modified nanosilica over equivalent vulcanizates filled with surface modified micro silica

Type of surface modifier	Enhanced TS % Level of filler addition (phr)			
	2.5	5	7.5	10
CE	24	20	32	24
CO	-4	11	12	32
CHO	11	-9	-0.1	18
GE	8	4	-0.4	7

Figures 4.57 and 4.58 illustrate the variation of EB of XNBR latex vulcanizates containing micro silica and nanosilica modified with NPs at different levels of addition respectively.

In the case of VN_3 filled vulcanizates, it is observed that the change of EB is only marginal. Both VN_3 and MMS_{CE2} filled vulcanizates show low EB than unfilled XNBR vulacnizate whilst the other modified filler filled vulcanizates show higher EB than unfilled XNBR latex vulcanizates.

As mentioned earlier, glove manufacturers must carefully balance strength with elasticity. Elongation is an important property to make it more comfort donning.

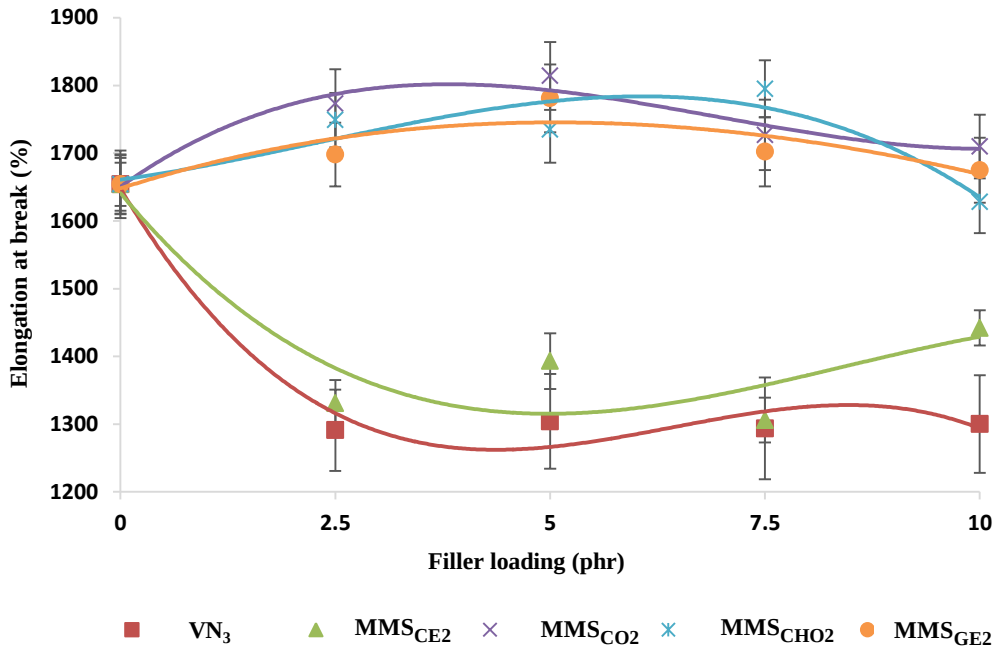

Figure 4.57: Variation of EB of XNBR latex vulcanizates filled with VN_3, MMS_{CE2}, MMS_{CO2}, MMS_{CHO2} and MMS_{GE2} at different levels of filler loading

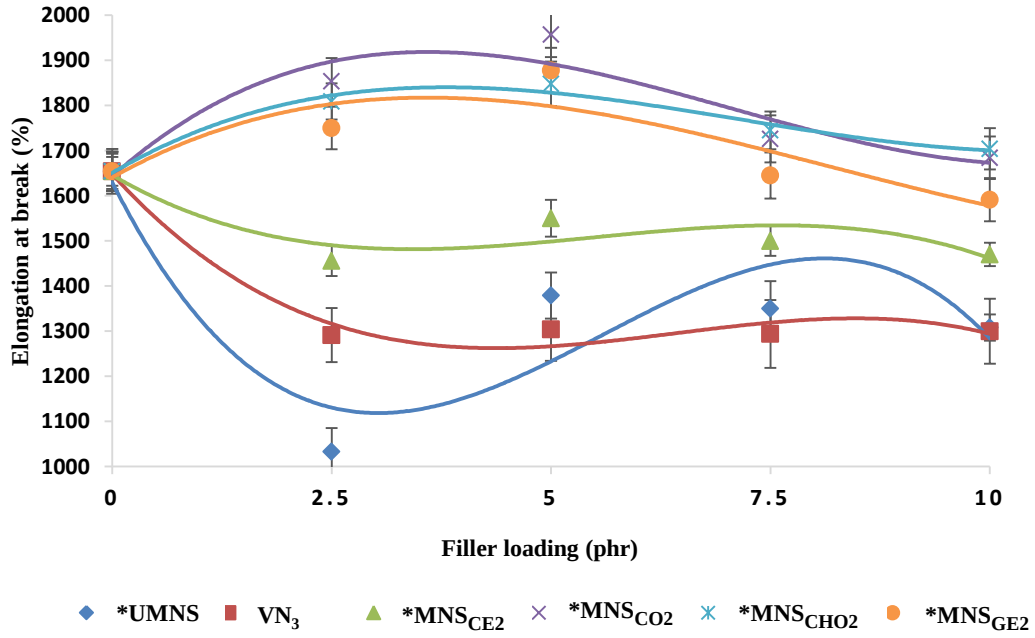

Figure 4.58: Variation of EB of XNBR latex vulcanizates filled with *UMNS, VN_3, $*MNS_{CE2}$, $*MNS_{CO2}$, $*MNS_{CHO2}$ and $*MNS_{GE2}$ at different levels of filler loading

Modified nanosilica filled vulcanizates show high EB, obtaining high ability to stretch. A slight reduction of EB was observed with increasing the levels of filler addition. Generally, *MNS_{CO2} filled vulcanizates show the highest in EB at all levels of filler addition from 2.5 to 10 phr and second, third and fourth performance could be observed for *MNS_{CHO2}, *MNS_{GE2} and *MNS_{CE2} filled vulcanizates respectively. NPs modified nanosilica filled vulcanizates display higher EB than the NPs modified microsilica except in some situations (See Table 4.15).

Table 4.15: Increase in EB of vulcanizates filled with surface modified nanosilica over equivalent vulcanizates filled with surface modified micro silica

Type of surface modifier	Enhanced EB Level of filler addition (phr)			
	2.5	5	7.5	10
CE	9	11	15	2
CO	5	8	-0.06	-1
CHO	3	7	-3	5
GE	3	5	-3	-5

Figures 4.59 and 4.60 illustrate the variation of M300 of XNBR vulcanizates containing micro silica and nanosilica modified with NPs at different levels of addition respectively.

It is observed that of all types of vulcanizates enhance M300 continuously with the level of filler addition. It can also be seen that the moduli of the filled vulcanizates are higher than that of the unfilled vulcanizates and increased with increasing filler content. The increase in moduli is due to the stiffening effect caused by the F/R interactions. This interaction increases with increasing filler loading. The highest M300 could be observed for MMS_{CO2} filled vulcanizates over 5 to 10 phr level of filler addition than other types of modified silica filled vulcanizates. Apparently, this observation indicates that the surface modification of silica filler, enhances the F/R interactions.

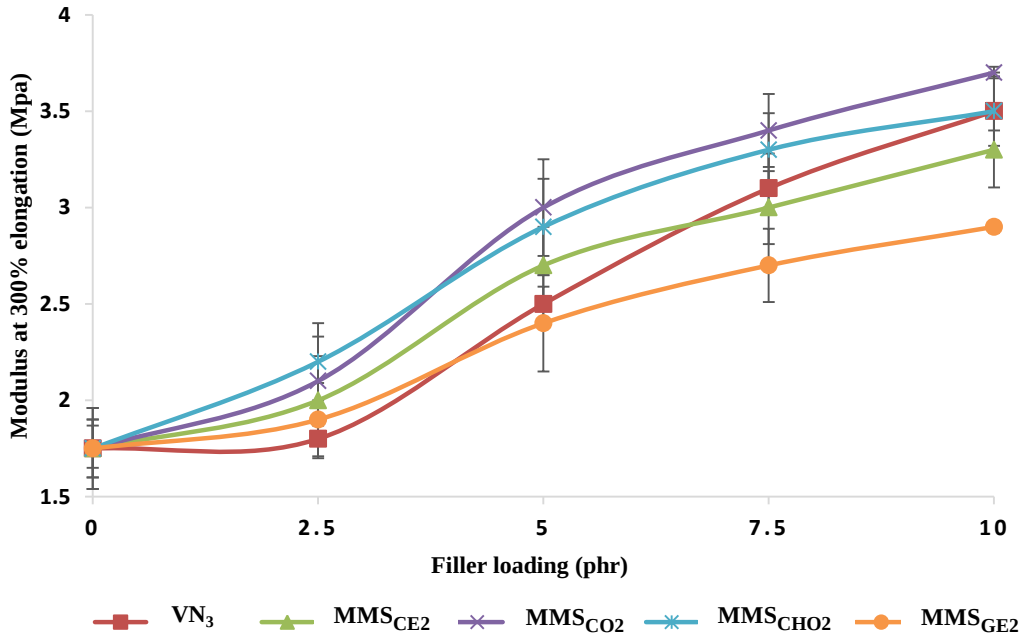

Figure 4.59: Variation of M300 of XNBR latex vulcanizates filled with VN_3, MMS_{CE2}, MMS_{CO2}, MMS_{CHO2} and MMS_{GE2} at different levels of filler loading

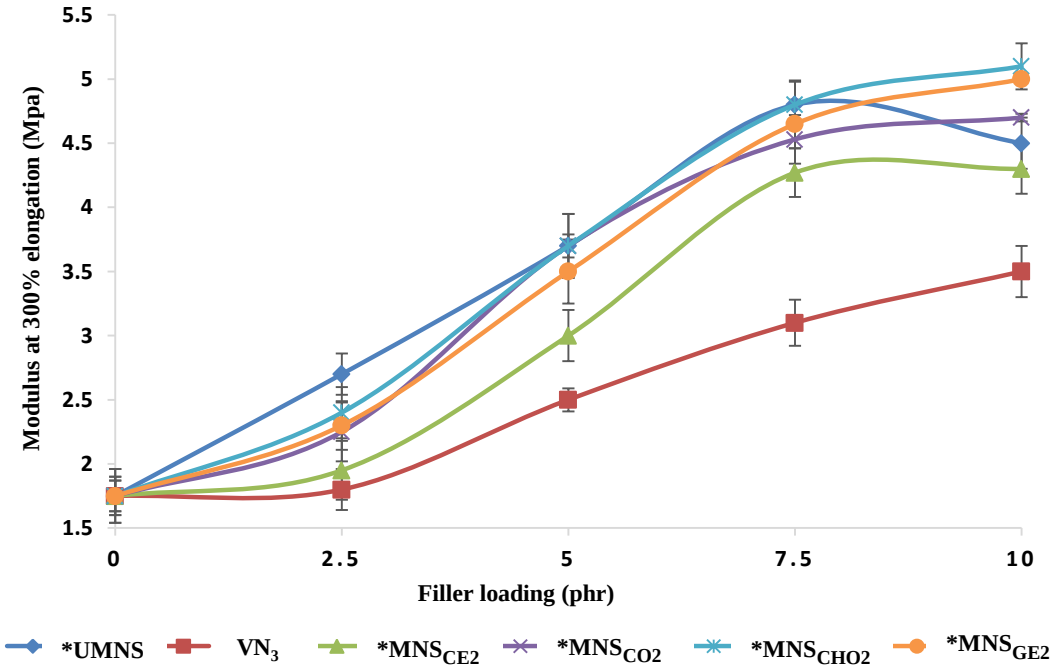

Figure 4.60: Variation of M300 of XNBR latex vulcanizates filled with *UMNS, VN_3, $*MNS_{CE2}$, $*MNS_{CO2}$, $*MNS_{CHO2}$ and $*MNS_{GE2}$ at different levels of filler loading

Table 4.16: Increase in M300 of vulcanizates filled with surface modified nanosilica over equivalent vulcanizates filled with surface modified micro silica

Type of surface modifier	Enhanced M300 Level of filler addition (phr)			
	2.5	5	7.5	10
CE	-3	11	42	30
CO	7	23	33	27
CHO	9	28	46	46
GE	21	46	72	72

All types of modified nanosilica filled vulcanizates show a higher M300 than that of surface modified microsilica and VN_3 filled vulcanizates over all levels of filler addition due to the better F/R interactions (See Table 4.16). This is due to the presence of high surface area of nanosilica compared to microsilica, having a high potential of surface modification. Taking a combination of optimum values of TS, M300 and EB is very important for the industrial applications rather than the highest values of each property.

Figures 4.61 and 4.62 illustrate the variation of TRS of XNBR latex vulcanizates containing micro silica and nanosilica modified with NPs at different levels of addition respectively.

Increasing pattern of TRS could be observed for all types of filler added vulcanizates. This is because, addition of filler act as a reinforcement to the polymer network making it more stiff in structure. Peak value of TRS could be observed at 10 phr level of filler addition in all types of fillers.

It is noticeably revealed that the highest TRS enhancement % could be observed for $*MNS_{CE2}$ filled vulcanizates compared to MMS_{CE2} filled vulcanizates, over all the levels of filler additions (See Table 4.17). The highest TRS could be observed for $*MNS_{CE2}$ whilst second and third highest TRS could be observed for $*MNS_{GE2}$ and $*MNS_{CO2}$ filled vulcanizates respectively (See Figure 4.62).

Considering the physical properties discussed above: tensile strength, modulus values, elongation and tear strength, the optimum physical properties which are more suitable for glove manufacturing could be observed for *MNS_{CE2} filled vulcanizates.

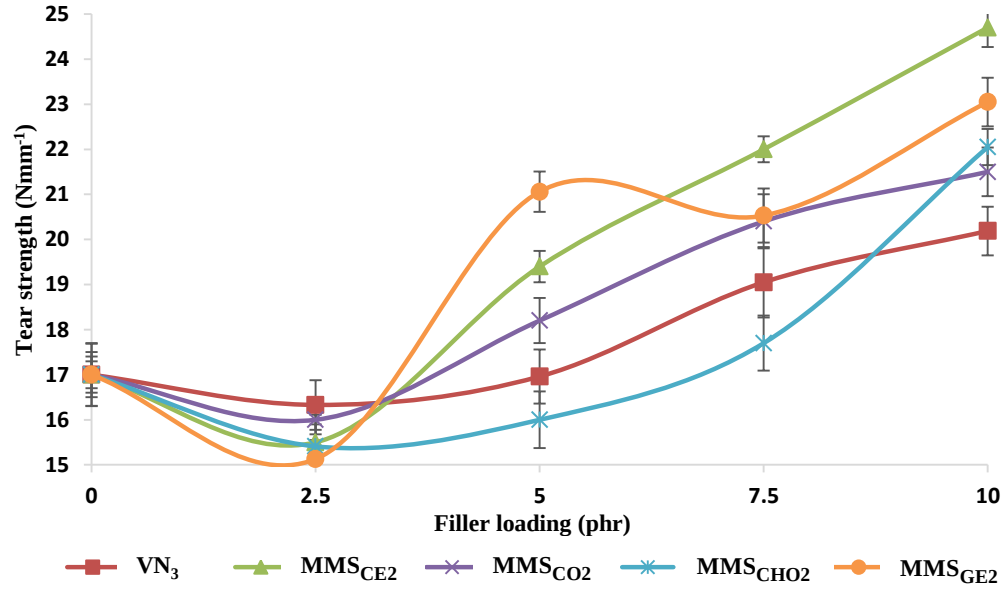

Figure 4.61: Variation of TRS of XNBR latex vulcanizates filled with VN_3, MMS_{CE2}, MMS_{CO2}, MMS_{CHO2} and MMS_{GE2} at different levels of filler loading

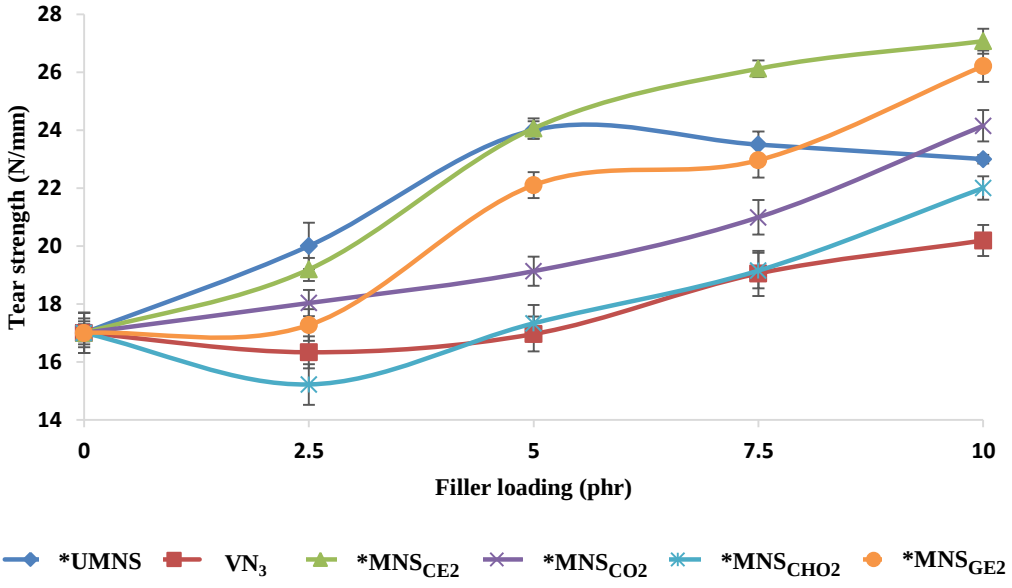

Figure 4.62: Variation of TRS of XNBR latex vulcanizates filled with *UMNS, VN_3, *MNS_{CE2}, *MNS_{CO2}, *MNS_{CHO2} and *MNS_{GE2} at different levels of filler loading

Table 4.17: Increase in TRS of vulcanizates filled with surface modified nanosilica over equivalent vulcanizates filled with surface modified micro silica

Type of surface modifier	Enhanced TRS % Level of filler addition (phr)			
	2.5	5	7.5	10
CE	24	24	19	10
CO	13	5	3	12
CHO	-1	8	8	-0.2
GE	14	5	12	14

4.1.5.2 Swelling properties

Figures 4.63 and 4.64 illustrate the variation of swelling % of XNBR latex vulcanizates containing micro silica and nanosilica modified with NPs at different levels of addition respectively.

It is observed that all NPs modified micro and nanosilica filled XNBR latex films show lower swelling % than VN_3 filled vulcanizates. The addition of filler reduces the swelling %.

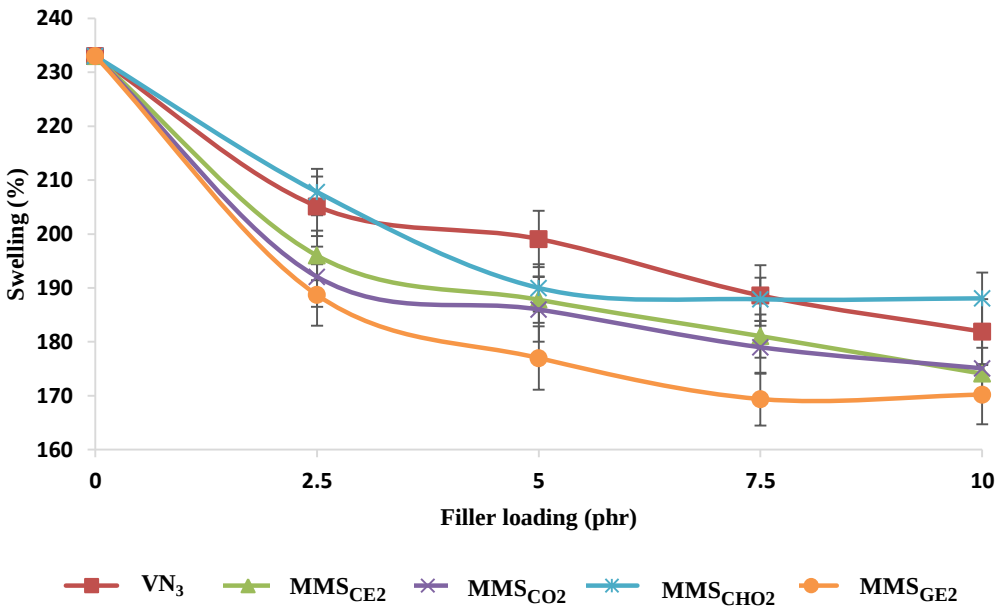

Figure 4.63: Variation of swelling (%) of XNBR latex vulcanizates filled with VN_3, MMS_{CE2}, MMS_{CO2}, MMS_{CHO2} and MMS_{GE2} at different levels of filler loading

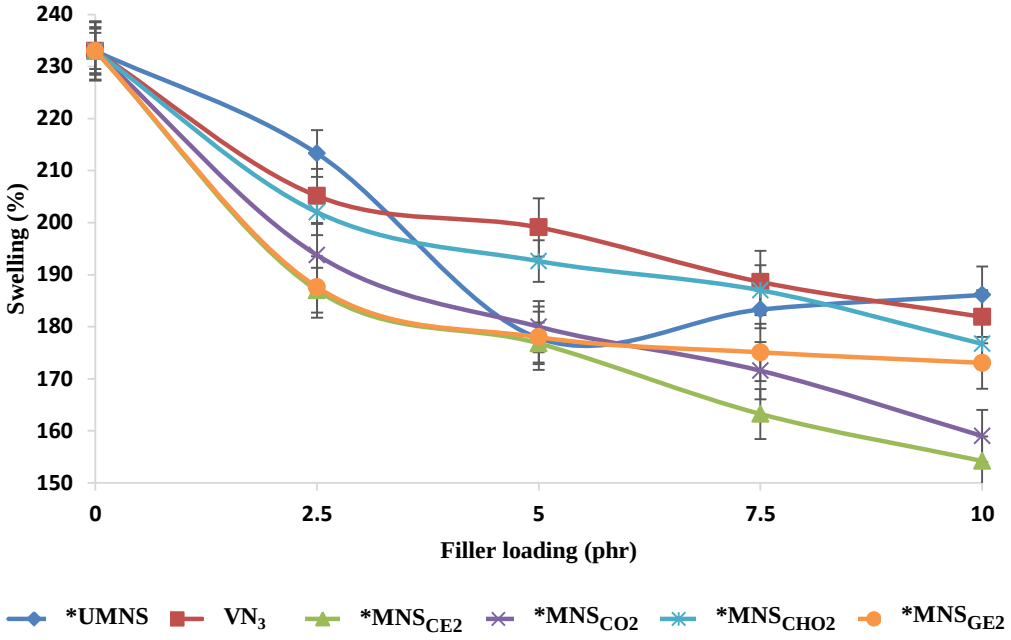

Figure 4.64: Variation of swelling (%) of XNBR latex vulcanizates filled with *UMNS, VN_3,*MNS_{CE2}, *MNS_{CO2}, *MNS_{CHO2} and *MNS_{GE2} at different levels of filler loading

This is probably due to the lack of void spaces in modified cast films than unmodified cast films. The lowest swelling % could be observed for MMS_{GE2} filler filled films among the microsilica filled films whilst the lowest swelling shows for MNS_{CE2} filler filled vulcanizates among the nanosilica filled films, throughout the all levels of filler loadings.

Figures 4.65 and 4.66 illustrate the variation of crosslink density of XNBR latex vulcanizates containing micro silica and nanosilica modified with NPs at different levels of addition respectively.

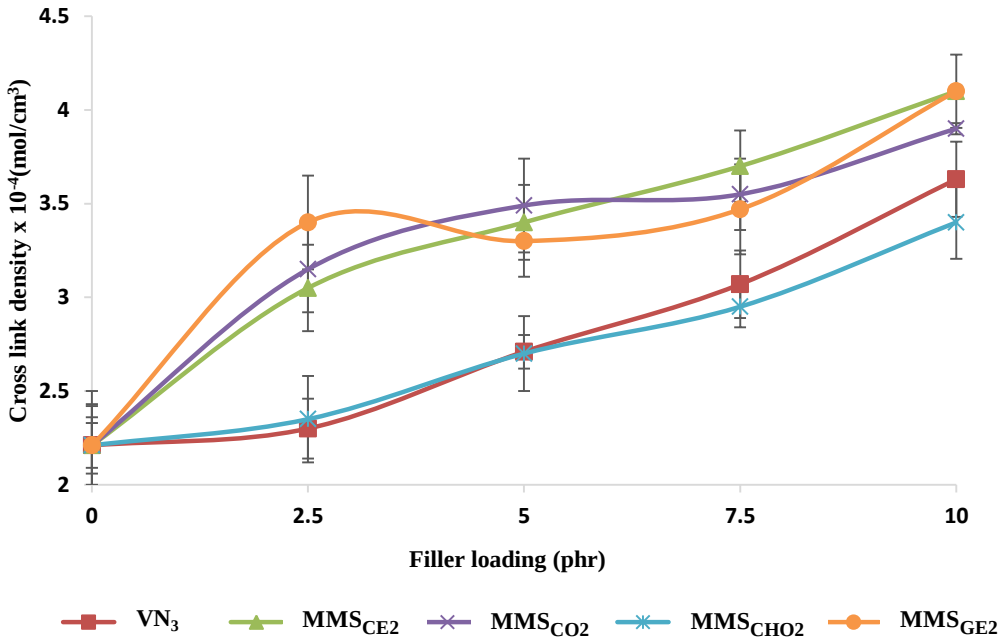

Figure 4.65: Variation of crosslink density of XNBR latex vulcanizates filled with VN_3, MMS_{CE2}, MMS_{CO2}, MMS_{CHO2} and MMS_{GE2} at different levels of filler loading

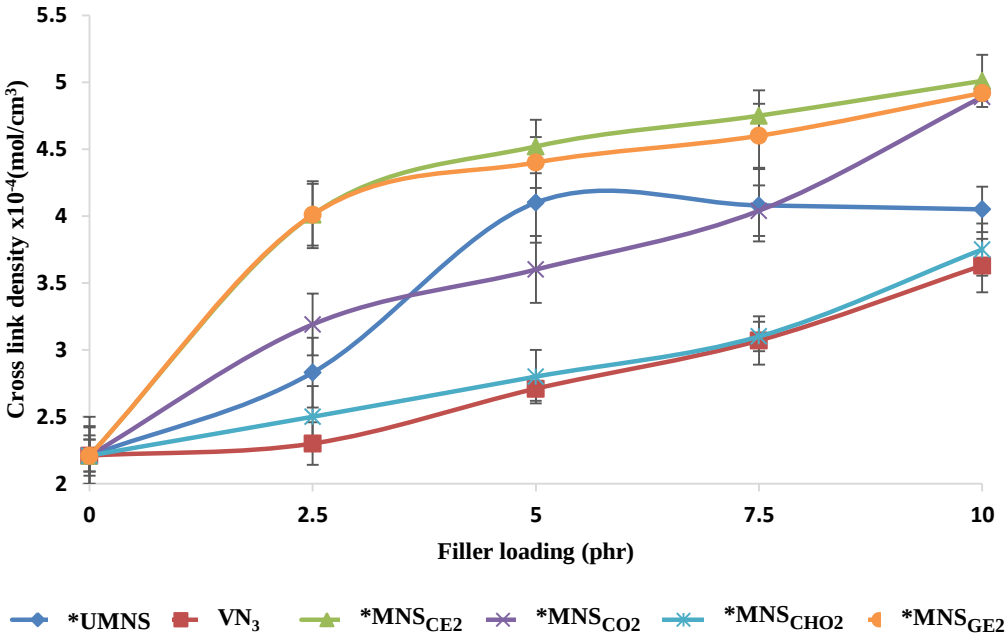

Figure 4.66: Variation of crosslink density of XNBR latex vulcanizates filled with *UMNS, VN_3, $*MNS_{CE2}$, $*MNS_{CO2}$, $*MNS_{CHO2}$ and $*MNS_{GE2}$ at different levels of filler loading

The surface modification of silica using NPs leads to better interaction between filler not only with polar –COOH part of latex but also with non-polar part of the latex matrix. Hence, this surface modification leads to more interaction between filler and polymer matrix than the unmodified filler. In the case of nano filler, high surface area of filler, leads to more filler-polymer interactions than micro filler. *MNS_{CE2} show highest crosslink density over all the levels of nanosilica addition.

Figures 4.67 and 4.68 demonstrate Qf/Qg of XNBR vulcanizates containing micro silica and nanosilica modified with NPs at different levels of addition respectively.

As mentioned earlier, lower the Qf/Qg value, higher the interactions between rubber and filler segments in the composite. The Qf/Qg value decreases with increasing the level of filler addition due to the fact that increasing filler portion definitely increases the interactions between them. Albeit, F/R interaction values were not affected much with the change of type of surface modifier. However, both surface modified nano and micro filler filled vulcanizates show higher F/R interactions compared to VN_3 filled vulcanizates at all levels of filler additions concluding that the surface modification leads to better interaction between rubber and filler regions.

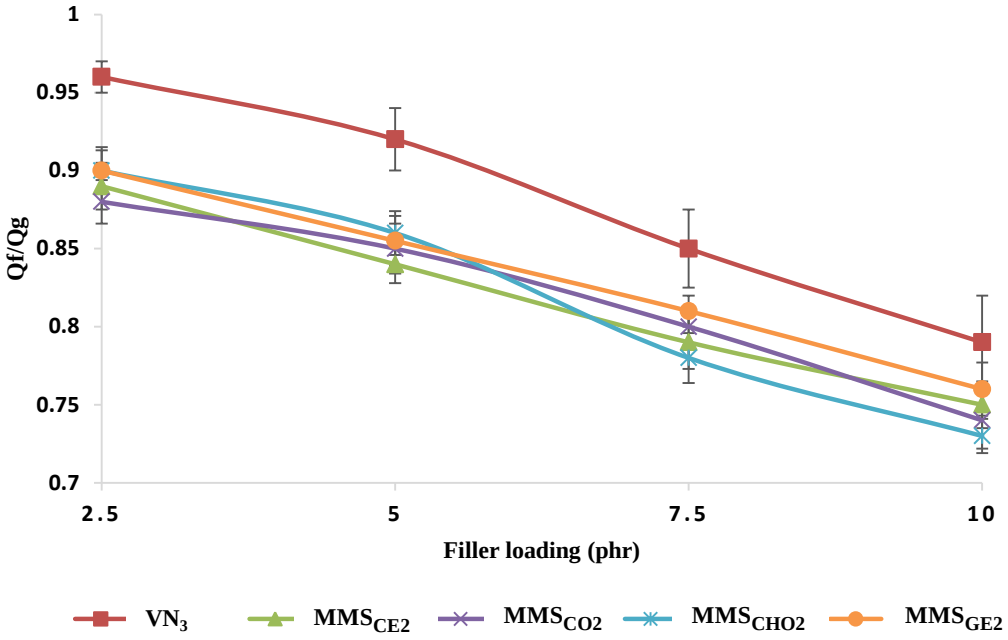

Figure 4.67: Variation of Qf/Qg of XNBR latex vulcanizates filled with VN_3, MMS_{CE2}, MMS_{CO2}, MMS_{CHO2} and MMS_{GE2} at different levels of filler loading

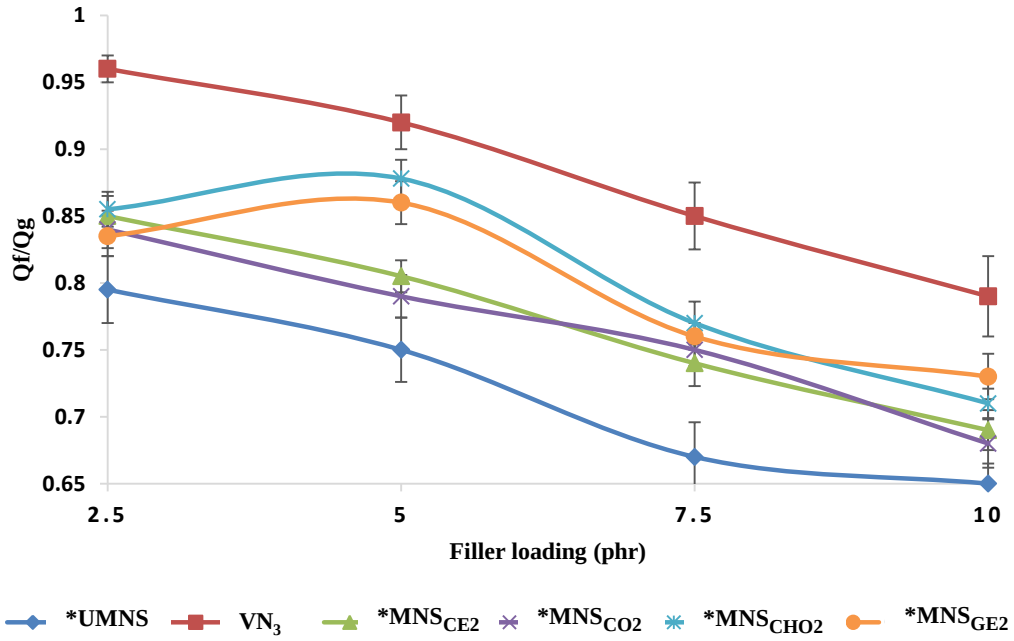

Figure 4.68: Variation of Qf/Qg of XNBR latex vulcanizates filled with *UMNS, VN_3, $*MNS_{CE2}$, $*MNS_{CO2}$, $*MNS_{CHO2}$ and $*MNS_{GE2}$ at different levels of filler loading

4.1.5.3 Morphology

Figure 4.69 illustrates the cross sectional micrographs of VN_3, *MNS_{CE2}, *MNS_{CO2}, *MNS_{CHO2} and *MNS_{GE2} filled XNBR vulcanizates at 10phr level of filler addition. These micrographs do not show any significant different senario with the type of surface modifier. The nanosilica distribution within the film is not affected by the type of natural surface modifiers as indicated by Figure 4.69. Surface modified nanosilica filled vulcanizates show higher extent of distribution of compounding ingredients than in the case of VN_3 filled vulcanizates at 10 phr level of filler addition, confirming the improvement in mechanical properties obtained for NPs modified nanosilica filled vulcanizates.

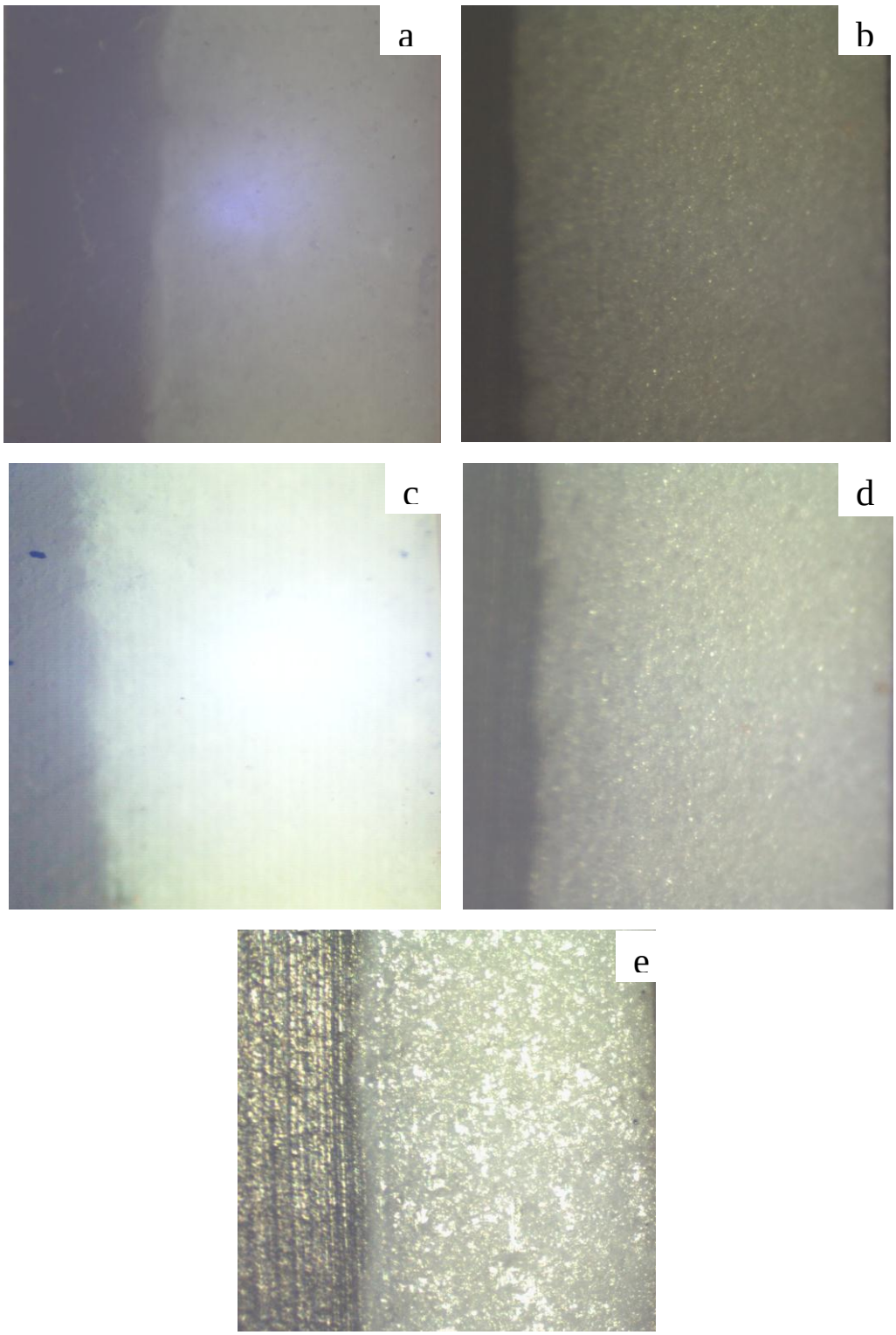

Figure 4.69: Morphology of (a) VN_3 (b) *MNS_{CE2} (c) *MNS_{CO2} (d) *MNS_{CHO2} (e) *MNS_{GE2} filled XNBR latex vulcanizates at 10 phr level of filler addition

CONCLUSIONS

Amorphous spherical nanosilica particles can be synthesized by hydrolysis of aqueous sodium metasilicate solutions under acidic conditions in the presence of a surface modifier to retard aggregation of silica particles which occur through interactions of surface polar groups. PMAA and P(MAA-EHA) are quite capable of performing the function of surface modifier in this particular synthesis. The level of surface modifier required to obtain the optimum extractable yield depends on its composition. **FTIR** analysis confirms the surface modification via the formation of ester bonds between hydroxyl group of surface modifier and surface silanol groups of nanosilica. **TGA** analysis results confirms the surface modification of nanosilica particles with acrylic polymers due to the higher thermal stability of modified nanosilica compared to unmodified nanosilica. **XRD** analysis reveals that the amorphous nature of synthesized nanosilica. **SEM** confirms the synthesized particles are in nanometer scale & spherical in shape. **Particle size distribution** results further confirms the synthesized silica particles have well-defined size range in nanometer scale & narrow size distribution.

TS of acrylic polymer modified filler filled vulcanizates were found to be high over all levels of filler addition compared to unmodified filler filled vulcanizates. Meanwhile, 2% PMAA modified filler filled vulcanizates exhibit better performance and best TS could be observed at 5phr level of filler addition. **EB** of 2% PMAA modified filler filled vulcanizates show the highest over all levels of filler addition. Compared to modified and unmodified filler filled vulcanizates while the highest EB could be observed at 5phr level of addition. **M300** increases up to 7.5 phr level of filler addition & then decrease for unmodified and modified nanosilica filled vulcanizates. M300 of acrylic polymer modified filler filled vulcanizates show lower value than unmodified filler filled vulcanizates. Swelling propertise further confirm the pattern of physical propertise. The lowest swelling % & highest crosslink density could be observed for 2% PMAA modified filler filled vulcanizates at 5ohr level of filler addition. 2% PMAA modified filler filled vulcanizates obtained balance strength with stretch & comfort.

FTIR and TGA results confirms the surface modification of nanosilica with NPs like cellulose, collagen, chitosan and gelatin. The optimum properties such as TS, M300, EB & TRS could be observed for 2% cellulose modified filler filled vulcanizates for glove manufacturing.

RECOMMENDATIONS FOR FUTURE WORK

1. Investigation of surface modification pattern of nanosilica at the optimize surface modifier levels (i.e. 2% for PMAA and 1.5% for P(MAA-EHA))
2. Investigation of effect of molecular weight of surface modifier on synthesis of nanosilica particles.
3. Obtaining further quantitative measurements on rubber-filler interactions in surface modified nanosilica filled XNBR latex vulcanizates.

REFERENCES

Ain, Z., & Azura, A. (2011). Effect of different types of filler and filler loadings on the properties of carboxylated acrylonitrile–butadiene rubber latex films. *Journal of Applied Polymer Science, 119*(5), 2815-2823.

Al-Oweini, R., & El-Rassy, H. (2009). Synthesis and characterization by FTIR spectroscopy of silica aerogels prepared using several Si (OR) 4 and R″ Si (OR′) 3 precursors. *Journal of Molecular Structure, 919*(1), 140-145.

Alexandre, M., & Dubois, P. (2000). Polymer-layered silicate nanocomposites: preparation, properties and uses of a new class of materials. *Materials Science and Engineering: R: Reports, 28*(1-2), 1-63.

Andrianov, K. m. A. (1955). Organic silicon compounds (Vol. 1): State Scientific technical Pub. House for Chemical Literature, 101-106.

Baes, C. F., & Mesmer, R. E. (1976). The Hydrolysis of Cations (Vol. 489).

Bhowmik, S., Islam, J. M., Debnath, T., Miah, M. Y., Bhattacharjee, S., & Khan, M. A. (2017). Reinforcement of Gelatin-Based Nanofilled Polymer Biocomposite by Crystalline Cellulose from Cotton for Advanced Wound Dressing Applications. *Polymers, 9*(6), 222.

Blackley, D. (1997). Polymer Latices Science and Technology, Vol. 2 'Types of Latices', 445 et seq. In: Chapman & Hall 2. Unpublished data.

Bogush, G., Tracy, M., & Zukoski, C. (1988). Preparation of monodisperse silica particles: control of size and mass fraction. *Journal of non-crystalline solids, 104*(1), 95-106.

Bogush, G., & Zukoski, C. (1991). Studies of the kinetics of the precipitation of uniform silica particles through the hydrolysis and condensation of silicon alkoxides. *Journal of Colloid and Interface Science, 142*(1), 1-18.

Bokobza, L. (2004). The reinforcement of elastomeric networks by fillers. *Macromolecular Materials and Engineering, 289*(7), 607-621.

Brinker, C. (1988). Hydrolysis and condensation of silicates: effects on structure. *Journal of non-crystalline solids, 100*(1-3), 31-50.

Brinker, C. J. (1990). GW Scherer Sol-Gel Science. *The Physics and Chemistry of Sol-Gel Processing, Academic, San Diego, CA*, (21-228).

Brinker, C. J. (1994). Sol-gel processing of silica (No. CONF-900802-). American Chemical Society, Washington, DC (United States).

Brinker, C. J., & Scherer, G. W. (2013). *Sol-gel science: the physics and chemistry of sol-gel processing*: Academic press.

Chakraborty, S., Bandyopadhyay, S., Ameta, R., Mukhopadhyay, R., & Deuri, A. (2007). Application of FTIR in characterization of acrylonitrile-butadiene rubber (nitrile rubber). *Polymer testing, 26*(1), 38-41.

Ciolacu, D., Ciolacu, F., & Popa, V. I. (2011). Amorphous cellulose-structure and characterization. *Cellulose Chemistry and Technology, 45*(1), 13.

Ciprari, D., Jacob, K., & Tannenbaum, R. (2006). Characterization of polymer nanocomposite interphase and its impact on mechanical properties. *Macromolecules, 39*(19), 6565-6573.

Das, D., Parida, K., & Mishra, B. (2009). Synthesis and surface properties of silica spheres with core shell structure by one convenient method. *Advances in Materials Science and Engineering, 2009*.

Erdemir, D., Lee, A. Y., & Myerson, A. S. (2009). Nucleation of crystals from solution: classical and two-step models. *Accounts of Chemical Research, 42*(5), 621-629.

Evans, M. S. (2002). Tyre compounding for improved performance (Vol. 12): iSmithers Rapra Publishing, 68-72.

Flory, P. J. (1950). Statistical mechanics of swelling of network structures. *The Journal of Chemical Physics, 18*(1), 108-111.

Freundlich, H., & Hatfield, H. S. (1926). Colloid and capillary chemistry: Methuen And Co. Ltd; London, 53-61.

Gojny, F., Wichmann, M., Köpke, U., Fiedler, B., & Schulte, K. (2004). Carbon nanotube-reinforced epoxy-composites: enhanced stiffness and fracture toughness at low nanotube content. *Composites Science and Technology, 64*(15), 2363-2371.

Green, D., Lin, J., Lam, Y.-F., Hu, M.-C., Schaefer, D. W., & Harris, M. (2003). Size, volume fraction, and nucleation of Stober silica nanoparticles. *Journal of Colloid and Interface Science, 266*(2), 346-358.

Iler, K. R. (1979). The chemistry of silica. Solubility, Polymerization, Colloid and Surface Properties and Biochemistry of Silica, (43-78).

Jarnthong, M., Peng, Z., Nakason, C., & Lopattananon, N. (2010). Surface modification of silica nanoparticles for reinforcement of epoxidized natural rubber. In Advanced Materials Research (Vol. 93, pp. 370-376). Trans Tech Publications.

Jasso-Gastinel, C. F. (2017). Gradients in Homopolymers, Blends, and Copolymers. In Modification of Polymer Properties (pp. 185-210).

Jing, S.-Y., Lee, H.-J., & Choi, C. K. (2002). Chemical bond structure on Si-OC composite films with a low dielectric constant deposited by using inductively coupled plasma chemical vapor deposition. *Journal of the Korean Physical Society, 41*(5), 769-773.

Koo, J. H. (2006). Polymer nanocomposites: McGraw-Hill Professional Pub,79-93.

Lim, H., Vivayganathan, K., & Amir-Hashim, M. (2012). Properties of Carboxylated Nitrile Latex Film with Varying Thickness. *Journal of Rubber Research*, *15*, 3.

Lipatov, I. U. r. S., & Lipatov, Y. S. (1995). Polymer reinforcement: ChemTec Publishing (Vol. 1), 69-96.

Luo, Y., Feng, C., Wang, Q., Yi, Z., Qiu, Q., Lx, K., & Peng, Z. (2013). Preparation and characterization of natural rubber/silica nanocomposites using rule of similarity in latex. *Journal of Wuhan University of Technology-Mater. Sci. Ed.*, *28*(5), 997-1002.

Mahipal, Y. K., Agrawal, R. C., Hanisah, Y., Arshed, N., & Ramesh, S. (2016). Materials and Electrical Property Studies on Polymer Electrolyte Membranes Incorporating with Room Temperature Ionic Liquid. Int. J. Emerg. Technol. Adv. Eng., 6, 18-25.

Malafaya, P. B., Silva, G. A., & Reis, R. L. (2007). Natural–origin polymers as carriers and scaffolds for biomolecules and cell delivery in tissue engineering applications. *Advanced drug delivery reviews, 59*(4), 207-233.

Matsoukas, T., & Gulari, E. (1988). Dynamics of growth of silica particles from ammonia-catalyzed hydrolysis of tetra-ethyl-orthosilicate. *Journal of Colloid and Interface Science, 124*(1), 252-261.

Matsoukas, T., & Gulari, E. (1989). Monomer-addition growth with a slow initiation step: a growth model for silica particles from alkoxides. *Journal of Colloid and Interface Science, 132*(1), 13-21.

McNeil, K., DiCaprio, J., Walsh, D., & Pratt, R. (1980). Kinetics and mechanism of hydrolysis of a silicate triester, tris (2-methoxyethoxy) phenylsilane. *Journal of the American Chemical Society, 102*(6), 1859-1865.

Mihara, S. (2009). Reactive processing of silica-reinforced tire rubber: new insight into the time-and temperature-dependence of silica rubber interaction, 52-78.

Mujkanović, V. L., & Ostojić, G. (2009). NON-BLACK FILLERS FOR ELASTOMERS 13th International Research. In Expert Conference Tunisia (pp. 16-20).

Nair, K. P., Nair, A. B., & Joseph, R. (2014). Carboxylated acrylo nitrile butadiene rubber latex/kaolin nanocomposites: preparation and properties. *Composite Interfaces, 21*(6), 571-583.

Nair, K. P., Thomas, P., & Joseph, R. (2012). Latex stage blending of multiwalled carbon nanotube in carboxylated acrylonitrile butadiene rubber: mechanical and electrical properties. *Materials & Design, 41*, 23-30.

Nguyen, T.-D. (2013). From formation mechanisms to synthetic methods toward shape-controlled oxide nanoparticles. *Nanoscale, 5*(20), 9455-9482.

Nishinari, K., & Takahashi, R. (2003). Interaction in polysaccharide solutions and gels. *Current opinion in colloid & interface science, 8*(4), 396-400.

Nozawa, K., Gailhanou, H., Raison, L., Panizza, P., Ushiki, H., Sellier, E., . . . Delville, M. (2005). Smart control of monodisperse Stöber silica particles: effect of reactant addition rate on growth process. *Langmuir, 21*(4), 1516-1523.

Oliver, R. C., Lipfert, J., Fox, D. A., Lo, R. H., Doniach, S., & Columbus, L. (2013). Dependence of micelle size and shape on detergent alkyl chain length and head group. *PloS one, 8*(5), 62488.

Ostwald, W. (1900). About the supposed isomerism of red and yellow mercuric oxide and the surface tension of solid bodies. *Zeitschrift für physikalische Chemie, 34*(1), 495-503.

Patel, B., & Patel, P. (2014). Synthesis and characterization of silica nano-particles by acid leaching technique. *Research Journal of Chemical Sciences, 4*(5), 52-55.

Paul, D., & Robeson, L. M. (2008). Polymer nanotechnology: nanocomposites. *Polymer, 49*(15), 3187-3204.

Pavia, D. L., Lampman, G. M., Kriz, G. S., & Vyvyan, J. A. (2008). Introduction to spectroscopy. Cengage Learning, 108-199.

Pontoni, D., Narayanan, T., & Rennie, A. (2002). Time-resolved SAXS study of nucleation and growth of silica colloids. *Langmuir, 18*(1), 56-59.

Rafiee, E., Shahebrahimi, S., Feyzi, M., & Shaterzadeh, M. (2012). Optimization of synthesis and characterization of nanosilica produced from rice husk (a common waste material). *International Nano Letters, 2*(1), 29.

Rallini, M., & Kenny, J. (2017). Nanofillers in Polymers. In *Modification of Polymer Properties* (pp. 47-86): Elsevier.

Ramasinghe, R. L. P., Gannoruwa, G. K. B. M., & Liyanage, N. M. V. K. (2016, April). Use of surface modified silica in reinforcing carboxylated nitrile rubber latex. In Moratuwa Engineering Research Conference (MERCon), 2016 (pp. 361-366). IEEE.

Rida, M. A., & Harb, F. (2014). Synthesis and characterization of amorphous silica nanoparitcles from aqueous silicates uisng cationic surfactants. *Journal of Metals, Materials and Minerals, 24*(1).

Rothon, R. N. (2002). Particulate fillers for polymers (Vol. 12): iSmithers Rapra Publishing. 49-110.

Sadeghi, M., Dorodian, M., & Rezaei, M. (2013). Synthesis and Characteristic of Precipitated Nano-Silica. *Journal of Advances in Chemistry, 6*(1), 917-922.

Sae-oui, P., Sirisinha, C., Thepsuwan, U., & Hatthapanit, K. (2006). Roles of silane coupling agents on properties of silica-filled polychloroprene. *European polymer journal, 42*(3), 479-486.

Sala, R. L., Arantes, T. M., Longo, E., Leite, E. R., Paranhos, C. M., & Camargo, E. R. (2014). Evaluation of modified silica nanoparticles in carboxylated nitrile rubber nanocomposites. *Colloids and Surfaces A: Physicochemical and Engineering Aspects, 462*, 45-51.

Sarawade, P. B., Kim, J.-K., Hilonga, A., & Kim, H. T. (2010). Preparation of hydrophobic mesoporous silica powder with a high specific surface area by surface modification of a wet-gel slurry and spray-drying. *Powder Technology, 197*(3), 288-294.

Shimura, N., & Ogawa, M. (2007). Preparation of surfactant templated nanoporous silica spherical particles by the Stöber method. Effect of solvent composition on the particle size. *Journal of materials science, 42*(14), 5299-5306.

Skelhorn, D. (2003). Particulate fillers in elastomers. *Particulate-Filled Polymer Composites. 2nd ed. Shrewsbury, UK: Rapra Tec. Lim*, 324.

Somaratne, M., Liyanage, N., & Walpalage, S. (2014). Surface modification of silica with a hydrophilic polymer and its influence on reinforcement of natural rubber latex. *Journal of the National Science Foundation of Sri Lanka, 42*(4).

Stanley, R., & Nesaraj, A. S. (2014). Effect of surfactants on the wet chemical synthesis of silica nanoparticles. *International Journal of Applied Science and Engineering, 12*(1), 9-21.

Stöber, W., Fink, A., & Bohn, E. (1968). Controlled growth of monodisperse silica spheres in the micron size range. *Journal of Colloid and Interface Science, 26*(1), 62-69.

Tennakoon, D. (2015). Study on the Effect of Filler Combinations to the Cost and Quality of an Industrial Nitrile Glove (Doctoral dissertation, University of Sri Jayewardenepura, Nugegoda).

Thuc, C. N. H., & Thuc, H. H. (2013). Synthesis of silica nanoparticles from Vietnamese rice husk by sol–gel method. *Nanoscale research letters, 8*(1), 58.

Vansant, E. F., Van Der Voort, P., & Vrancken, K. C. (1995). *Characterization and chemical modification of the silica surface* (Vol. 93): Elsevier. 59-74.

Voronkov, M. G. e., IUzhelevsk'ii, I. A., & Mileshkevich, V. P. (1978). *The Siloxane bond: physical properties and chemical transformations*: Consultants Bureau.

Wang, J., Jia, H., Zhang, J., Ding, L., Huang, Y., Sun, D., & Gong, X. (2014). Bacterial cellulose whisker as a reinforcing filler for carboxylated acrylonitrile-butadiene rubber. *Journal of materials science, 49*(17), 6093-6101.

Xie, Y., Hill, C. A., Xiao, Z., Militz, H., & Mai, C. (2010). Silane coupling agents used for natural fiber/polymer composites: A review. *Composites Part A: Applied Science and Manufacturing, 41*(7), 806-819.

Yin, Y., & Alivisatos, A. P. (2005). Colloidal nanocrystal synthesis and the organic–inorganic interface. *Nature, 437*(7059), 664-670.

Zawrah, M., El-Kheshen, A., & Abd-El-Aal, H. M. (2009). Facile and economic synthesis of silica nanoparticles. *Journal of Ovonic Research, 5*(5), 129-133.

Zhang, Y., Fang, Y., Wang, S., & Lin, S. (2004). Preparation of spherical nanostructured poly (methacrylic acid)/PbS composites by a microgel template method. *Journal of Colloid and Interface Science, 272*(2), 321-325.

Zhang, Y., Ge, S., Tang, B., Koga, T., Rafailovich, M., Sokolov, J., . . . McElrath, K. (2001). Effect of carbon black and silica fillers in elastomer blends. *Macromolecules, 34*(20), 7056-7065.

Zulfiqar, U., Subhani, T., & Husain, S. W. (2016). Synthesis of silica nanoparticles from sodium silicate under alkaline conditions. *Journal of sol-gel science and technology, 77*(3), 753-758.